

Division of Geological & Geophysical Surveys

**PUBLIC-DATA FILE 98-29**

**PROJECT REPORT OF THE AEROMAGNETIC SURVEY  
FOR THE HOLITNA BASIN AREA, WESTERN ALASKA**

by

Sial Geosciences Inc./  
On-Line Exploration Services Inc.

August 1998

THIS REPORT HAS NOT BEEN REVIEWED FOR  
TECHNICAL CONTENT (EXCEPT AS NOTED IN TEXT) OR FOR  
CONFORMITY TO THE EDITORIAL STANDARDS OF DGGs.

Released by

STATE OF ALASKA  
DEPARTMENT OF NATURAL RESOURCES  
Division of Geological & Geophysical Surveys  
794 University Avenue, Suite 200  
Fairbanks, Alaska 99709-3645

**DEPARTMENT OF NATURAL RESOURCES  
DIVISION OF GEOLOGICAL & GEOPHYSICAL SURVEY  
STATE OF ALASKA**

**Contract 10-98-001**

**PROJECT REPORT OF THE AEROMAGNETIC SURVEY  
FOR THE HOLITNA BASIN AREA, WESTERN ALASKA**

---

**May 1998**

**DEPARTMENT OF NATURAL RESOURCES  
DIVISION OF GEOLOGICAL & GEOPHYSICAL SURVEYS  
STATE OF ALASKA**

**PROJECT REPORT OF THE  
AEROMAGNETIC SURVEY FOR THE  
HOLITNA BASIN AREA, WESTERN ALASKA**

**Contract 10-98-001**

**Project 97-A03-36**

by

**SIAL GEOSCIENCES INC./  
ON-LINE EXPLORATION SERVICES INC.**

**May 1998**

## TABLE OF CONTENTS

	Page
1.0 INTRODUCTION .....	1
2.0 MANAGEMENT OF SURVEY .....	3
3.0 SURVEY AREA .....	4
4.0 SURVEY EQUIPMENT .....	5
4.1 Aircraft .....	5
4.2 Digital and Analog Acquisition System .....	5
4.3 Airborne Magnetometer .....	6
4.4 Compensator .....	6
4.5 Radar altimeter .....	6
4.6 Barometric altimeter .....	6
4.7 Navigation and Flight Path Recovery Systems .....	7
4.7.1 Video Camera .....	7
4.7.2 GPS .....	7
4.7.3 Pilot Guidance .....	7
4.8 Base stations .....	8
4.8.1 Main magnetic base station .....	8
4.8.2 Remote magnetic base station .....	8
4.8.3 GPS base station .....	10
4.9 Field Data Plotting and Verification System .....	10
4.9.1 Hardware .....	10
4.9.2 Software .....	10

## TABLE OF CONTENTS (cont'd)

	Page
<b>5.0 OPERATIONS - FIELD PROCESSING - VERIFICATIONS . . . . .</b>	<b>11</b>
5.1 Summary . . . . .	11
5.2 Quality control . . . . .	12
5.2.1 Lag . . . . .	12
5.2.2 Magnetic . . . . .	13
5.2.3 Altimeters . . . . .	13
5.2.4 Magnetic base data . . . . .	13
5.2.5 Differential GPS . . . . .	14
5.3 Levelling . . . . .	14
5.4 Gridding and color plotting . . . . .	15
<b>6.0 OFFICE COMPILATION . . . . .</b>	<b>15</b>
6.1 Total field levelling and gridding . . . . .	15
6.2 Altimeters . . . . .	16
<b>7.0 DELIVERIES . . . . .</b>	<b>17</b>
7.1 Maps . . . . .	17
7.2 Digital Data Recording . . . . .	18
7.3 Miscellaneous Items . . . . .	18
7.4 In-depth Analysis and Modelling . . . . .	19
<b>8.0 GEOLOGICAL CONTEXT . . . . .</b>	<b>19</b>

## TABLE OF CONTENTS (cont'd)

	Page
<b>9.0 INTERPRETATION</b> .....	<b>26</b>
<b>9.1 Magnetic Signatures from some Geological Features</b> .....	<b>27</b>
<b>9.2 Analysis of the Total Field Magnetic Map</b> .....	<b>39</b>
<b>9.3 Qualitative Interpretation</b> .....	<b>40</b>
<b>9.4 Spectral Analysis</b> .....	<b>41</b>
<b>9.5 2.5-D Modelling</b> .....	<b>51</b>
<b>9.6 Euler Deconvolution</b> .....	<b>69</b>
<b>10.0 CONCLUSIONS</b> .....	<b>75</b>
<b>SELECTED REFERENCES</b> .....	<b>76</b>

## LIST OF FIGURES

	Page
Figure 1:	Holltna basin survey area . . . . . 2
Figure 2:	Base station localization, Sleetmute . . . . . 9
Figure 3:	Tectonic map of the survey area . . . . . 20
Figure 4:	Generalized geologic map of Holitna basin showing gravity trends and surrounding upland terraces . . . . . 21
Figure 5:	Magnetic anomaly shapes . . . . . 28
Figure 6:	Fault in the underlying rocks (1) . . . . . 29
Figure 7:	Fault in the underlying rocks (2) . . . . . 30
Figure 8:	Belt of volcanic rocks . . . . . 31
Figure 9:	Serpentinized peridotite sill . . . . . 32
Figure 10:	Gneissic terrain . . . . . 33
Figure 11:	Discordant intrusive (1) . . . . . 34
Figure 12:	Discordant intrusive (2) . . . . . 35
Figure 13:	Weakly magnetic metasediments . . . . . 36
Figure 14 a-b:	Magnetic Mapping of an oil field . . . . . 37
Figure 14 c-d:	Magnetic Mapping of an Oil Field . . . . . 38
Figure 15:	The residual magnetic field. The survey area divided in six blocks . . . . . 44
Figure 16:	Power Spectrum for the North-West part of the survey area 45
Figure 17:	Power Spectrum for the North-Centre part of the survey area 46
Figure 18:	Power Spectrum for the North-East part of the survey area 47
Figure 19:	Power Spectrum for the South-West part of the survey area 48
Figure 20:	Power Spectrum for the South-Centre part of the survey area 49
Figure 21:	Power Spectrum for the South-East part of the survey area 50
Figure 22:	Location of the 2.5-D modelled magnetic profiles . . . . . 52
Figure 23:	2.5-D modelled magnetic profile 1 . . . . . 53
Figure 24:	2.5-D modelled magnetic profile 2 . . . . . 54
Figure 25:	2.5-D modelled magnetic profile 3 . . . . . 55
Figure 26:	2.5-D modelled magnetic profile 4 . . . . . 56
Figure 27:	2.5-D modelled magnetic profile 5 . . . . . 57
Figure 28:	2.5-D modelled magnetic profile 6 . . . . . 58
Figure 29:	2.5-D modelled magnetic profile 7 . . . . . 59
Figure 30:	2.5-D modelled magnetic profile 8 . . . . . 60
Figure 31:	2.5-D modelled magnetic profile 9 . . . . . 61
Figure 32:	2.5-D modelled magnetic profile 10 . . . . . 62
Figure 33:	2.5-D modelled magnetic profile 11 . . . . . 63
Figure 34:	2.5-D modelled magnetic profile 12 . . . . . 64
Figure 35:	2.5-D modelled magnetic profile 13 . . . . . 65
Figure 36:	2.5-D modelled magnetic profile 14 . . . . . 66
Figure 37:	2.5-D modelled gravity profile A-A' . . . . . 67

## LIST OF FIGURES (cont'd)

	page
Figure 38:	2.5-D modelled gravity profile B-B' . . . . . 68
Figure 39:	Magnetic field (flux lines) and fall-off rates for various geological models . . . . . 71
Figure 40:	Euler depth interpretation (dike model) . . . . . 72
Figure 41:	Euler depth interpretation (step model) . . . . . 73
Figure 42:	Interpretation sketch map . . . . . 74

## FORWARD

A contractor provided this report to us. Upon review, it became apparent that the geologic terminology used is no longer current. The geologic portion of this report (Section 8.0 Geologic Context) is based on data from Cady and others (1955) and a chapter from *The Geology of North America* (Volume G-1, *The Geology of Alaska*, Chapter 14 – Interior Basins of Alaska, by C.E. Kirschner) that are no longer current. Consequently, some of the terminology is outdated and much of the geology of the survey area is not discussed. A brief discussion is included here, and the reader is referred to Decker and others (1994), and references included therein, for a more complete discussion of the regional geology. For example, Adrain and others (1995) recommended abandoning “Holitna Group” as a stratigraphic term. That term is used in this report. Recent improvements in the biostratigraphic zonation of rocks in the area have shown that several systems (spanning the early and middle Paleozoic) were included in the original definition by Cady and others (1955).

The aeromagnetic survey described herein corresponds to a portion of the Farewell terrane bounded by the Denali-Farewell fault, the Kulukbuk thrust, and an unnamed northeast-trending fault located west of the Big River fault (Decker and others, 1994; see their fig. 1). They considered this part of the Farewell terrane as the Holitna basin. Decker and others (1994) describe the Holitna basin as including Proterozoic through Triassic age sedimentary rocks and minor Mesozoic age intrusive and extrusive igneous rocks.

Additionally, we disagree with the conclusions reached in this report regarding oil and gas potential in the Holitna basin area. Section 8.0 of this report concludes with a valid statement regarding the petroleum potential of the Cretaceous and Tertiary strata in the vicinity of the Holitna basin. Past studies of the region have suggested poor to fair petroleum potential for Paleozoic strata. However, recently acquired conodont data from the northeastern part of the Holitna basin suggests that Middle to Upper Paleozoic rocks between the Gagaryah River and Lime Lakes region (Lime Hills quadrangle) were heated to maximum temperatures within the oil window (CAIs between 1.5 and 2.0). This suggests that the petroleum potential of Paleozoic rocks in the region has not been adequately evaluated.

Forward written by Dave LePain

### Works Cited:

- Adrain, J.M., Chatterton, B.D.E., and Blodgett, R.B., 1995. Silurian trilobites from southwestern Alaska. *Journal of Paleontology*, v. 69, p. 723-736.
- Cady, W.M., Wallace, R.E., Hoare, J.M., and Weber, F.R., 1955, *The central Kuskokwin region, Alaska*: U. S. Geological Survey, Professional Paper 268, 132 p.
- Decker, John, Bergman, S.C., Blodgett, R.B., Box, S.E., Bundtzen, T.K., Clough, J.G., Coonrad, W.L., Gilbert, W.G., Miller, M.L., Murphey, J.M., Robinson, M.S., and Wallace, W.K., 1994, *Geology of southwest Alaska*: in Pfäfer, George, and Berg, Henry C., eds., *The Geology of Alaska*: Boulder, Colorado, Geological Society of America, *The Geology of North America*, vol. G-1, p. 285-310.
- Kirschner, C. E., 1994. Interior basins of Alaska: *The Geology of North America*, Vol. G-1, *Geology of Alaska*. The Geological Society of America, pp. 469-493.

## 1.0 INTRODUCTION

On-Line Exploration Services Inc. (OLES) was awarded State of Alaska contract 10-98-001 by the Natural Resources Department, Division of Geological & Geophysical Surveys, on August 26th. This contract required OLES to carry out a high-sensitivity airborne magnetic survey over a 3 234 square mile area located in the Holitna basin, western Alaska. The survey area is shown in Figure 1.

The primary goal of this project was to acquire and publish aeromagnetic data that will aid in the evaluation of the hydrocarbon potential of the Holitna basin area. A thorough detailed analysis of the aeromagnetic data and modelling of selected magnetic profiles add to the understanding of the basin.

The survey was carried out between September 8th and October 7th, 1997. Preliminary maps were delivered at the end of November 1997, followed by final maps and digital products in April and May, 1998.

This report describes the data acquisition and processing procedures, parameters and delivery products for this survey as well as the qualitative and quantitative interpretation methodology and results.



## 2.0 MANAGEMENT OF SURVEY

Coordination and general management of the project were carried out by OLES. The Project Manager, Mr. Kevin P. Adler, acted as liaison between the Project Manager for the State of Alaska, Dr. Laurel E. Burns, other governmental agencies, subcontractors and the local suppliers and vendors. Mr. Adler worked closely with the geophysical subcontractor to ensure timely delivery of survey results.

SIAL Geosciences Inc. (SIAL) was the geophysical subcontractor for the project. The survey and office crews consisted of the following permanent employees of SIAL:

**Table 1: Field Survey Crew**

POSITION	NAME
Project Manager, Field Geophysicist & Data Processing	Ms. Josée Potvin
Field Operator & Electronic Technician	Mr. Pierre Filion
Pilot	Mr. Eric Gauthier-Raymond
Office Data Processing	Ms. Josée Potvin, Geophysicist Mr. Ji Ma, M.Sc., Geophysicist Mr. Weizhong Shen, M.Sc., Geophysicist Mr. François Caty, Geologist Ms. Sylvie Robillard, Technician CAD Mr. Albert Sayegh, Technician CAD
Interpretation and Report	Camille St-Hilaire, M.Sc.A, Geophysicist

### 3.0 SURVEY AREA

The survey area, shown on Figure 1, covers portions of the Sleetmute and Lime Hills Quadrangles in western Alaska. A total of 13,192 line-km (8,215 miles) were flown. Cultural effects in the data are almost absent. Minor exceptions are the villages of Stony River and Sleetmute located to the north and northwest of the survey area.

Most of the survey area has flat to moderate topographic relief which did not present significant difficulty in meeting altitude and line spacing specifications. The exception was the Lime Hills area, located in the Southeast portion, where drape flying was required because of the steep mountains with incised drainage, which could not be safely flown by fixed-wing aircraft within the requested altitude specifications. In this area, the flight altitude varied to a maximum of 700 feet.

The grid characteristics were:

Flight-line direction:	N35°W
Flight-line spacing:	0.5 mile (2680 feet or 813 meters)
Tie-line spacing:	3 miles (4800 meters)
Flight-line tolerance:	Maximum deviations (from the specified flight path) of 500 feet over a distance of 0.5 mile (spacing of adjacent lines was less than 3140 feet or more than 2140 feet over a distance of 0.5 mile)

## 4.0 SURVEY EQUIPMENT

All the instrumentation used during the survey met the contractual specifications presented in appendix A.

### 4.1 Aircraft

A Piper Navajo 310 (registration C-GAKM) equipped with a 10-foot stinger, owned and operated by SIAL was used. Average flying speed was 130 knots while mean terrain clearance (averaged over any one mile distance) was 300 feet.

### 4.2 Digital and Analog Acquisition System

A RMS DAS-8/DGR-33A (serial 8108009) data logging system, an on-board graphical display data-acquisition system and a graphic recorder were used. This system:

- accepted digital data from the magnetometer, radar and barometric altimeters, time and raw GPS positions
- produced a hard-copy graphic record (analog) of both coarse and fine scales data from the magnetometer, 4th difference X-track, radar and barometric altimeter data, fiducial date and time.
- produced a digital machine-readable record of raw data on an external tape-drive

The analog records were of sufficient resolution to enable visual checks to be made of system performance. The chart speed of the analog recorder was 12 cm/sec. One-second intervals were indicated on the analog by means of short tics and fiducial numbers printed at 10-seconds intervals.

The data acquisition system was synchronized to GPS time through a one-second GPS pulse. Synchronization was checked at the end of each day of surveying.

### 4.3 Airborne Magnetometer

Airborne magnetometer:	Geometrics G-822A Cesium Vapour split beam (serial G098) in a tail stinger installation
Sensor static resolution:	better than 0.1 nT
In-flight sensibility:	$\pm 0.001$ nT
Dynamic range:	20,000 - 95,000 nT
In-flight noise envelope:	< 0.01 nT
Sampling rate:	ten (10) readings per second or approximately 22 feet at average aircraft speed of 130 knots
Heading error:	< 1 nT
Recording interval:	0.1 sec

### 4.4 Compensator

The aircraft generated magnetic field was compensated with an Automatic Aeromagnetic Digital Compensator unit (AADCI, serial 9502694) yielding digital signal correction of 18 to 30 terms based on the vector field components and their derivatives as measured by a 3-axis fluxgate sensor.

### 4.5 Radar altimeter

Radar altimeter:	King KRA-10
Range:	20-2500 ft
Resolution:	4 mV/foot
Accuracy:	1% over flat terrain
Sensitivity:	better than 10 feet

### 4.6 Barometric altimeter

Barometric altimeter:	Rosemount 1241
Range:	sea-level to 10,000 ft
Resolution:	1 Mv/foot
Accuracy:	$\pm 7$ feet
Electronic drift:	< 10 feet/hour

For each flight, the barometric altimeter was calibrated with the radar altimeter pre and post flight and the "drift" was determined by flying over an airstrip of known elevation at several altitudes. This drift and the GPS altitude were used to correct the barometric altitude of flight.

## **4.7 Navigation and Flight Path Recovery Systems**

### **4.7.1 Video Camera**

An ELMO TSN272 color video camera with audio capability (serial J3HB0074) recorded the flight path terrain beneath the aircraft. The video camera recorded alphanumerically the flight line number, fiducial, time and GPS generated X-Y UTM coordinates in the top portion of each frame.

### **4.7.2 GPS**

A Trimble 4000SE, 10 channel GPS receiver differentially-corrected in post-processing with a ground base station GPS receiver was used. The GPS receivers locked on to at least 4 satellites. Data from both GPS receivers were recorded simultaneously at 1 second intervals by the data acquisition systems. Post-processing position accuracy was better than 5 meters.

### **4.7.3 Pilot Guidance**

In conjunction with the GPS, a Picodas PNAV 2001 provided in-flight navigation control (XY guidance).

## 4.8 Base Stations

### 4.8.1 Main magnetic base station

The main base station was placed inside the survey area (figure 2), near the landing strip, at Sleetmute, in a magnetically clean environment, away from sources of electromagnetic interferences or excessive magnetic gradients. A digital record of the variation of the earth's magnetic field was continually recorded.

The airborne and digital base station magnetometers were synchronized with an accuracy better than 1.0 second.

Base station magnetometer:	GEM GSM-19 Overhauser with internal memory (14 days self-sufficiency)
Sensor static resolution:	better than 0.1 nT
Sensitivity:	$\pm 0.001$ nT
Dynamic range:	20,000 - 95,000 nT
Noise envelope:	less than 0.1 nT
Sampling rate:	once per 3 seconds

### 4.8.2 Remote magnetic base station

A second base station magnetometer was placed at the base camp located at McGrath. As this base station was located 100 km from the survey area, it was solely used to monitor the diurnal variations. Diurnal was not significant during the survey period but when variations exceeded 7.5 nT over a chord of 2.0 minutes, the corresponding airborne data were rejected.

Remote magnetometer:	Geometrics G-823W cesium (S/N 823001)
Sensor static resolution:	better than 0.1 nT
Sensitivity:	$\pm 0.001$ nT
Dynamic range:	20,000 - 95,000 nT
Noise envelope:	less than 0.1 nT
Sampling rate:	once per 3 seconds

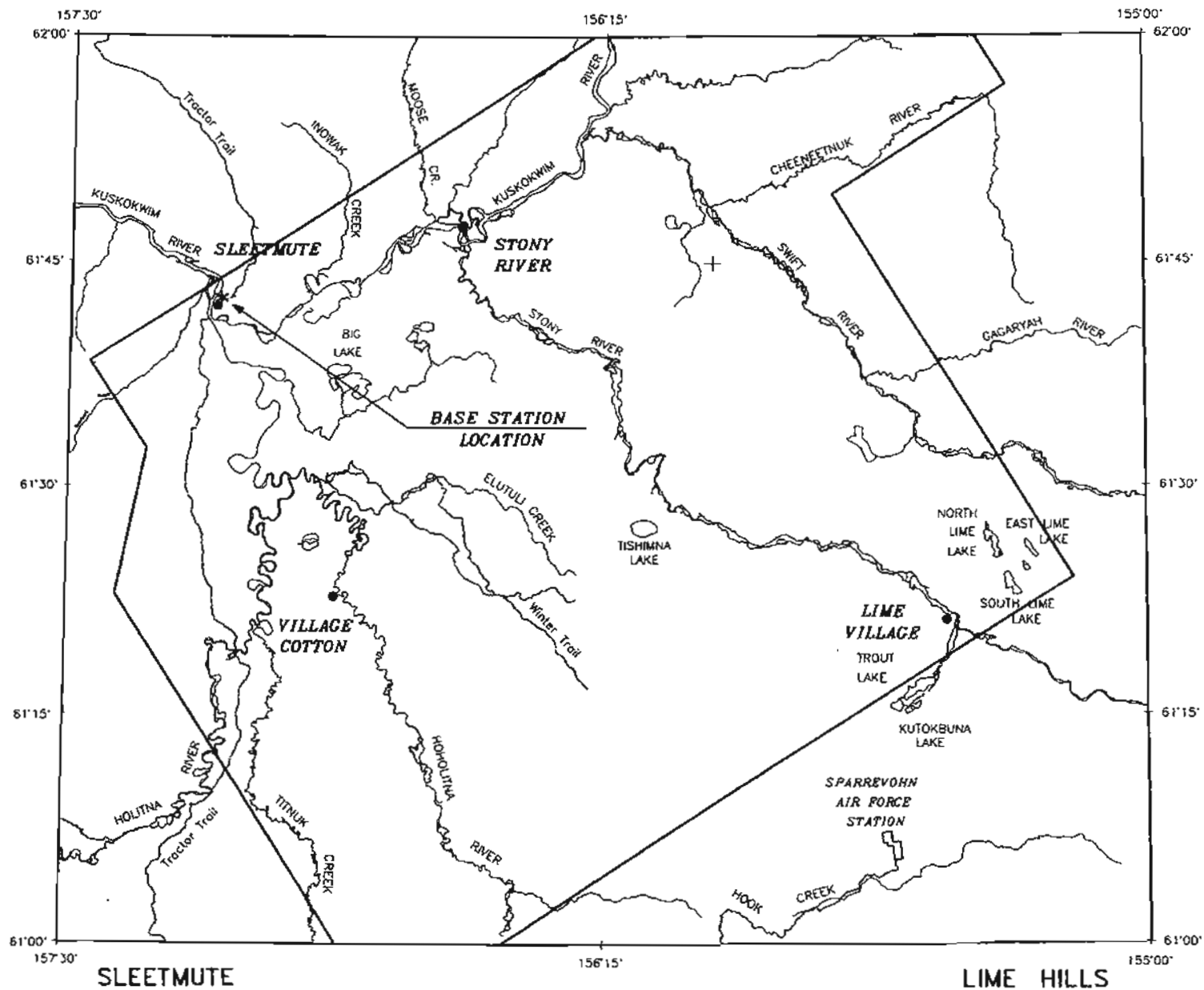


FIGURE 2  
 AIRBORNE GEOPHYSICAL SURVEY  
 HOLITNA BASIN, SOUTHWESTERN ALASKA  
 BASE STATION LOCATION, SLEETMUTE

### **4.8.3 GPS base station**

A GPS Trimble 4000SE receiver (identical to airborne unit) was also installed at the remote base station and used as a reference for post-processing. The recording interval was 1 second and at least 4 satellites were monitored at all times.

## **4.9 Field Data Plotting and Verification System**

### **4.9.1 Hardware**

The field processing system consisted of a Pentium-PC with a high-resolution screen, a Zip tape drive, a Cannon BJ-4000 color bubble-jet printer and a video player.

### **4.9.2 Software**

The computer was equipped with custom and commercial software capable of providing preliminary compilation through initial contours in addition to profile plots required to confirm the validity of data collected on each flight. The software package included Geosoft, Oasis and Nortech HPM differential processing software.

## 5.0 OPERATIONS - FIELD PROCESSING - VERIFICATIONS

### 5.1 Summary

The survey base was established at McGrath. The main magnetic base station, powered by a 12 volt car battery, was located at the airstrip at Sleetmute. The station was capable of recording data for 14 days (GEM memory) and no malfunctions or data losses occurred. The main and remote magnetic base stations were located away from any sources of magnetic interference.

The pre-survey Figure of Merit (FOM) and Bourget calibrations were carried out September 1st, 1997. The FOM was of 2.2 nT. The result of the Bourget and FOM calibrations are tabulated in Appendix B. The altimeter calibration results are also displayed in Appendix B.

Lag-tests, to determine the time difference between the magnetometer and positioning devices, were performed by flying in two directions, at the normal survey height, over a large steel tank that provided an anomaly sufficient to determine the system lag in relation to the GPS positioning data.

Mobilization to McGrath started September 2nd, 1997. All pre-survey tests and base installations were completed by September 7th. A new FOM value of 0.97 nT was obtained. Survey flying commenced on September 8th, 1997.

Spikes in the magnetic data, detected on September 22nd, resulted in the interruption of flights. A new magnetic sensor was received and installed on September 26th. New FOM and Heading tests were performed on September 28th. An FOM value of 1.37 nT was obtained (Appendix B).

A 100 hour aircraft inspection was carried out September 18th-19th.

Survey flights were completed on October 8th. Demobilization was completed by October 11th.

Field operations required 41 days, as follows:

• preparation and pre-survey calibration (Montreal)	1.0 day
• mob/demob (including customs)	7.5 days
• installation/de-installation	1.5 days
• McGrath pre-survey calibration	1.0 day
• survey flying	11 days
• down-time due to bad weather and diurnal	8.5 days
• aircraft inspection	3.5 days
• instrumentation problems	7.0 days

All the digital flight logs are presented in Appendix C.

## 5.2 Quality control

All flight records, the differentially corrected GPS and the ground station records were merged into a single GEOSOFTE-OASIS database on a flight by flight basis. Profiles were examined in detail, on the analog records and mainly using OASIS scrolling and zooming capabilities. The main concerns were the speed check of GPS data, diurnal activity, and altimeter data (mainly radar and GPS Z jumps).

### 5.2.1 Lag

RMS/GPS synchronization was achieved by the RMS acquisition software. This software uses the 1-pps transmission from the GPS-TRIMBLE console that contains the GPS time. Upon reception of the GPS signal, the corresponding RMS system time was logged. GPS and RMS were recorded as data fields in the raw RMS file at the rate of 1 per second.

### 5.2.2 Magnetic

Field quality control procedures were:

- 1) application of lag (see section 5.2.1).
- 2) application of a de-spiking filter. This filter only affects discrete spikes, leaving most of the data untouched.
- 3) monitoring of compensation quality, especially for flights made over topographic highs
- 4) visual inspection of magnetic profiles and flight path plots
- 5) preliminary color maps

### 5.2.3 Altimeters

No field processing was applied on the radar altimeter data.

Field barometric correction was based on pre- and post-flight barometric measurements made on the airstrip. Corrections were calculated using the known elevation of the airstrip, and were linearly interpolated over the flight data. The barometric data were then compared to the more stable GPS altitude.

The topographic profile was calculated from the difference between the barometric and radar altimeters, and used to detect and correct discontinuities in radar values.

### 5.2.4 Magnetic base data

After having been merged in the main OASIS database, the main and remote base magnetometers data were carefully inspected in order to remove any cultural noise and spikes. A 30 second low-pass filter was then applied to remove small amplitude noise.

OASIS profiles and SIAL software were then used to compare the degree of diurnal

activity with the contract tolerance of 7.5 nT over chords of 2 minutes in length. Periods of activity close to or above this tolerance were listed and re-flights done.

### **5.2.5 Differential GPS**

The GPS raw data were processed post-flight using the NORTECH HPM software. Statistics produced by HPM on the differential correction were used to minimize X,Y,Z jumps through de-selection of data from some satellites and modification of the horizon angle.

The velocity and acceleration of the aircraft were then calculated for the entire flight as a final check on the flight path. Any remaining errors were corrected or the data re-flown as appropriate. Gradient grids were also used to assess GPS quality.

Plots of the flight path were produced on a daily basis to inspect the quality of the coverage.

Before demobilization, to be sure that data were of good quality, a final check was carried out. Control line magnetic data were gridded separately and the result compared to the survey line grid.

## **5.3 Levelling**

The main base station (Sleetmute) level was determined and continuously updated by averaging all the observations collected during the course of the survey. At the end of the survey, the average value of the main base station was 54895 nT. Drift was obtained by subtracting the 54895 nT from the base magnetic readings. The drift amplitudes ranged from 54783 nT to 54964 nT. Although levelling improvements were significant, they still proved insufficient to produce useful preliminary total field maps.

#### 5.4 Gridding and color plotting

GEOSOFT line gridding (minimum curvature) software was used in the field. Color maps of the total field, as well as of its derivatives and shadow, were regularly produced in the field, with flight path overlay, in order to evaluate data quality.

### 6.0 OFFICE COMPILATION

Final compilation was completed in SIAL's head office, Montreal, under the supervision of Ms. Josée Potvin. Other personnel assigned to this project were Mr. Ji Ma and Weishong Shen, Geophysicists (Processing Support), Mr. François Caty Geologist, Ms. Sylvie Robillard, Technicians (AutoCad/Drafting), and Mr. Albert Sayegh, Technician (AutoCad/Drafting).

All field processing steps were exhaustively verified and updated before proceeding further. The steps to be completed at this stage were:

- intersection levelling of the total field
- final correction and levelling of altimeter data
- production of the deliverable items (maps and archives files).

#### 6.1 Total field levelling and gridding

After diurnal corrections were removed, the final levelling of the total magnetic field was done by intersection analysis. First, all the intersection differences were calculated and a statistical levelling was done on each tie-line by subtracting a first order curve. Secondly, any residual difference between tie-lines/traverse-lines were applied on each traverse-line to produce identical values for all the intersections. After this processing, no further correction was necessary.

The magnetic values were then reduced to a regular X-Y grid, using a numerical approximation technique referred to as gridding. This final 200 meter grid was produced using GEOSOFT line grid (minimum curvature) software for the areas with 800 metre line spacing.

The final grid was contoured using the GEOSOFT contouring routines. Hierarchies of contour intervals were defined, each with its own dropout density, pen weight, and periodic annotation.

A color contour map of the final total field magnetic intensity gridded data set was produced. Pseudo equal area color intervals were utilized wherein smaller increments were applied around the mean data values and increasingly larger increments were applied towards the minimum and maximum data values. This resulted in a better resolution of anomalies in the mid-range of the data. Such anomalies can become obscured when linear color intervals are used.

A color shadow map (illuminated image) of the final total field magnetic intensity gridded data set was produced. The orientation and value of the gradients of the individual grid cells determined the apparent brightness or darkness of each cell on the shadow map. This technique emphasizes even very small rates of change that may be obscured by large features in the data.

First and second derivatives were calculated for final check.

## **6.2 Altimeters**

The corrections to the GPS, barometric and radar altimeter data were done post-survey at the head office. All corrections were directed to the production of a non-corrugated topographic (ZGPS-radar) grid with a zero-level corresponding to sea level.

## 7.0 DELIVERIES

All final products required by the technical specifications of the contract (appendix A) were delivered in May 1998. All CAD map layouts and digital mapping files were prepared by M. Albert Sayegh. Appendix D contains a full description of the digital data archive format.

### 7.1 Maps

All maps were made at a scale of 1:125,000 on the Universal Transverse Mercator (UTM) projection using the following parameters:

-	Central Meridian	159°W
-	Zone	4
-	Spheroid	Clarke 1866
-	False Northing	0 meters
-	False Easting	500,000 meters

The total magnetic intensity and flight path maps display latitude/longitude reference marks and a topographic base. The following final maps were produced:

- The flight line maps on stable mylar base.
- The Magnetic total-field contours on stable mylar topographic base with flight path lines (scale 1:125,000).
- Paper-copies in full-color of the Magnetic total-field contours with Latitude/Longitude notations along border of map.
- Paper-copies in full-color shadow of the Magnetic total-field contours with Latitude/Longitude notations along border of map.
- An interpretation sketch map on stable mylar
- An interpretation sketch map (scale 1:500,000; figure 42).

## 7.2 Digital Data Recording

Digital data were supplied on CD-ROMS readable by standard common CD-ROM readers, including Mitsumi, Panasonic and Sun. The CD-ROMS contain flight number, line number, fiducial information, as well as latitude-longitude x-y UTM coordinates. Appendix D gives a description of the material CD-ROM's contents.

Each CD-ROM includes:

- final processed data for all systems in ASCII format
- flight path
- gridded data used in preparation of magnetic contour maps in Geosoft format
- gridded data used in preparation of magnetic contour maps in ASCII format
- magnetic total field contours in Geosoft vector format
- sections grids in Geosoft and "DXF" formats vector file for use as an overlay for the gridded data
- Interpretation overly from project report in Geosoft and dxf vector formats
- original raw profile data (with corrected locations) in ASCII format
- "Readme" file describing contents of CD-ROM

## 7.3 Miscellaneous Items

The following miscellaneous items were finally produced:

- Analogue records for airborne systems and ground monitor systems
- Video tapes
- A technical project report
- Records of the FOM tests (appendix B)
- Records of the altimeter calibrations (appendix B)

#### 7.4 In-depth Analysis and Modelling

In-depth analysis and modelling of the aeromagnetic data, and the accompanying maps, are included in this report.

### 8.0 GEOLOGICAL CONTEXT

The following geologic description and interpretation are taken from - W.M. Cady, R.E. Wallace, J.M. Hoare, and E.J. Webber, 1955; U.S. Geological Survey Professional Paper 268 - and - C.E. Kirschner, 1994; The Geology of North America. Vol. G-1, The Geology of Alaska; chapter 14, Interior Basins of Alaska.

The Holitna basin is a small Cenozoic basin of about 5,000 km<sup>2</sup> astride the Farewell fault zone (figure 3). It is located to the northeast of Kuskokwim Bay, and north of Bristol Bay, along the Kuskokwim river system. It covers portions of Sleetmute and Lime Hills Quadrangles in western Alaska. The survey area consists of low relief alluvial plain underlain entirely by unconsolidated Quaternary deposits.

The most conspicuous feature of the Holitna basin is a long, narrow gravity trough (Barnes, 1977) localized along the trend of the Farewell fault zone, which suggests a rift-graben with a few kilometers of Cenozoic fill (figure 4). Small outcrops of middle(?) and late Tertiary nonmarine coal-bearing strata are present locally along the Farewell fault zone, on trend with the Holitna basin (Kirschner, 1994).

The Lower Kuskokwim - Bristol Bay region is a tectonically active belt which borders the Pacific ocean. This region has been subjected to strong compressive forces operating northwest and southwest. Strata of Cretaceous age and older are compressed into tight folds and broken by numerous faults. Large areas of lava flows of Tertiary and Quaternary age are present which show that the region was the scene

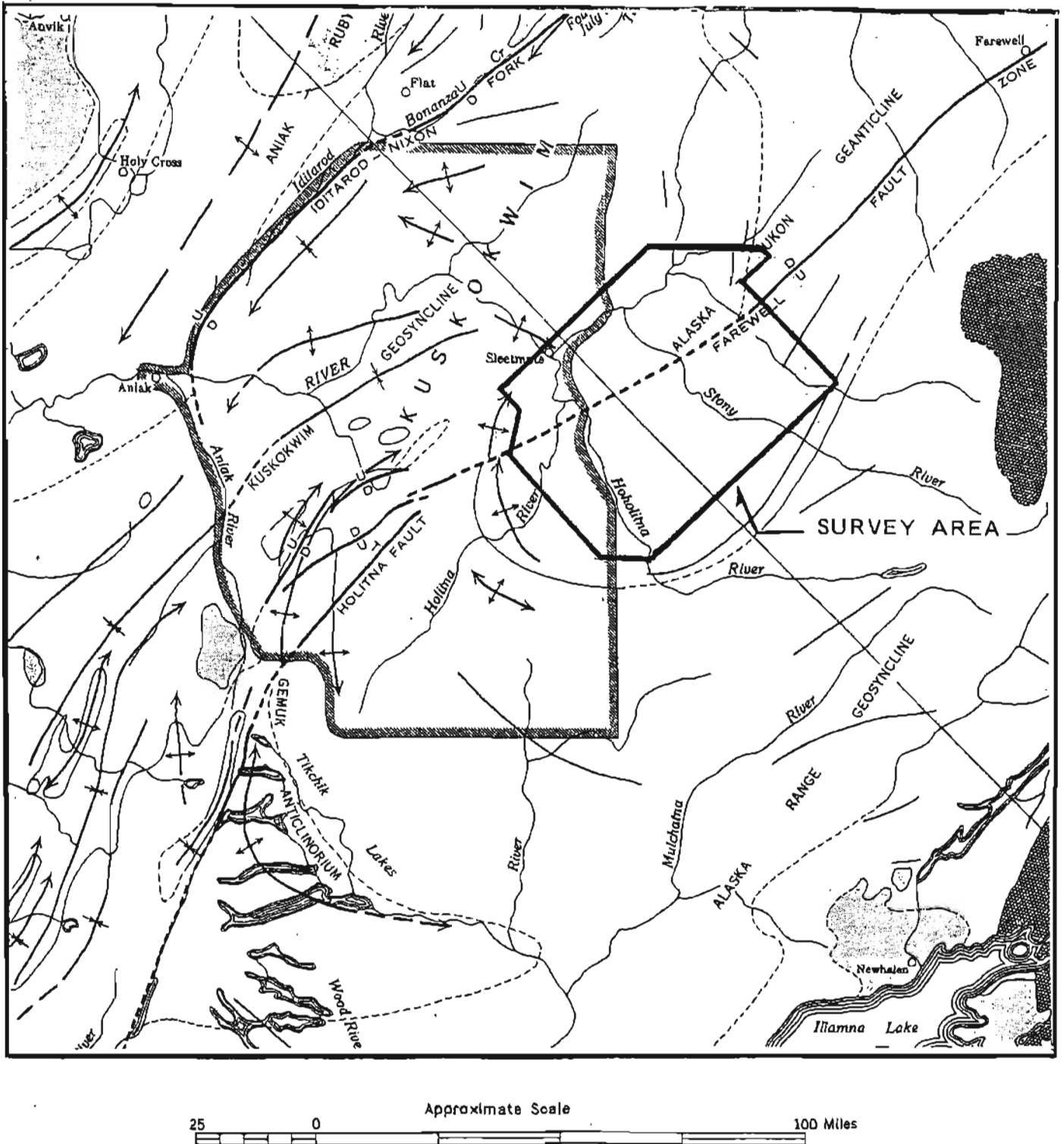


**FIGURE 3: Tectonic map of the survey area**

(Modified from W.M. Cady and J.M. Hoare, 1955; in U.S. Geological Survey Professional Paper 268, plate 2)

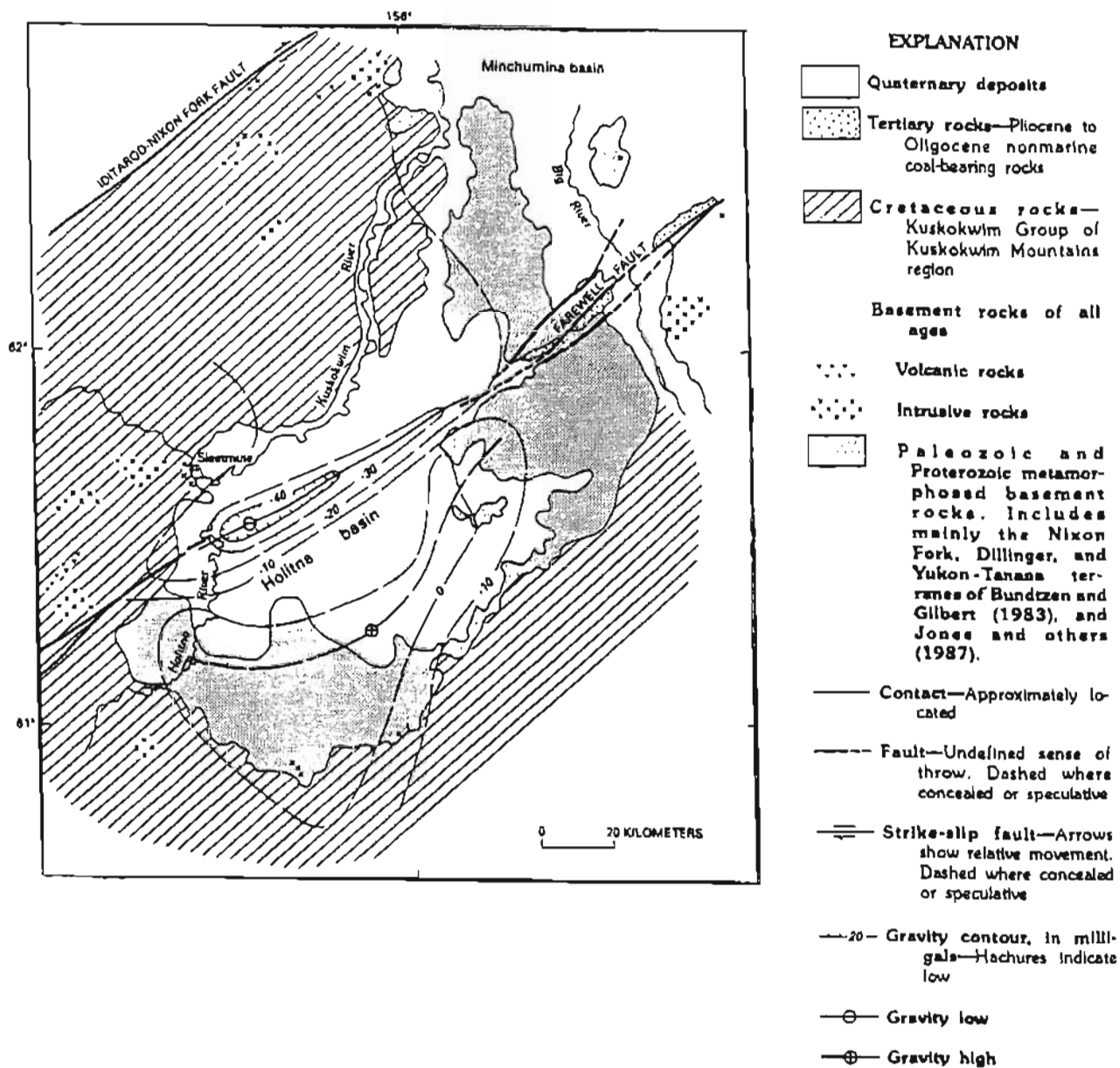


**Figure 4: Generalized geologic map of Holitna basin showing gravity trends and surrounding upland terranes**

Taken from C.E. Kirschner, 1994; *The Geology of North America*. Vol. G-1, *The Geology of Alaska*; chapter 14, Interior Basins of Alaska; p. 485, fig. 14.

of considerable volcanic activity a relatively short time ago.

Rocks exposed in the region are from Precambrian to Quaternary in age. These units from, oldest to youngest, consist of:

- metamorphic rocks of Precambrian age
- limestones of Devonian age (Holitna group)
- interbedded greywacke shale and conglomerate which make up the Kuskokwim group of Cretaceous age
- continental basalt of Tertiary and Quaternary age
- surficial deposits of Quaternary age

### **The Holitna Group**

A group of Devonian limestones which crop out in a hilly belt, about 20 miles wide, across the middle course of the Holitna River is designated the Holitna group. The actual extent of the limestone belt is undetermined. These hills are the southern continuation of the Lime Hills, which cross the eastern tributaries of the Kuskokwim River west of the Alaska Range. Comparable limestones, associated with various clastic rocks, are reported northeast of the central Kuskokwim region, northwest of the upper Kuskokwim River. The limestones in these two outlying areas lie in the southeast and northwest flanks respectively of the Alaska-Yukon geanticline (figure 3).

The Holitna group includes various types of limestone that have been changed from an originally dense, fine-textured rock to more coarsely crystalline types. The recrystallized facies are partly dolomitic. Small reef-like masses are found in several places. Intraformational conglomerate and breccia, composed of limestones fragments in a limestone matrix, are common locally.

The Holitna group is estimated, from the few measurable sections exposed, to be at least 5,000 and probably closer to 10,000 feet thick.

### **The Kuskokwim**

Interbedded greywacke, shale, breccia and conglomerate of Kuskokwim group extend several tens of miles from the north and northwest of the area. The Kuskokwim group is traceable into the basins of the upper Holitna and Stony Rivers. The rocks referred to as greywacke are a variety of sandstone. The shales, which are about half as abundant, are a siltstone facies of the greywacke that is intimately interbedded with the sandstone. Breccia and conglomerates, which also form facies of the greywacke similar to the sandstone, although coarse grained, are present in a few localities. All the rocks are dark.

Generally, the Kuskokwim group is extremely thick and is estimated to contain between 40,000 to 65,000 feet of strata. The group probably thins, chiefly by transgressive overlap of the higher strata on the Alaska-Yukon geanticline. Some of the highest strata possibly lie near the lower contact on the northwest flank of the geanticline at the northeasternmost localities in which the group is exposed. Studies of the relation of the Kuskokwim group to the Holitna group suggest that some presumably basal southeastern shale facies of the Kuskokwim group overlap the Alaska-Yukon geanticline.

### **Igneous rocks**

The bedded rocks of the area are intruded by many kinds of igneous rocks, mostly granitic. These rocks intrude sedimentary rocks as young as middle to late Cretaceous. They seem less abundant in the Holitna basin, but this is possibly because they are covered there by extensive surficial deposits.

Largest of the intrusive bodies are the stocks made up predominately of quartz monzonite and granite. These large tabular bodies, some of which are nearly elliptical in ground plan, consist of albite rhyolite. The smallest intrusive bodies are sills and dikes, chiefly of basalt, diabase, and rhyolite.

Horizontal basalt flows of late Tertiary and Quaternary age compose the youngest bedrock formation in the region.

### **The Surficial deposits**

In the surveyed area, surficial deposits cover most of the bedrock and are most abundant in the large stream valleys. They are accumulations of terrigenous sediments of which few, if any, were marine deposited. The succession of surficial deposits is generally as follows, in the order of appearance:

- residual deposits composed chiefly of rather coarse rocky soil and rubble produced by weathering of bedrock
- gravel deposits made up of gravel and smaller amounts of sand and silt deposited by streams
- glacial deposits include till and outwash gravel
- silt deposits composed of massive buff-colored silt deposited largely by the wind
- flood-plain deposits made up of stratified silt and smaller amounts of sand and gravel along the larger streams

The thickness of the surficial deposits may only be estimated, because depths to bedrock, except in river cut-banks, have not as yet been determined. Some of the surficial deposits are possibly more than 100 feet thick. The surficial deposits are probably mostly of Quaternary age.

## Structural Geology

Geanticlines that were uplifted in the Mesozoic established the structural framework of Alaska, and mark the first phase of mountain building that has been fairly continuous since that time. The geanticlines extend southwestward in southwestern Alaska as finger-like projections of a much more extensive geanticlinal uplift, the Cordilleran geanticline of the western United States and Canada. The broadest of these, here designated the Alaska-Yukon geanticline, may be traced from the eastern part of the central Kuskokwim region northeastward into central Alaska, and thence eastward and southeastward into Yukon Territory (figure 3).

Most of the mountains of Alaska, with the exception of those formed by volcanic accumulation, attained their present altitudes by vertical uplift at various times in the middle and late Cenozoic, after folding. Connected with the mountain uplifts are extensive faults, many of which transect the geanticlinal framework in southwestern Alaska. One of these, the Farewell Fault, crosses the survey area in a northeast-southwest direction (figure 3).

The Farewell Fault may be traced southwestward on the aerial photographs to within 25 miles of the Stony River or about 80 miles from Farewell. It is generally believed that the fault probably accounts for an apparent southwestward offset in the contact between the limestones of the Holitna group along the axis of the Alaska-Yukon geanticline on the east, and the greywacke and shales of Kuskokwim group that overlap the western flank of the geanticline. The offset is believed to be produced in that area, on the western flank of the geanticline, by westward "down-dip" shift of the contact between the Holitna group and the overlying Kuskokwim group with progress of erosion, in response to uplift southeast of the fault.

## Petroleum Potential

Flysch of the Cretaceous Kuskokwim Group may underlie parts of the Holitna basin (Kirschner, 1994). Generally, this flysch is strongly deformed and extensively intruded. Overall, these Cretaceous flysch rocks are unlikely to have oil source or reservoirs rocks, or to provide a petroleum source for the overlying Tertiary fill.

According to the geological knowledge of the Holitna basin, Kirschner concluded that the area of the Holitna basin that could have 3 km or more of nonmarine Tertiary fill is less than 1 percent of the total basin area. Although coal-bearing beds in the basin could generate gas, and fluvial sandstones are likely reservoirs, the size of any accumulation would probably be small.

## 9.0 INTERPRETATION

The basic objective of this section was to produce an interpretation sketch map (figure 42) of the project area and a depth evaluation of the basement and of the observed magnetic anomalies. It contains:

- An analysis describing the geophysical signatures from gross geological features (section 9.1)
- An analysis of the Total-Field Magnetic Map (section 9.2)
- A qualitative interpretation of the total-field magnetic contours, first vertical derivative and shadow maps (section 9.3)
- Depth estimates from:
  - Spectral Analysis (section 9.4)
  - Automated profile analysis using EULER deconvolution (section 9.5)
- 2.5-D modelling of selected aeromagnetic anomalies and interpretation of available gravity data (section 9.6)

### 9.1 Magnetic signatures from some geological features

Magnetic anomalies can be produced by a number of causative features such as lithology changes, variations in the thickness of magnetic units, faulting, folding, and topographic relief. A significant amount of information can be obtained from a qualitative review of the residual total-field magnetic anomaly map. The aeromagnetic map, when interpreted, gives basic information about the geophysical properties of the rocks, which can enhance the geologic interpretation. Interpreted maps show magnetic and non-magnetic units, folds and faults which affect certain igneous, sedimentary and metamorphic rocks and intrusions. The value of the survey does not end with the first interpretation, but rather increases as more is discovered about the geology.

For a particular body, the inclination of the magnetic field, strike and dip of the body, will change the shape of the magnetic anomaly and the interpreter must have a mental image in order to relate magnetic anomalies to rock bodies. Figure 5 illustrates these phenomena.

Figures 6 to 14 show magnetic anomaly patterns over some causative geological features.

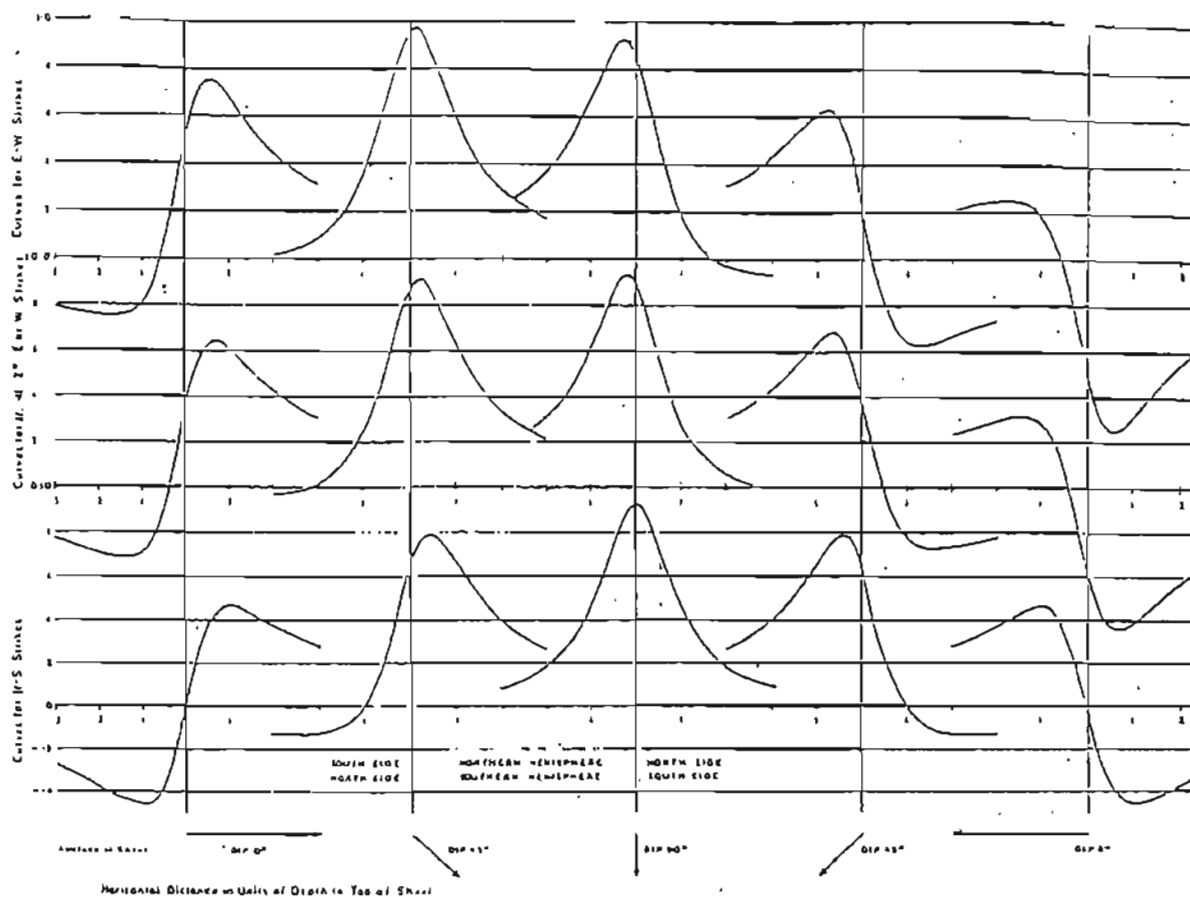


**FIGURE 5:**

**Magnetic anomaly shapes.** This diagram takes a particular body, the infinitely long thin sheet, and shows the anomaly shapes for different attitudes. The bottom of the diagram shows various dips. The three strips of anomaly profiles correspond to different strikes: N-S at the bottom, then NE or NW, and E-W at the top. With the steep inclination of the magnetic field, 75 degrees, the anomaly shape is not much changed by strike, but for lower inclination, the shape is drastically changed.

From: Reford, M.S., 1964. Magnetic anomalies over thin sheets, *Geophysics* vol. 29, p. 532-536.

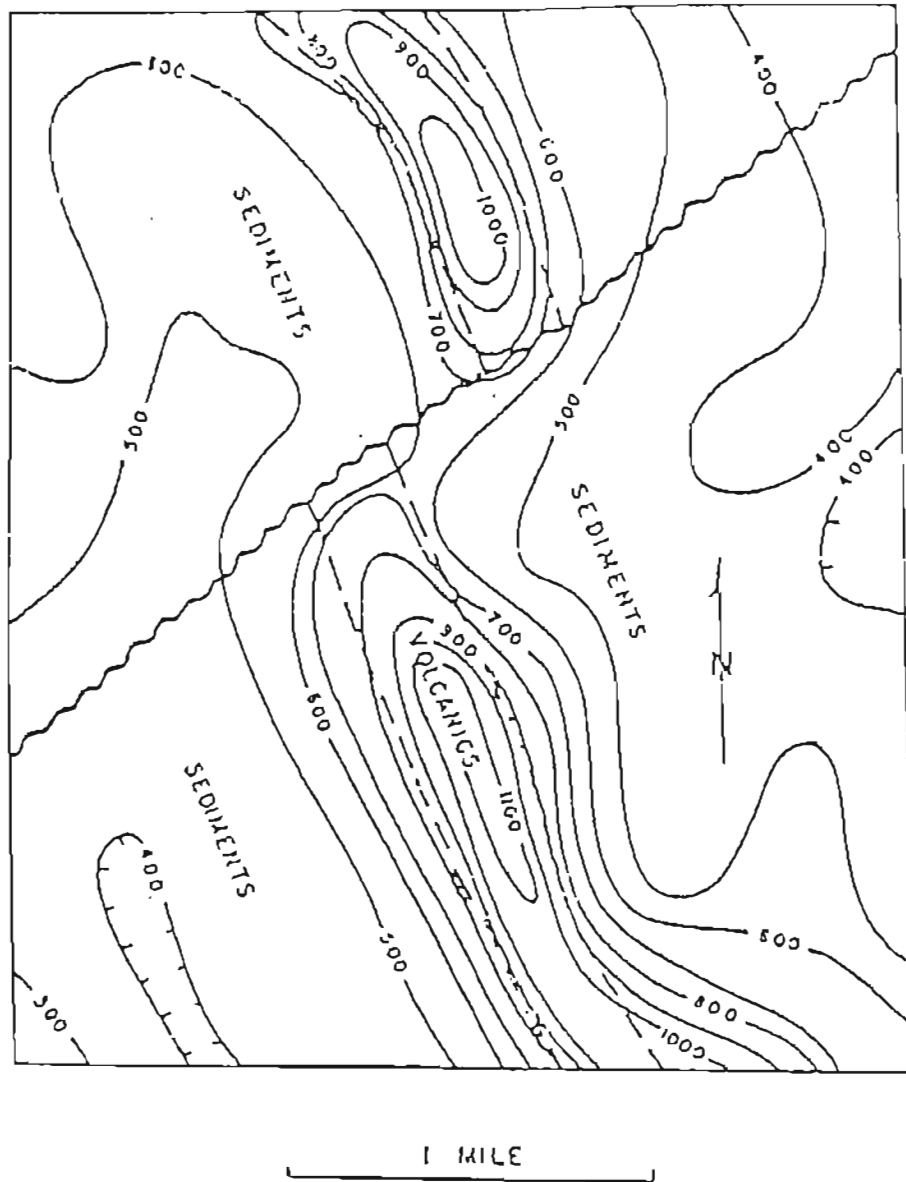


FIGURE 6

Fault in the underlying rocks (1). The abrupt horizontal displacement of magnetic contours is indicative of a fault.

From: Methods and Case Histories in Mining Geophysics. 6th Commonwealth Mining & Metallurgical Congress, 1957. p. 30-33.

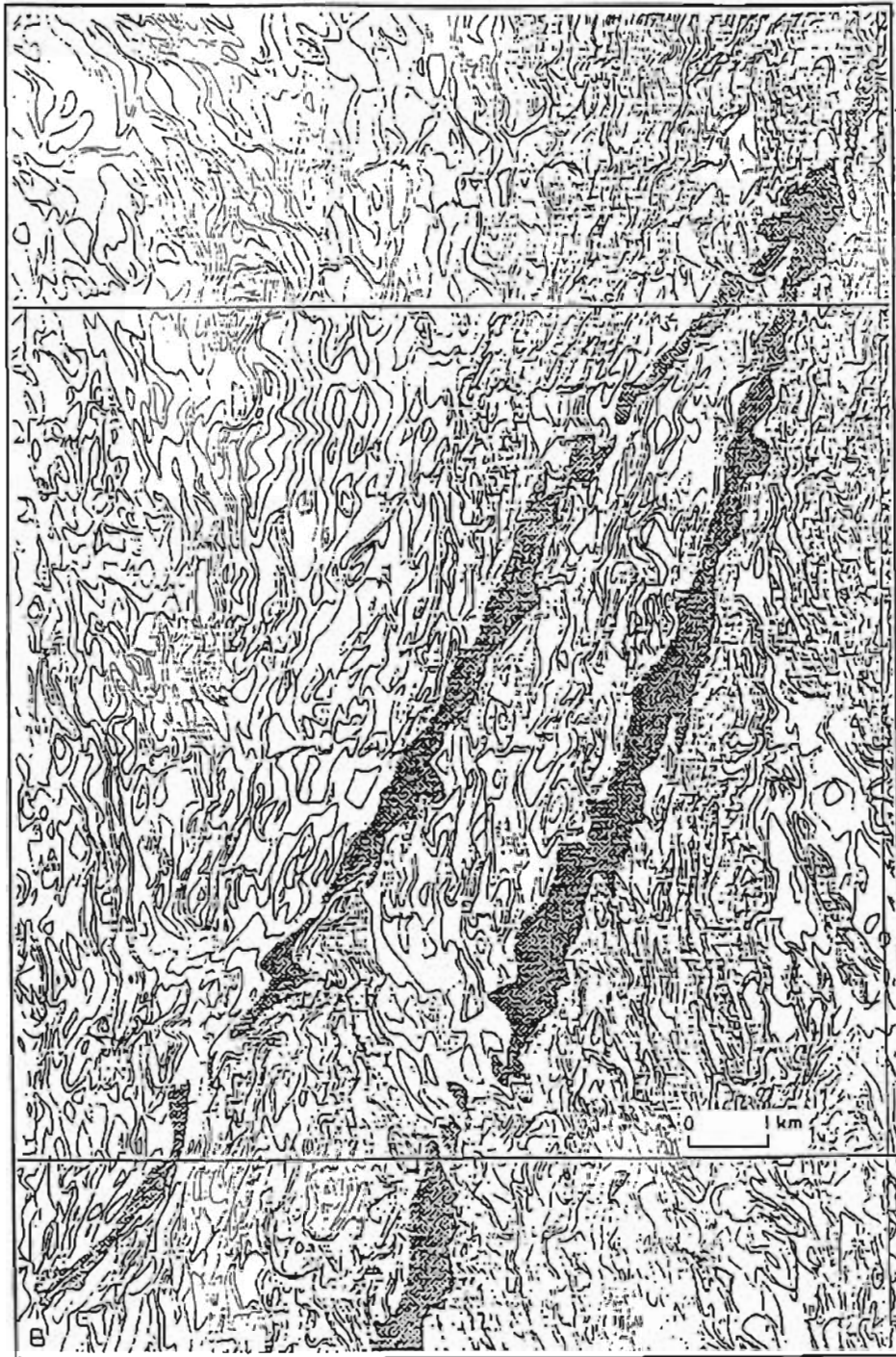
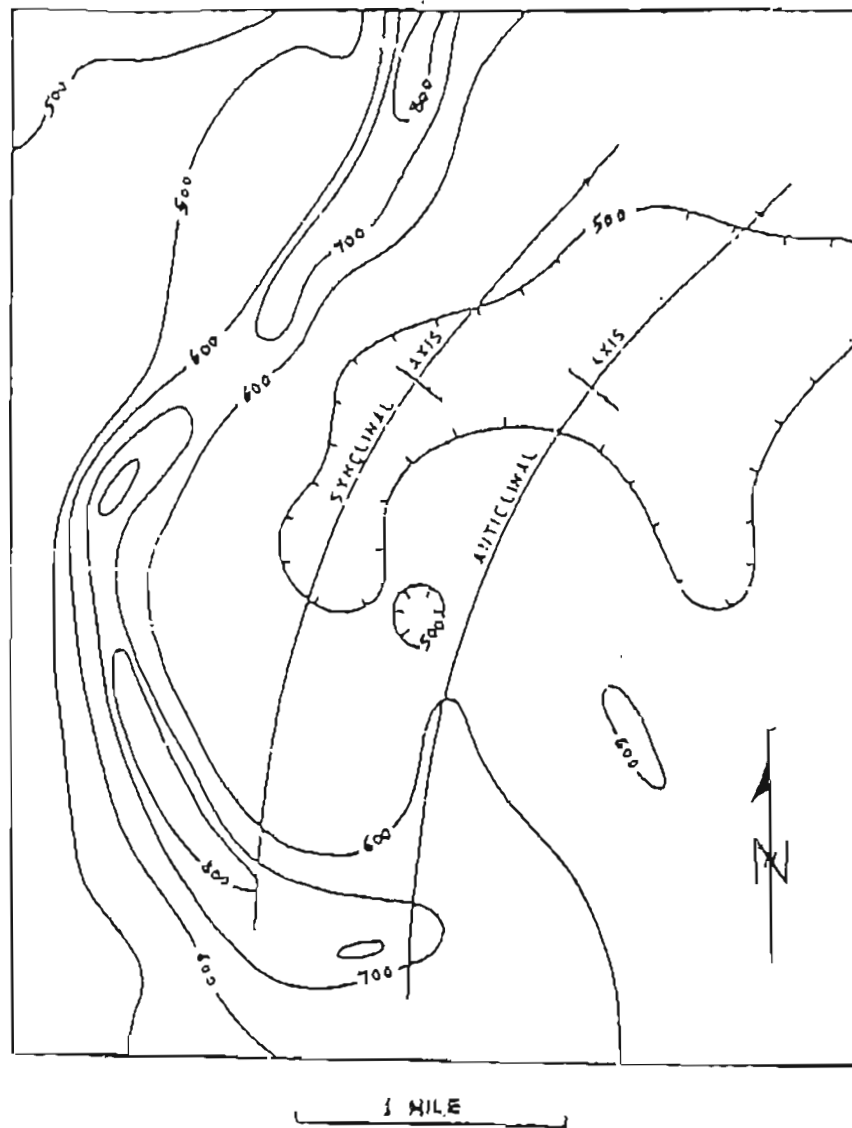


FIGURE 7 Fault in the underlying rocks (2). The linear magnetic minima are related to faults. The magnetization is believed to be reduced through oxidation and hydration from water percolation along the faults (map area 28 J NE).

From: Henkel and Guzman, 1977. *Geoexploration*, vol 15, p. 173-181.



**FIGURE 8** Belt of volcanic rocks. Aeromagnetic contours outlining a belt of basic volcanic rocks, to the left.  
From: *Methods and Case Histories in Mining Geophysics*. 6th Commonwealth Mining & Metallurgical Congress, 1957. p. 30-33.

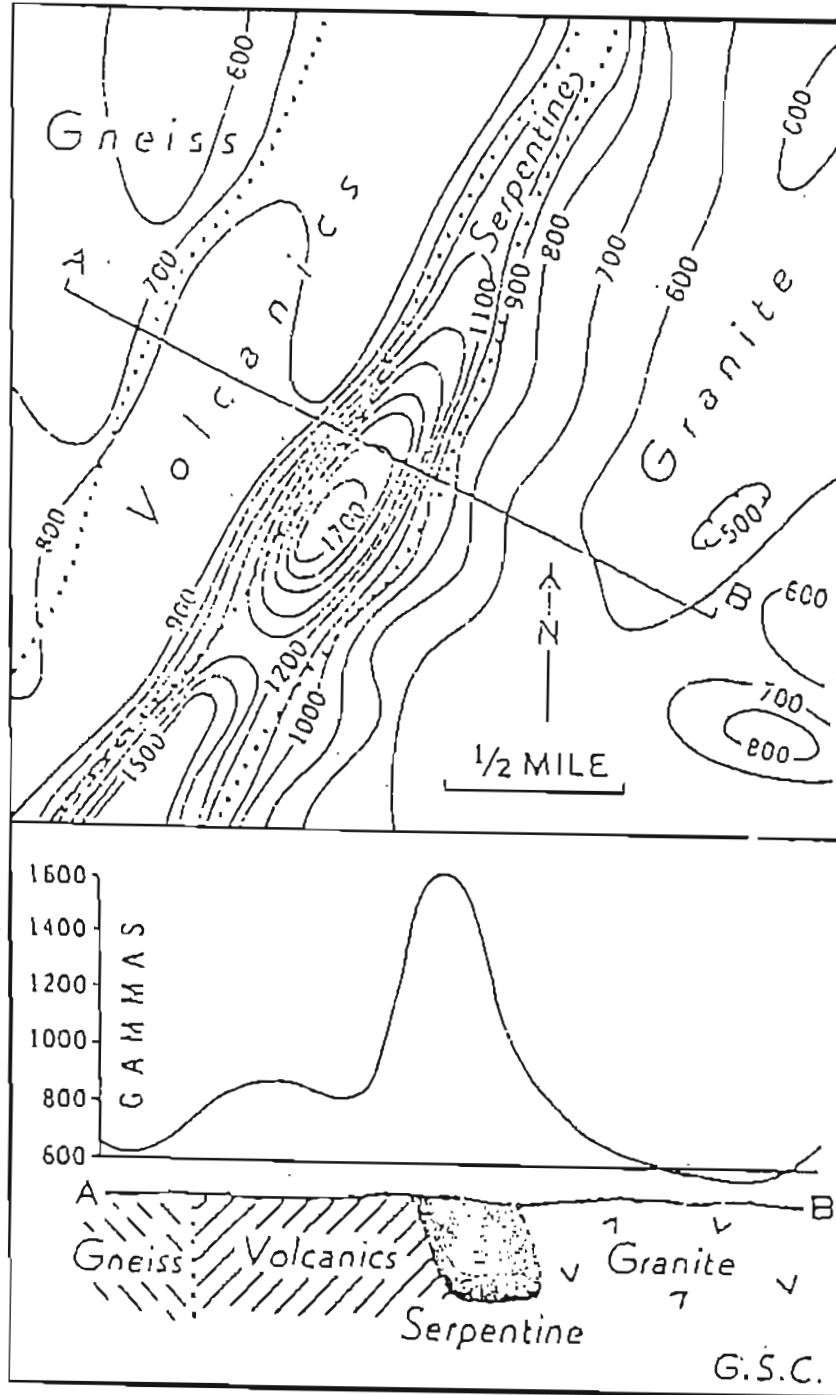
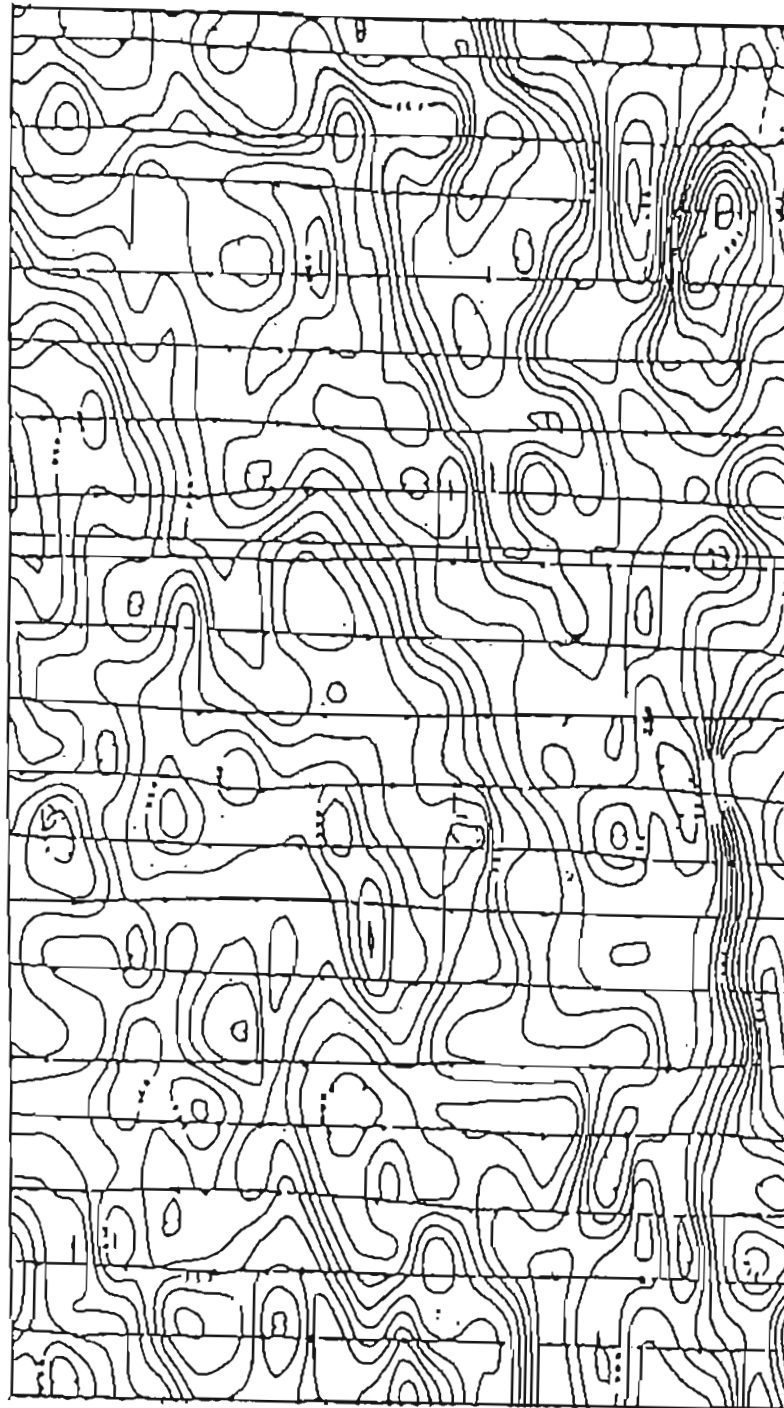
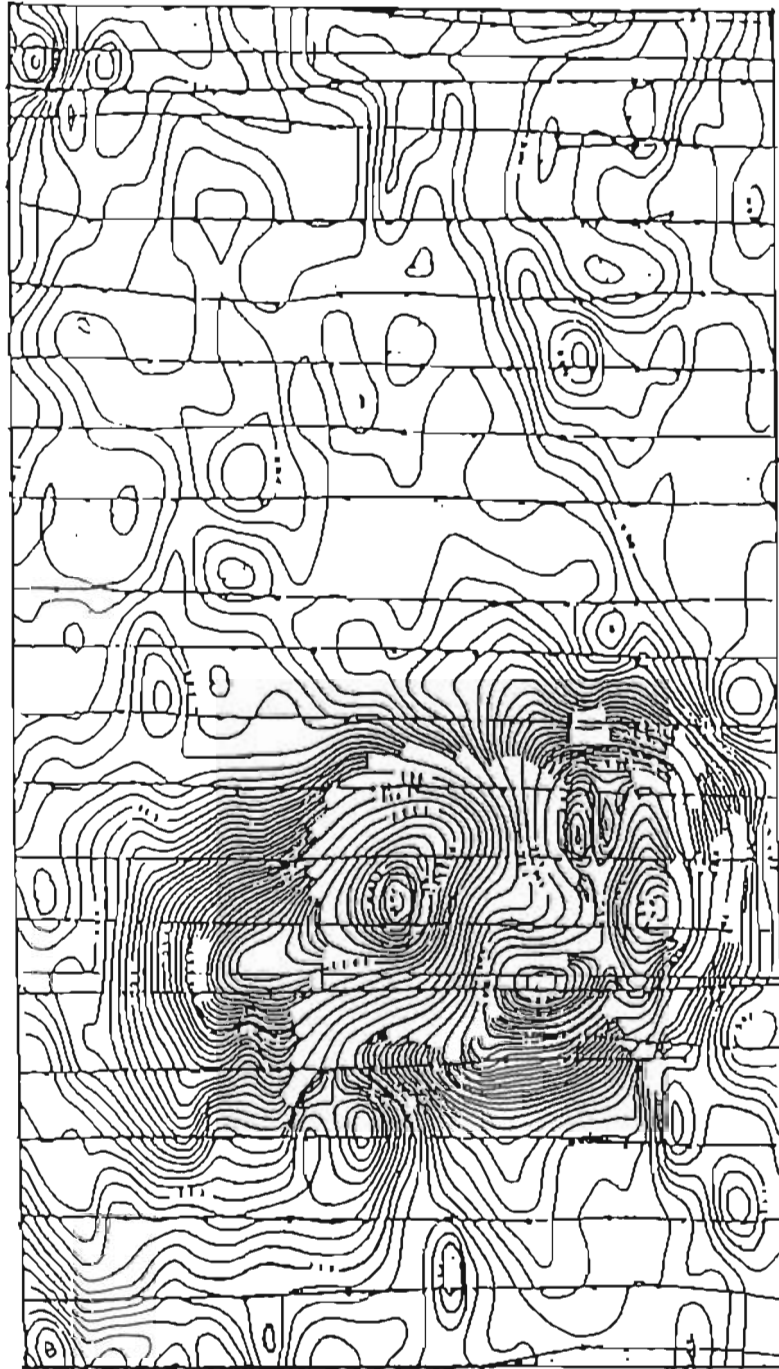


FIGURE 9 Serpentinized peridotite sill. Plan and profile showing the magnetic field over a serpentized peridotite sill in Newfoundland. From: Methods and Case Histories in Mining Geophysics. 6th Commonwealth Mining & Metallurgical Congress, 1957. p. 30-33.



**FIGURE 10: Gneissic terrain.** An area of low magnetic relief with only vaguely defined strike directions. This is typical of the magnetic expression of a granitic or gneissic terrain. If this pattern were intensified, it could easily represent a greenstone signature. Greenstone creates an intensely distorted, dipolar magnetic signature.

From: Reeves, C.V., 1978. Geological Survey Department, Botswana.



**FIGURE 11** Discordant intrusive (1). A clear example of a highly magnetic discordant body intruded into an area of relatively low magnetic relief. This is interpreted as a basic or ultrabasic intrusive, some 15 km in diameter, intruded into an area of granitic gneiss. To the north-west of the intrusive, there is a possible extension of the magnetic body at depth, within the basement  
From: Reeves, C.V., 1978. Geological Survey Department, Botswana.

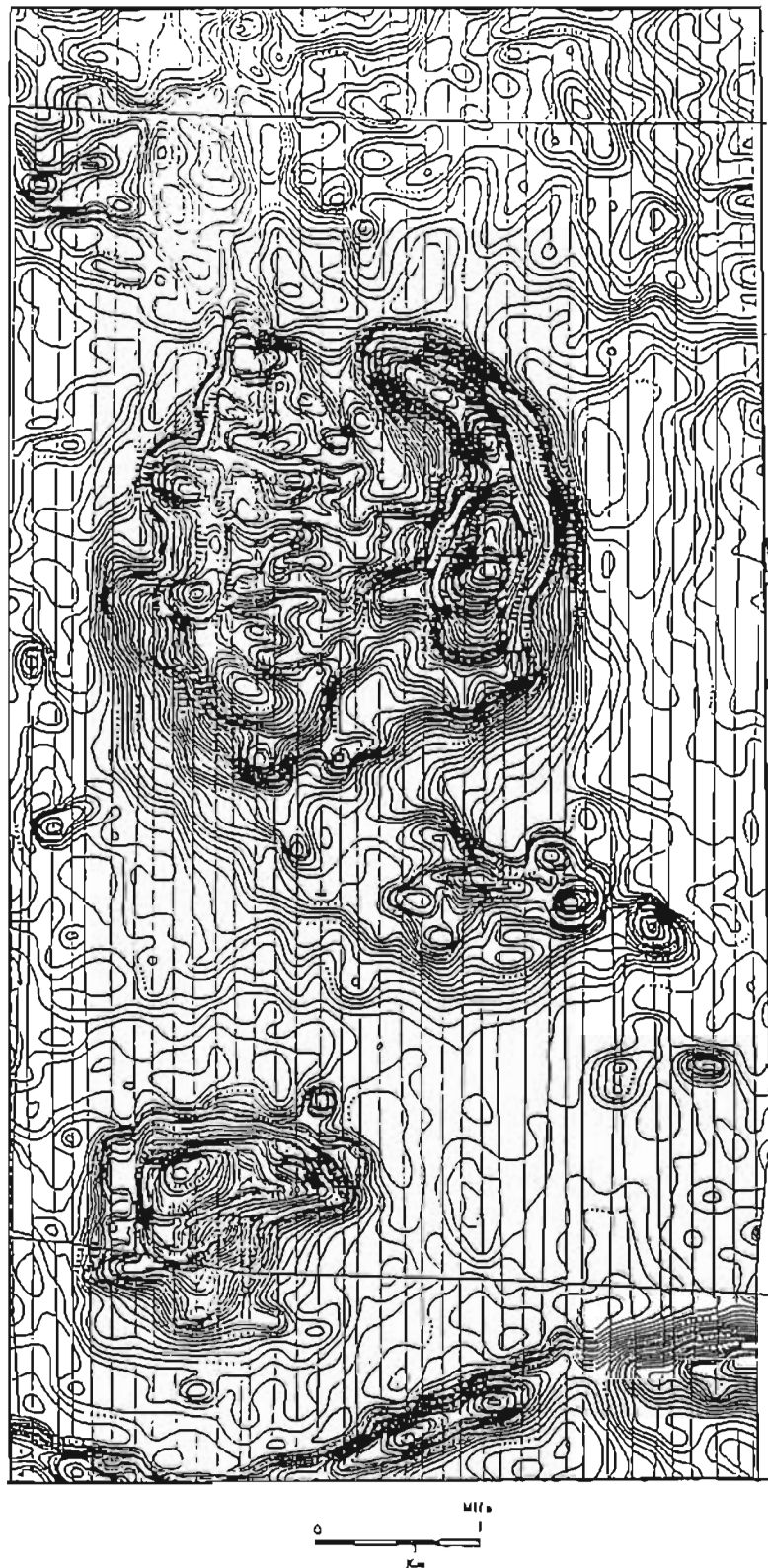


FIGURE 12 Discordant intrusive (2). A Canadian Carbonatite complex located north of Kapuskasing (Flight altitude 150 feet above ground level, traverse interval 1/8 mile).

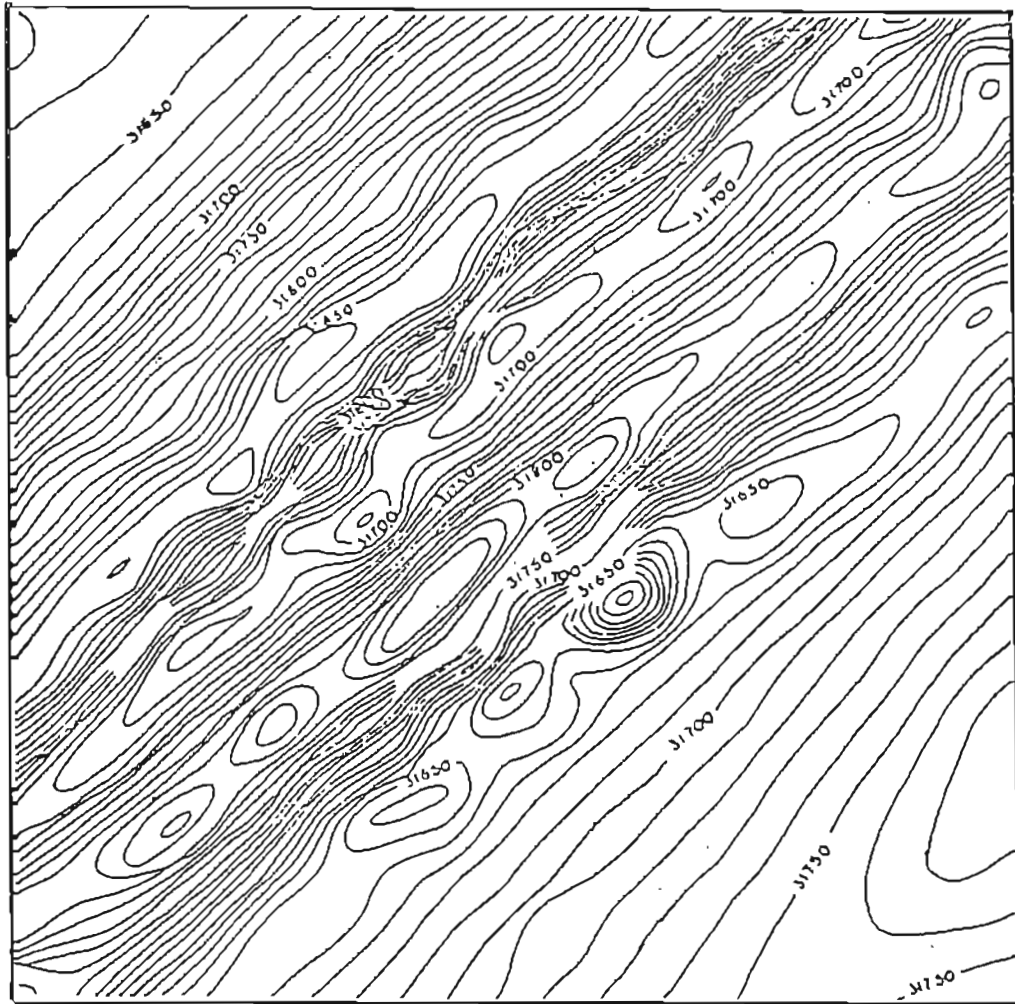


FIGURE 13 Weakly magnetic metasediments. Magnetic metasediments are illustrated by linears with localized zones of higher magnetic response - here the Meguma terrane of Eastern Nova Scotia. From: Brant and Fuller, 1978. Geophysical Exploration and Problems in Metamorphic Terranes - in Mineralization in Metamorphic Terranes (ed. W.J. Verwoerd, Pretoria), p. 7-40.

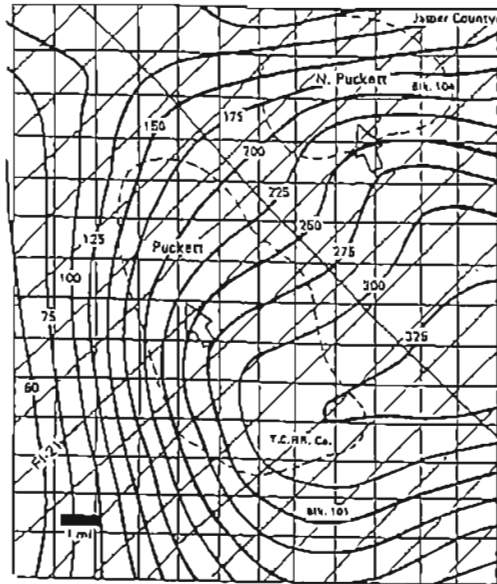


FIGURE 14-A

Puckett Field. The airborne magnetic survey (one mile flight line spacing) shows a very extensive and steep gradient on the westerly side and an irregular high nose in the central part of the map.

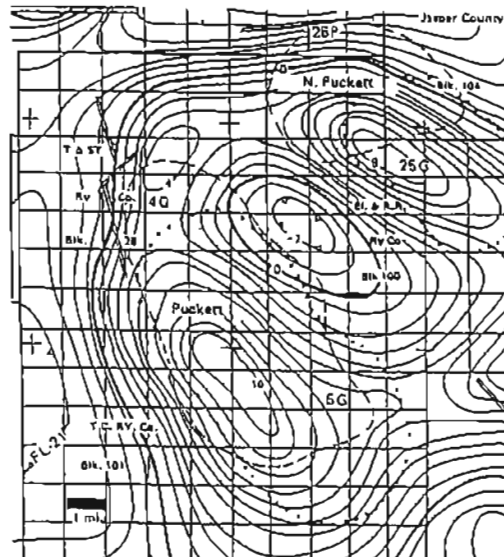


FIGURE 14-B

Puckett Field. The second-vertical-derivative map develops the local anomalies and shows a large closed maximum in the southwesterly part of the map and a smaller closed positive anomaly to the northeast.

FIGURE 14

Magnetic Mapping of an Oil Field. The Puckett Field, Pecos County, Texas. (From Steenland, N.C., 1965. *Oil Fields and Aeromagnetic Anomalies*. *Geophysics*, vol.30, no.5, pp.706-739.

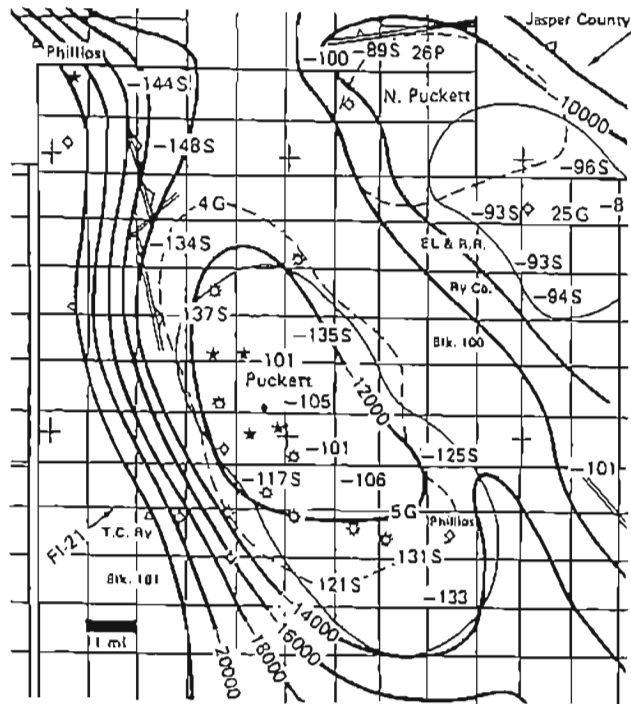


FIGURE 14-C Puckett Field. Magnetic basement map. Contour interval 2000 ft with possible local structures and oil fields indicated by dashed lines.

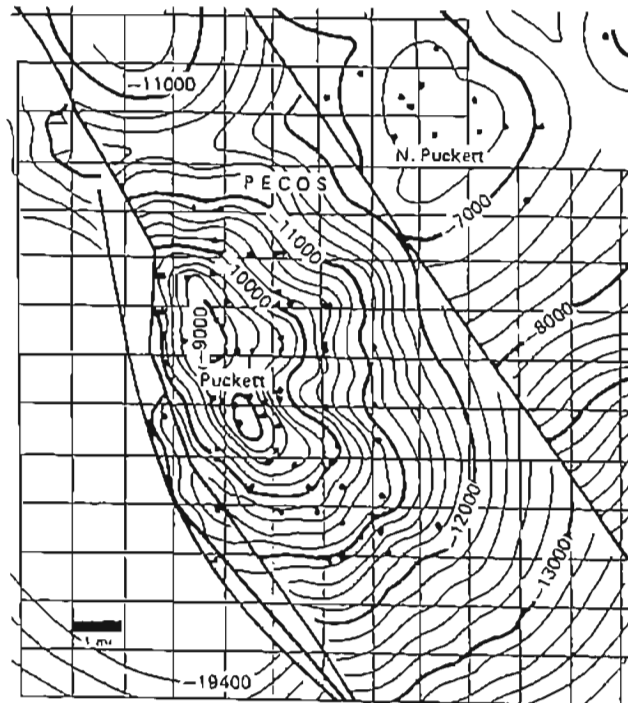


FIGURE 14-D Puckett Field. Subsurface contours showing structure from drilling.

## 9.2 Analysis of the Total-Field Magnetic Map

The maximum variation of the magnetic field seen on the total field magnetic map over the survey area is 682 nT, ranging from 54670 nT to 55352 nT. On the residual field (IGRF removed), this variation is lowered to 349 nT, ranging from 54788 nT to 55137 nT.

In general, most of the prominent higher amplitude anomalies (100 nT or more) are related to shallow intrusive bodies and volcanics while other anomalies associated with magnetic basement are on the order of 100 nT or less.

The prominent orientations of magnetic trends are in a N70°E direction. However, in the northern part of the survey area, expressions of N30°E trends are also significant.

In general, the magnetic anomalies can be divided into three categories on the basis of their wavelength and the reciprocal frequency or wavenumber (low, medium and high). On the average, low wave number anomalies have half wavelengths (peak to trough distances) of greater than 20,000 feet (approximately 6 km), medium wavenumber anomalies exhibit half wavelengths on the order of 5,000 to 20,000 feet and high wavenumber anomalies have half wavelengths less than 5,000 feet.

Characteristically, low wavenumber anomalies are related to the basement, medium wavenumber anomalies are related to intrusive and basement, and high wavenumber anomalies are related to volcanic rocks, intrusive rocks and other shallow geologic sources.

Based on the wavenumber, amplitude and characteristic patterns of the anomalies, an inspection of the total field magnetic map suggests the following points:

- High wavenumber and high amplitude anomalies are predominant at

- several locations of the map
- Approximately northeast-southwest trending fault systems
- Intrusive bodies are distributed throughout the survey area and are often recognizable by their high amplitudes and distinct circular patterns
- Volcanic and intrusive zones are predominant on the eastern portion of the survey area.

### 9.3 Qualitative Interpretation

The high resolution aeromagnetic data over the survey area were obtained at a constant terrain clearance of 300 feet (91 meters) utilizing a high sensitivity split beam cesium vapour magnetometer in an on-board "tailstinger" installation. The raw field data, in digital form, were subsequently edited, corrected for earth's field regional and diurnal variations, adjusted to remove datum level differences (IGRF), gridded and contoured. The data (residual) were then presented in color contours of the total-field, first derivative (gradient) and shadow maps. These maps were finally used for the generation of the interpretation sketch map presented at a scale of 1:500,000 at figure 42. Displayed on the interpretation sheet are magnetic sources and volcanic horizons both more shallow than the basement surface, structures (faults), intrusive bodies, dikes and areas of possible structural disturbance within the sedimentary section, and the basement depth obtained from the Euler depth interpretation (section 9.6).

Based on the characteristic patterns of the magnetic total field, an inspection of the magnetic maps suggests the following points:

- The prominent orientations of magnetic trends are in N70°E and N30°E directions
- The magnetic pattern is characterized by a series of magnetic highs along the Farewell fault. The Farewell fault is oriented N65°E
- An interesting north-south trend of highs is observed crossing the Farewell fault in the centre of the survey area
- A major magnetic high located along the Farewell fault corresponds to the dominant gravity low

- Mafic dikes are recognizable by their high amplitudes and distinct elongated patterns
- A round-shaped magnetic pattern is observed in the centre-south of the area. This feature represents probably a batholith present in the bedrock.

#### 9.4 Spectral Analysis

A grid of aeromagnetic data is a discrete representation of a continuous function. The frequency content of a data grid can be described in terms of spatial frequency in units of radian/sampling interval or as its wavenumber in units of cycles/sampling interval. From the fundamental sampling theorem (Hall, 1979) it can be shown that the highest resolvable wavenumber, called the Nyquist wavenumber, that can be expressed in a square grid is equal to one half of the grid spacing (in our case, 200 m). The Nyquist wavenumber is important because any higher wavenumber in the measured field will be reflected, or aliased, back into the frequency spectrum as a lower wavenumber. The possible range of wavenumber on a grid is therefore from 0, for an non-oscillating or constant component, to 0.5 cycles/grid cell, the Nyquist wavenumber.

The grid of data can be transferred to the spatial frequency, or wavenumber domain, by the application of a 2-dimensional Fourier Transform to the data. All of the information in the original grid is present in the transformed frequency domain grid but it is described in terms of its component frequencies instead of position. In practice the transform is done using faster algorithms called the fast Fourier Transform (FFT). The complex wavenumber spectrum  $F(u,v)$ , which results from the application of a Fourier Transform, can be analysed more easily by calculating the energy spectrum:

$$E(u,v) = a^2 + b^2$$

where:                     $a$  = real part of  $F(u,v)$  containing amplitude information  
                                $b$  = imaginary part of  $F(u,v)$  containing phase information

The energy spectrum  $E(u,v)$  shows the spectral energy distribution of the data in terms

of its wavenumber composition.

The power spectrum of airborne magnetometer total field data can be used to determine average depth values to buried magnetic rocks (Spector, 1967; Spector and Grant, 1970; Battacharya, 1966). These depths are established from the slope of the log-power spectrum at the lower end of the total wavenumber, or spatial frequency band. The method is based on the assumption that the magnetic effect of the basement surface can be simulated by an uncorrelated distribution of blocks of varying depth, width, thickness, and magnetization. On the log-power spectrum plot, if a group of blocks has a similar depth, they will fall into a line of constant slope. Thus, if there are groups of blocks with the individual groups at widely different depths, such as shallow volcanic over a deep basement, the plot will be separable into parts with different slopes and the magnitude of the slope is a measure of depth.

The method has its application primarily to evaluation of general conditions over broad areas and to give relatively objective separation of the sharp and broad anomalies in such a way that multiple depth zones could be recognized. It is not applicable to determination of depths to individual anomalies, as used for mapping a basement surface, but give an objective confirmation of the general depth of such a surface.

## **Results**

The survey area was first divided in six blocks (figure 15). The spectral analysis was then applied to each block in order to obtain six power spectrum (upper part of figures 16 to 21) and six estimated maximum depths (lower part of figures 16 to 21). On each power spectrum, we observe that the Nyquist wavenumber, which depends on the grid cell dimension, is equal to 5. From the lower end of the total wavenumber plots, we obtains the maximum depths of each blocks:

-NW 4.7 km  
-NC 4.0 km  
-NE 4.1 km  
-SW 6.3 km  
-SC 5.5 km  
-SE 5.0 km

In conclusion, the maximum depth to the basement is of the order of 4.0 to 6.3 kilometers.

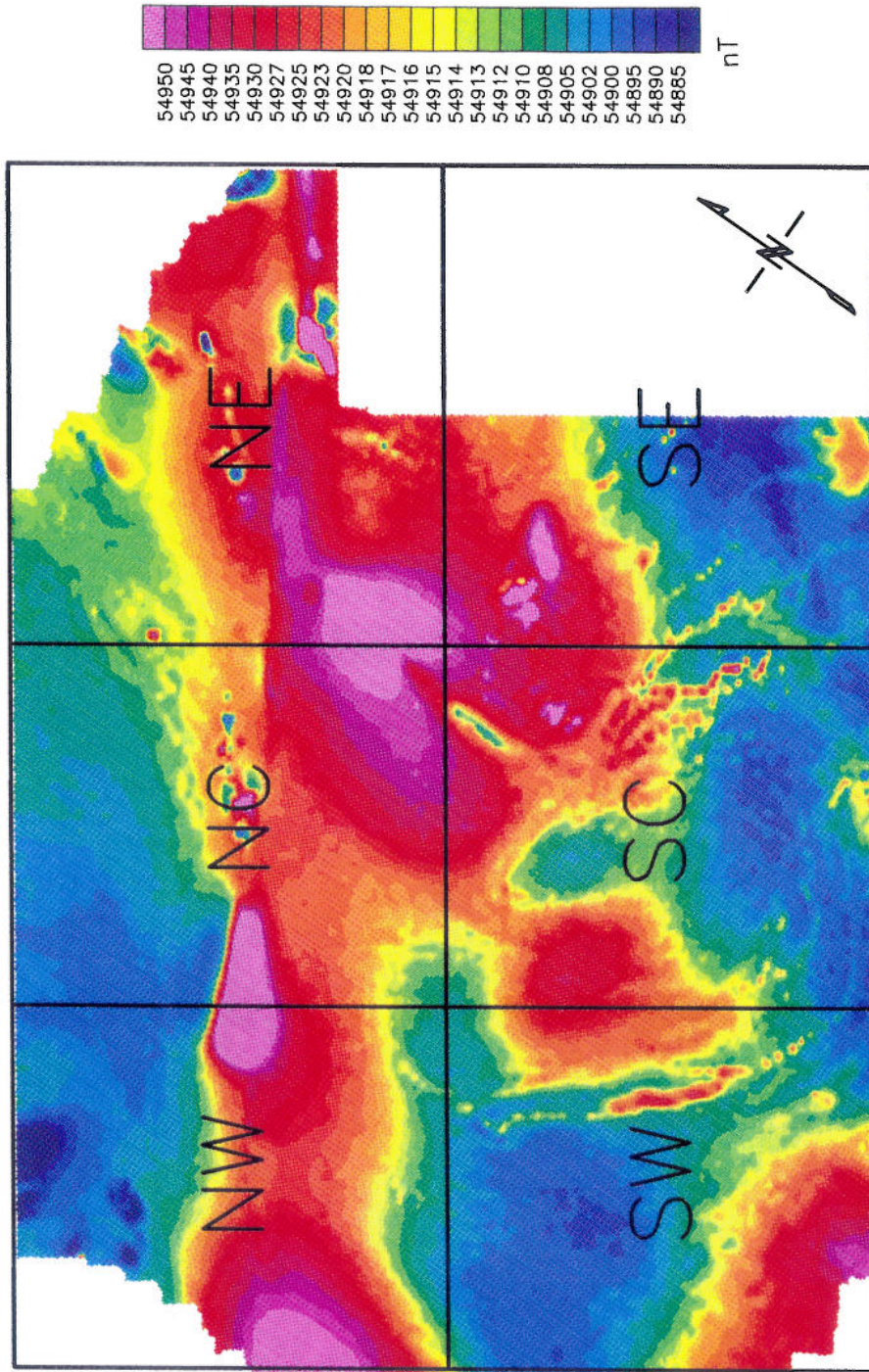
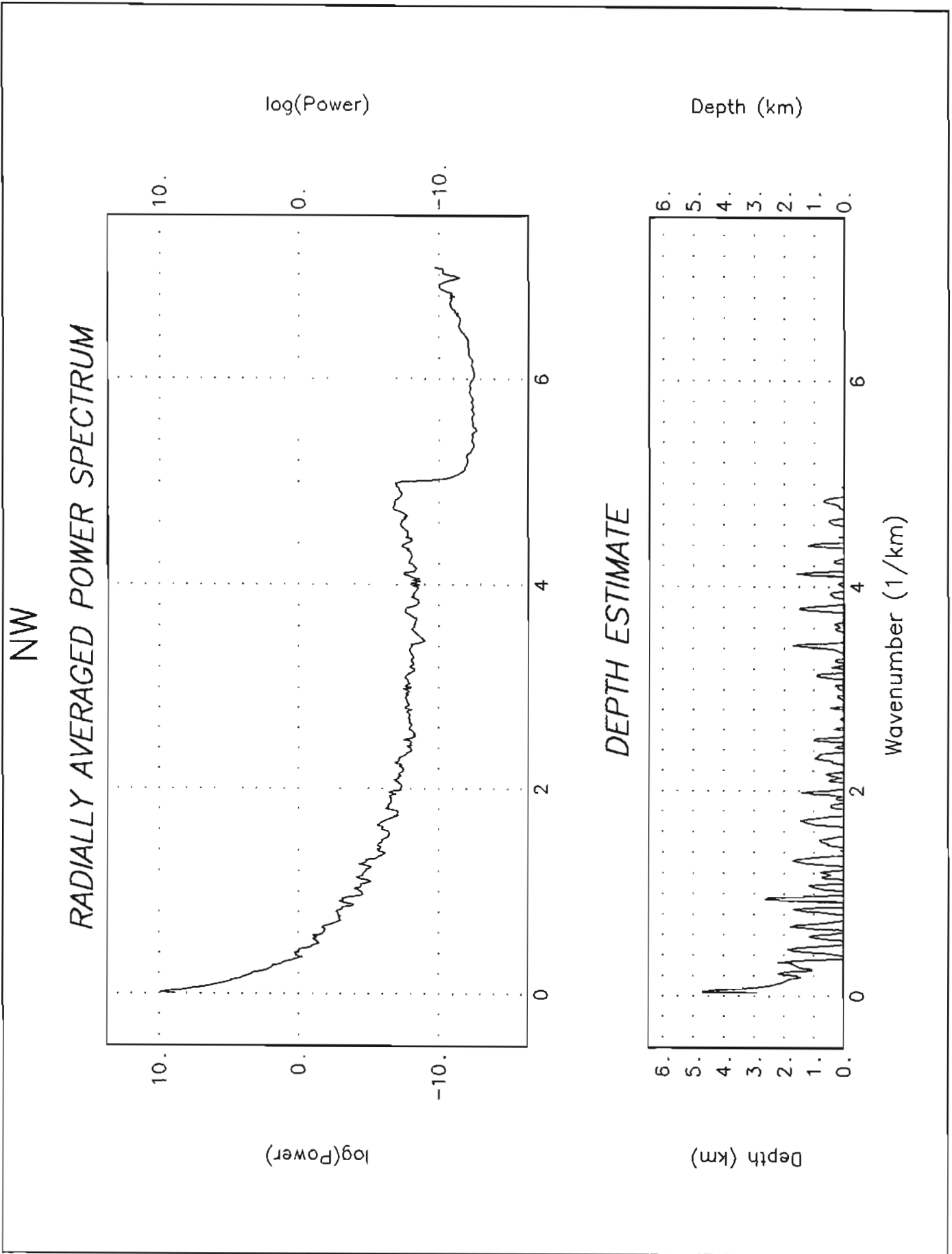
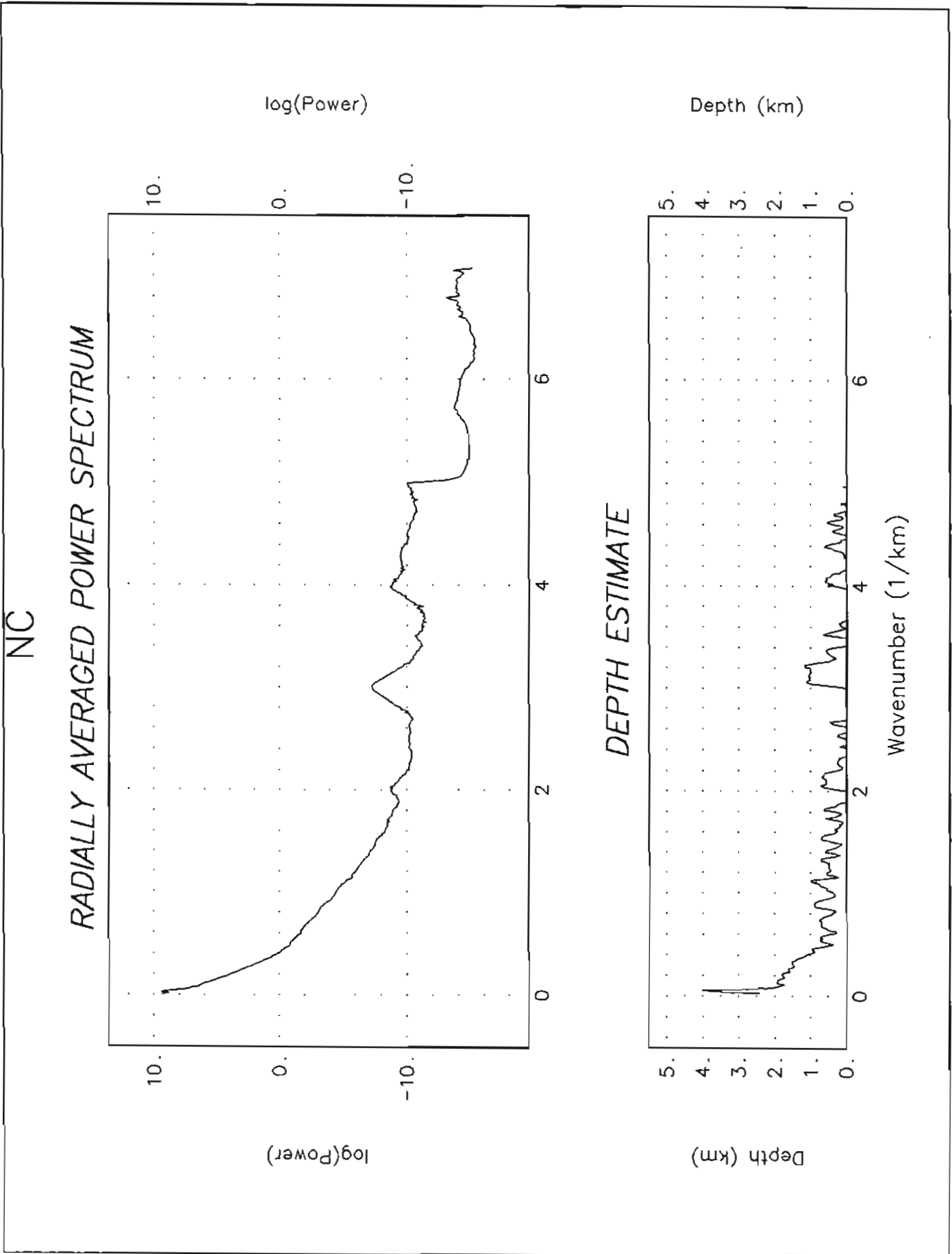


FIGURE 15: The residual magnetic field  
(the survey area divided in six blocks)



**FIGURE 16: Power Spectrum for the North-West part of the survey area**



**FIGURE 17: Power Spectrum for the North-Centre part of the survey area**

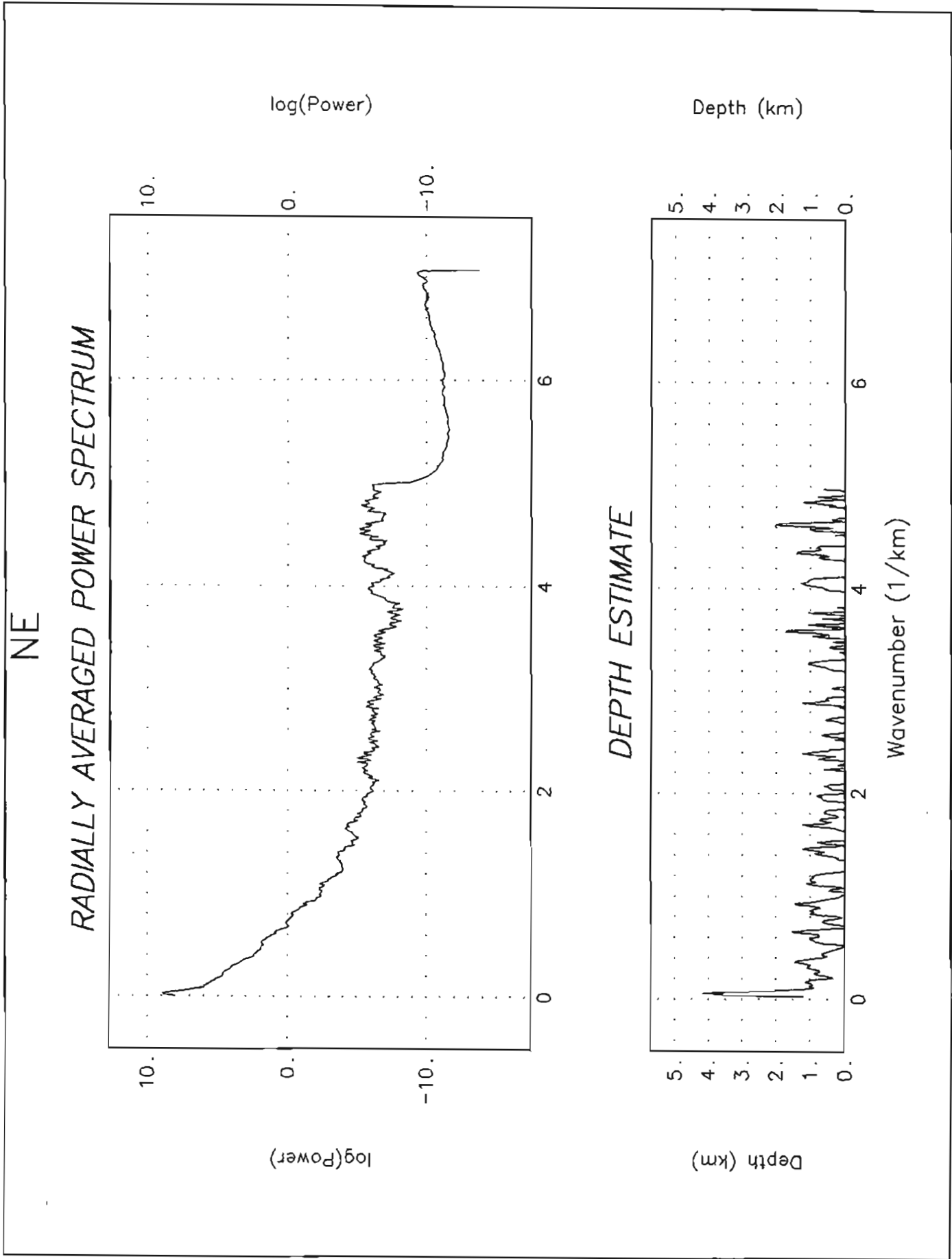


FIGURE 18: Power Spectrum for the North-East part of the survey area

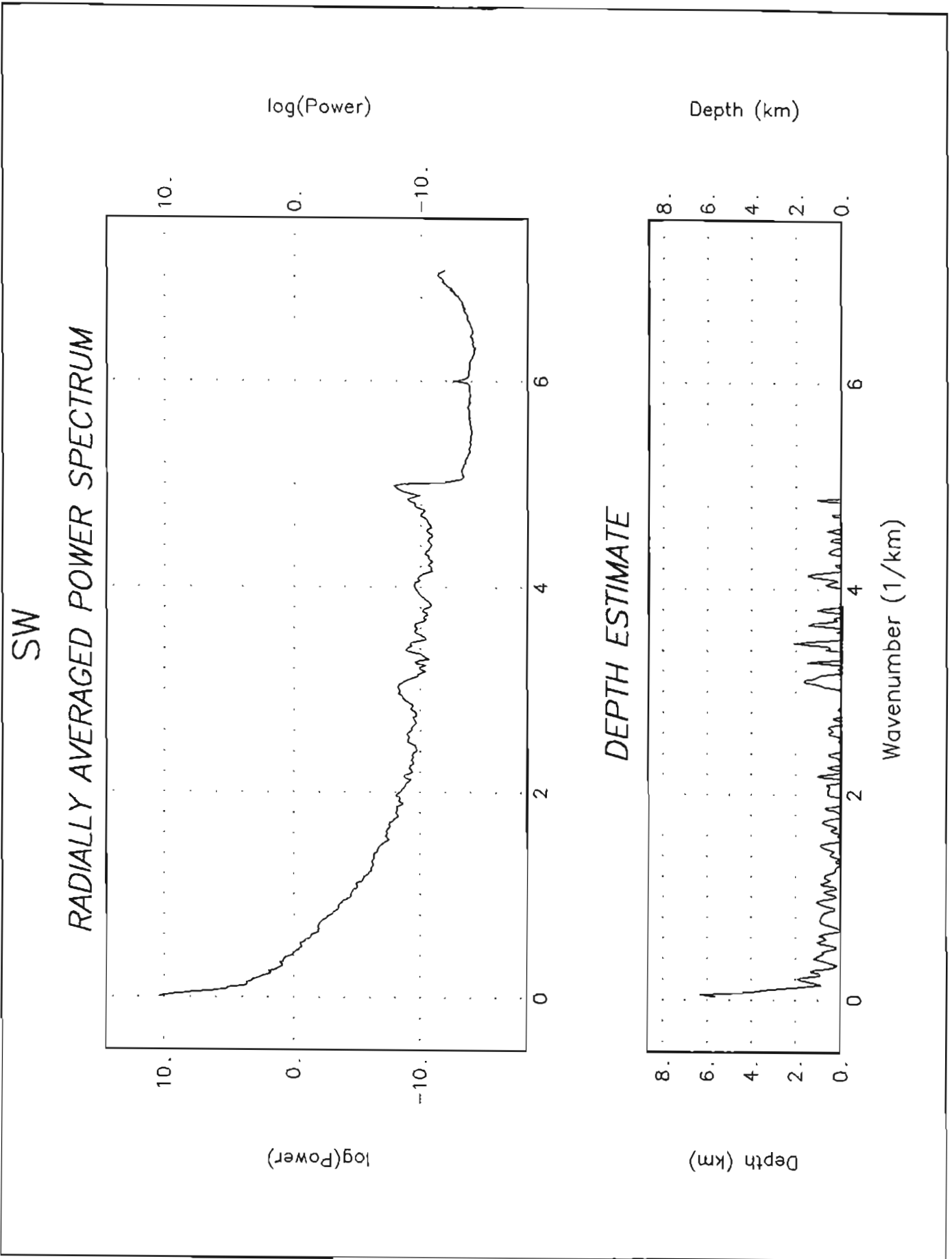


FIGURE 19: Power Spectrum for the South-West part of the survey area

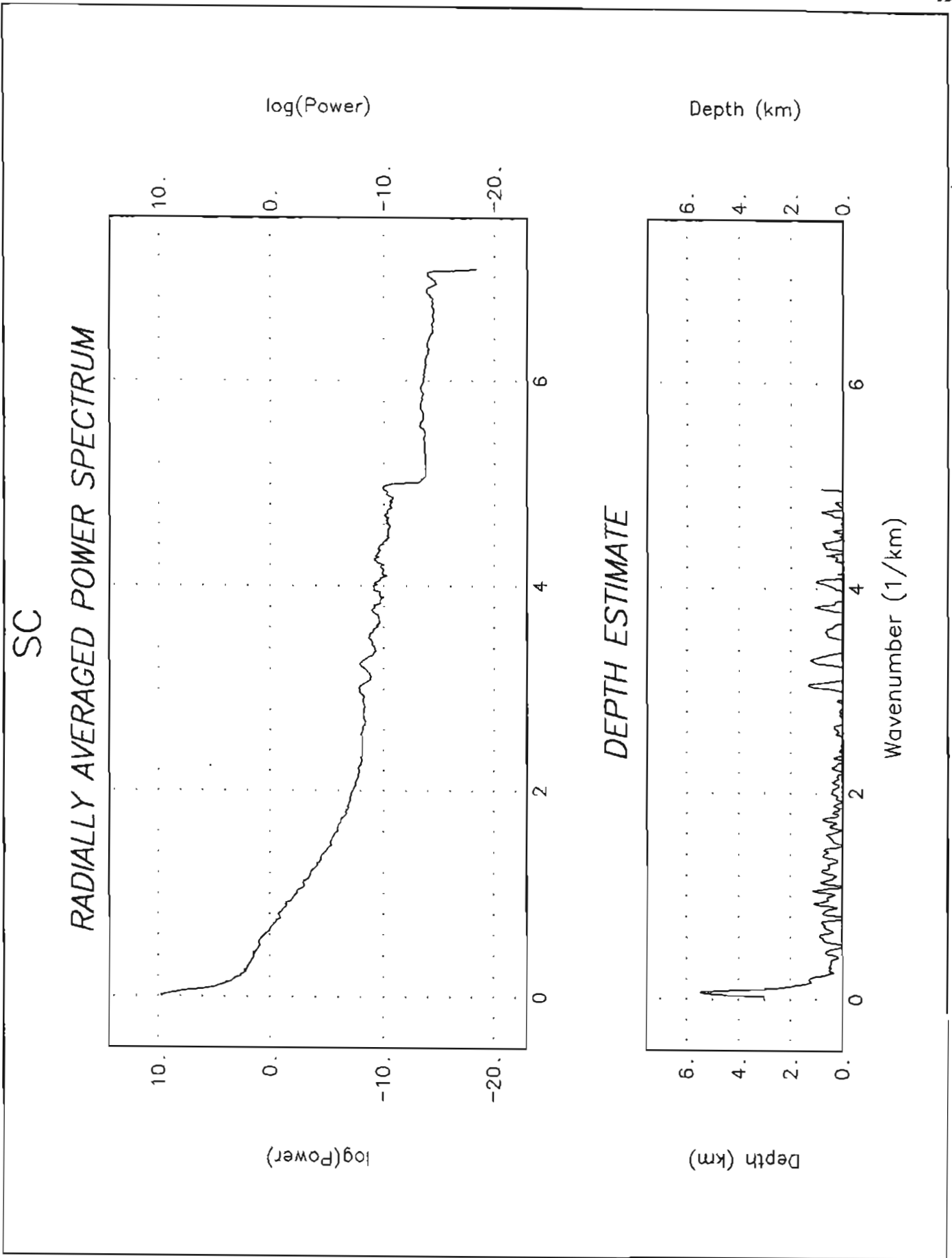
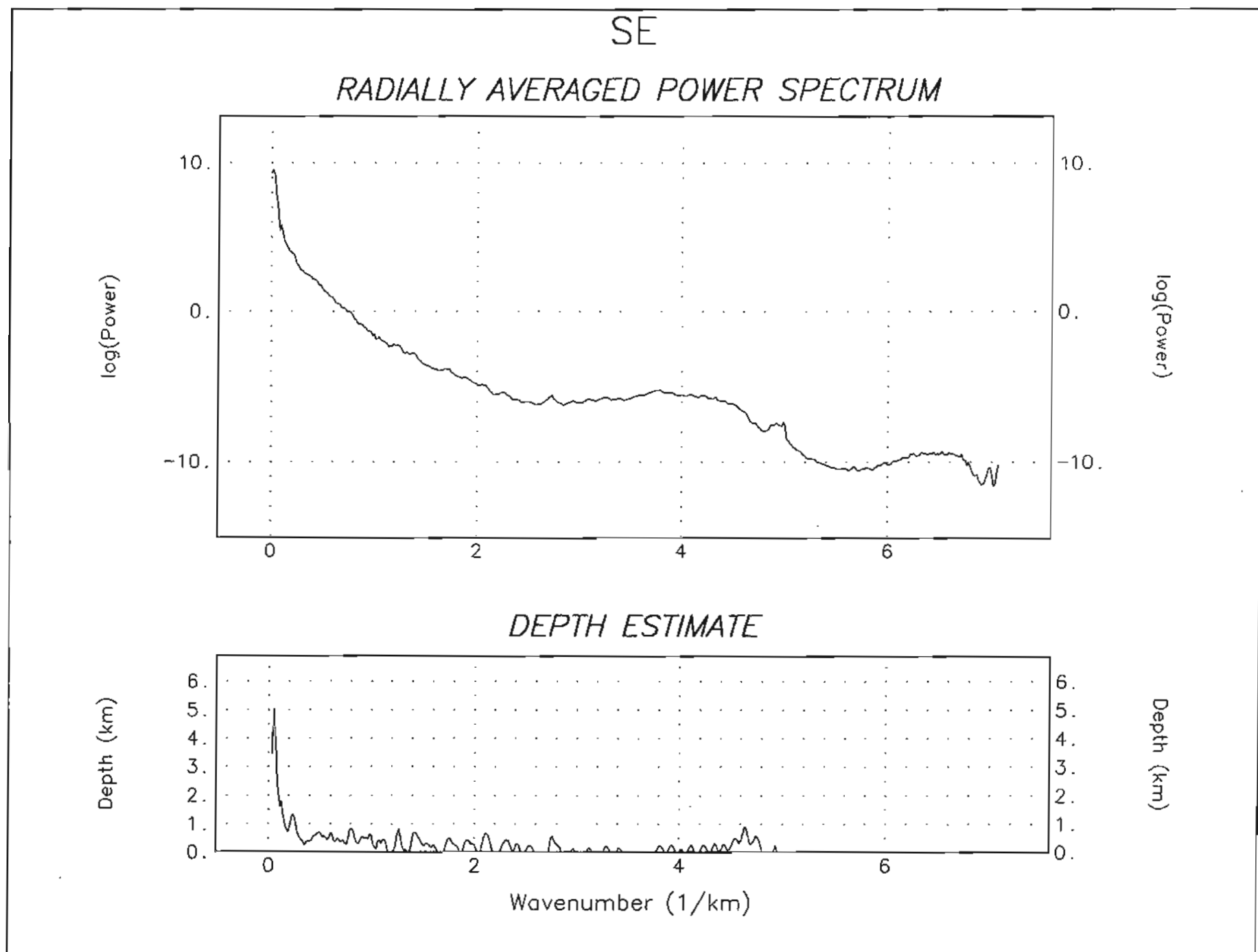


FIGURE 20: Power Spectrum for the South-Centre part of the survey area



**FIGURE 21: Power Spectrum for the South-East part of the survey area**

## 9.5 2.5-D Modelling

The interactive computer program used to model the magnetic and gravity anomalies is of the curve-fitting type. To represent anomalous geological bodies, the computer program uses the two-dimensional  $n$ -sided polygonal model of Talwani and Heirtzler (1964) modified for finite strike (2.5 dimensional body) length using mathematical expressions developed for the magnetic case by Shuey and Pasquale (1973, eq.19, p.510), and for the gravity case by Rasmussen and Pederson (1979, eq.8, p.753). Modifications to the model(s) to improve the fit of the calculated to the observed anomaly are performed either manually, or in a partial automatic mode using the non-linear least-squares method of Powell (1965).

The modelling program, MAGIX-XL, used to create magnetic models of 14 traverses, and gravity models of two traverses, which are all located on figure 22, has been developed by Interpex Ltd (Colorado). The traverses were selected to optimize the modelling. The intent was to estimate basement depth and structure. The results are shown on figures 23 to 38. The gravity profiles (figure 37 and 38) were interpolated from data downloaded from the USGS.

Since neither magnetization or gravity contrasts are known, it was necessary to use the assumption of minimum complexity for the modelling. That is, wherever possible, a constant magnetization, which was allowed to adjust to give a best fit, was used on any given profile. In addition, the fewest number of vertices necessary to adequately represent the data were inserted. The resulting depth surface therefore represents the simplest surface that can satisfy the data, with a uniform basement magnetization (magnetic susceptibility contrast varying between 0.0005 and 0.0016 in CGS units). Further study or information, such as drill hole data or magnetization values will therefore result in some changes to the model.

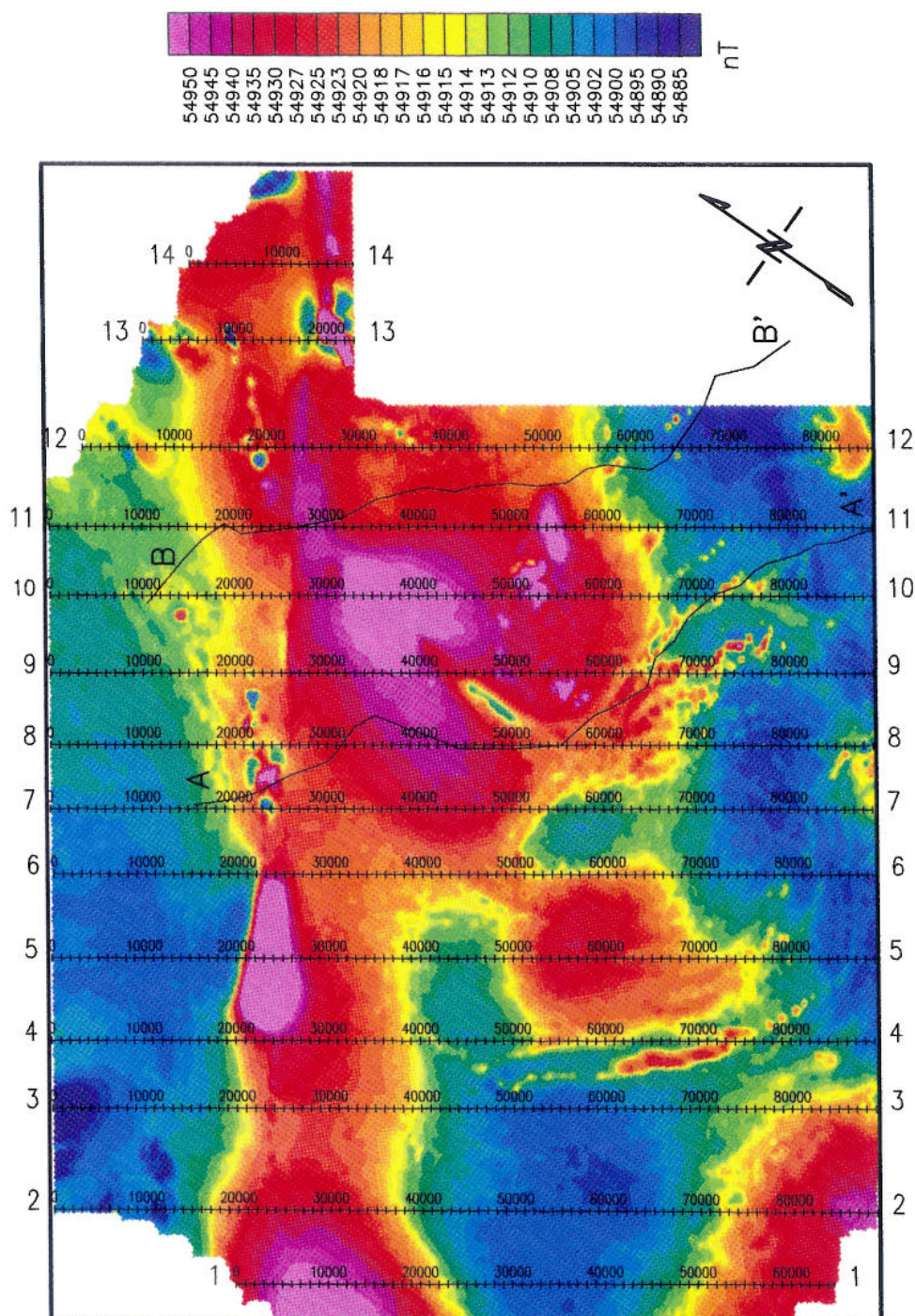


FIGURE 22: Location of the 2.5-D modelled magnetic and gravity profiles

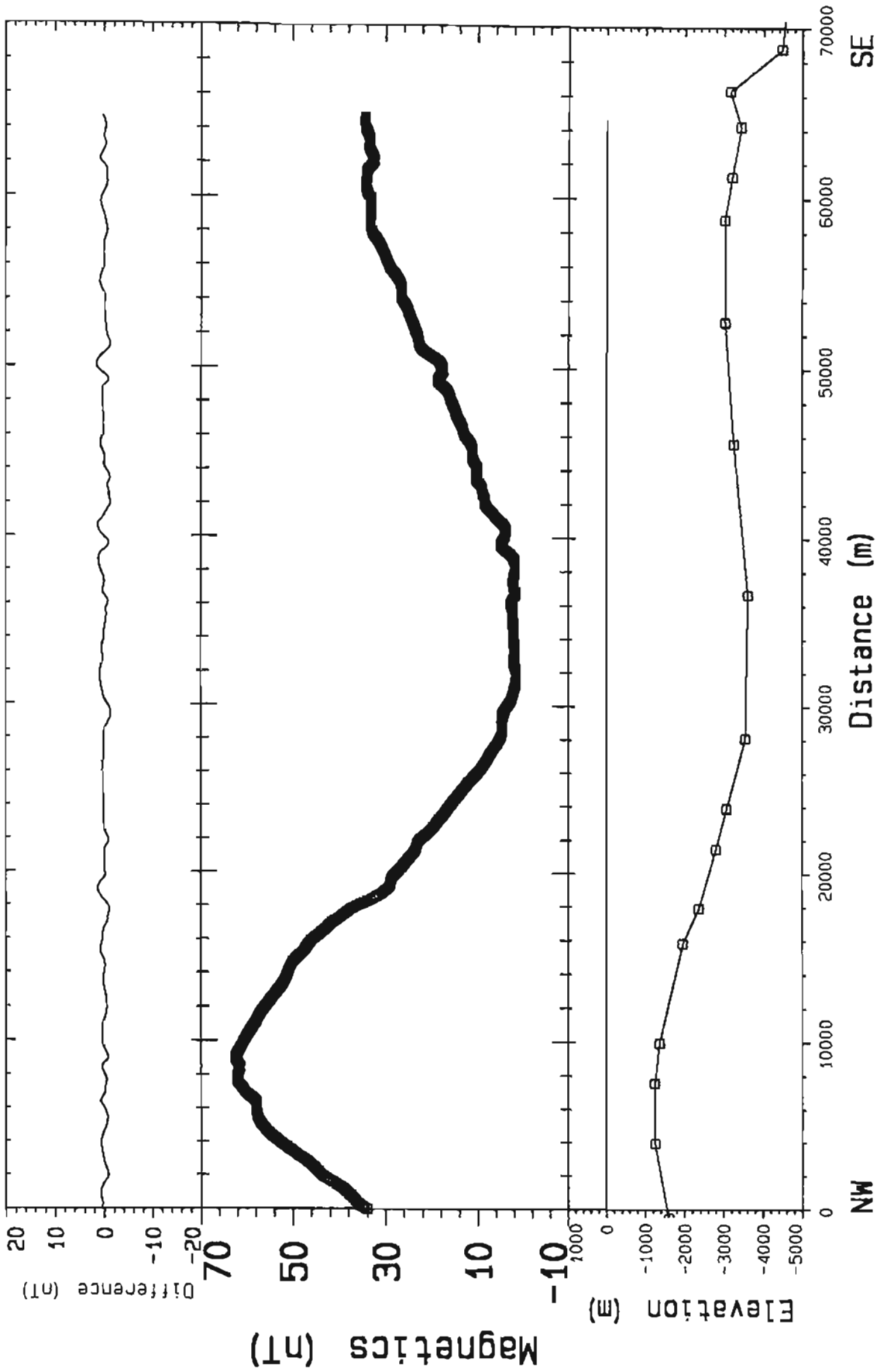


FIGURE 23: 2.5-D modelled magnetic profile 1

Inducing field : 54000. nT		Bedrock Magnetization: 0.001	
Inc: 72.00 deg	Dec: 20.00 deg	Dept. of Natural Resources	
Strike Direction : 65.00 de		State of Alaska	
Profile Direction : 155.00 de		Hollita Basin	
All Directions are Clockwise from true north		Data Set: 1	Date: 25 May 98
		Profile: 1	
		Profile Scale: 1:336005 Vert. Exagg. 2.28:1	

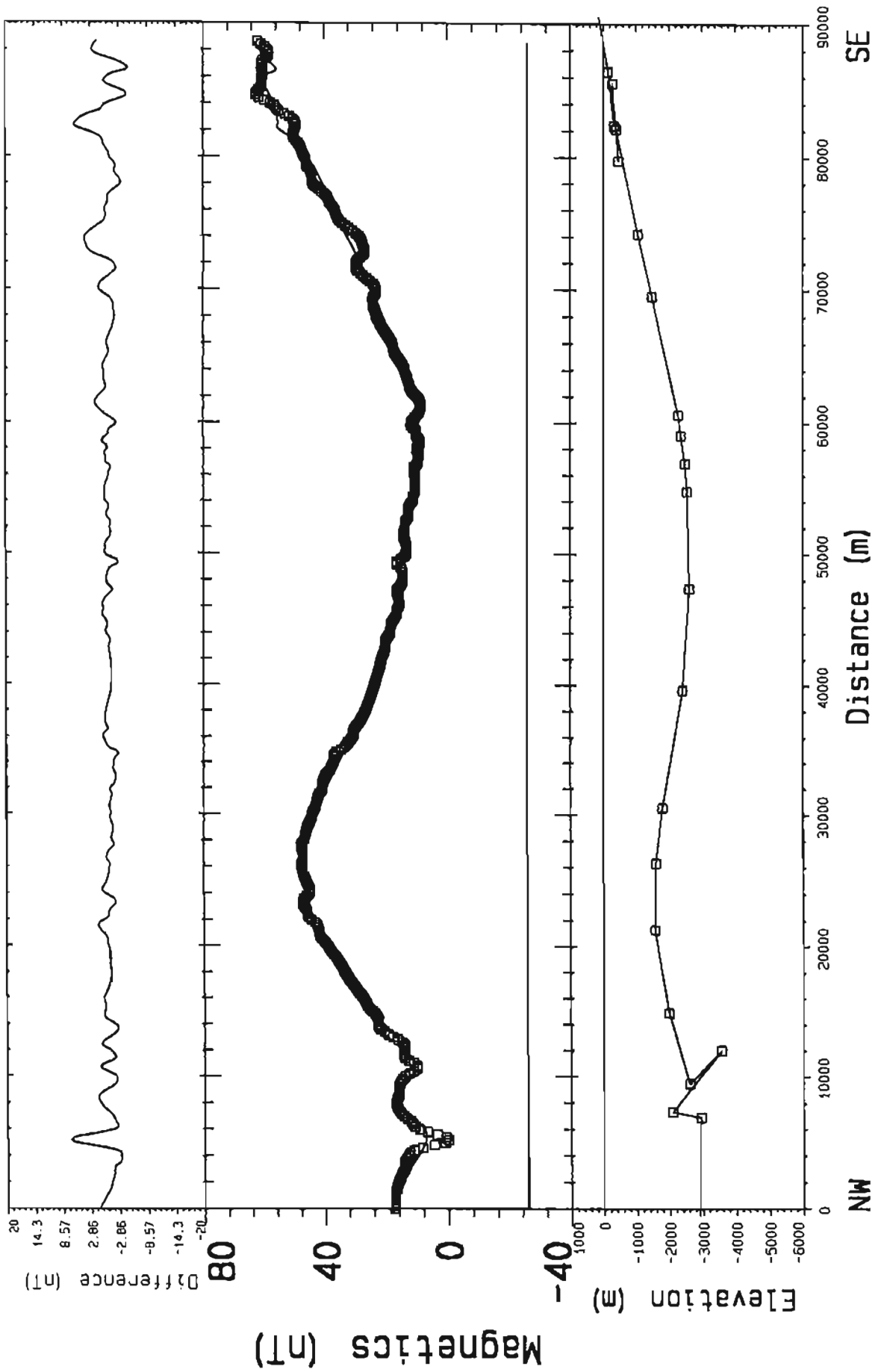


FIGURE 24: 2.5-D modelled magnetic profile 2

Inducing field : 54000. nT	Dept. of Natural Resources		Bedrock Magnetization: 0.001
Inc: 72.00 deg Dec: 20.00 deg	SIAL GEOSCIENCES INC.		State of Alaska
Strike Direction : 65.00 de	Data Set: 2	Date: 25 May 98	Holittna Basin
Profile Direction: 155.00 de	Profile: 2		Profile Scale: 1:422110 Vert. Error 2.51'
All Directions are Clockwise from True North			

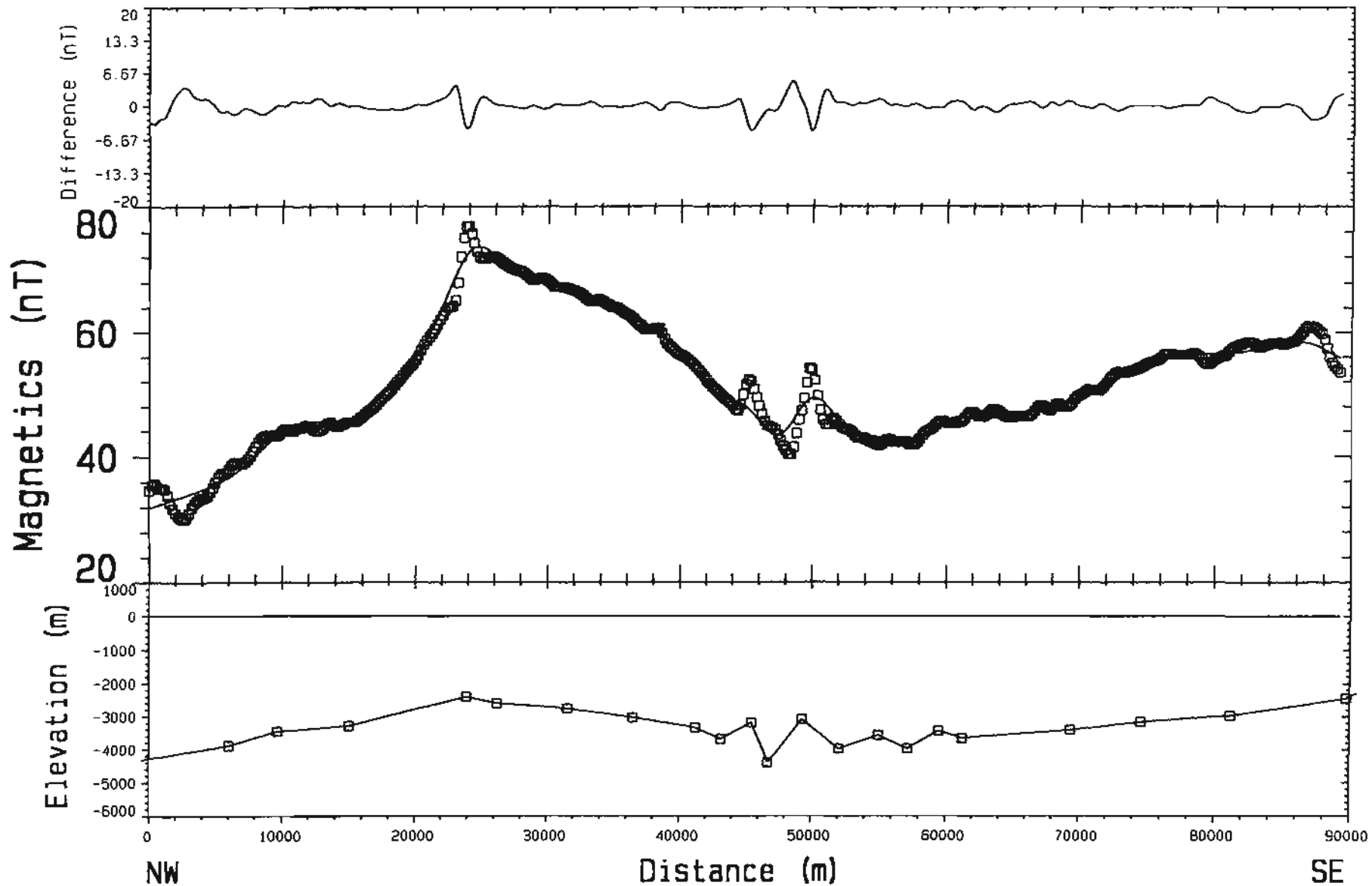
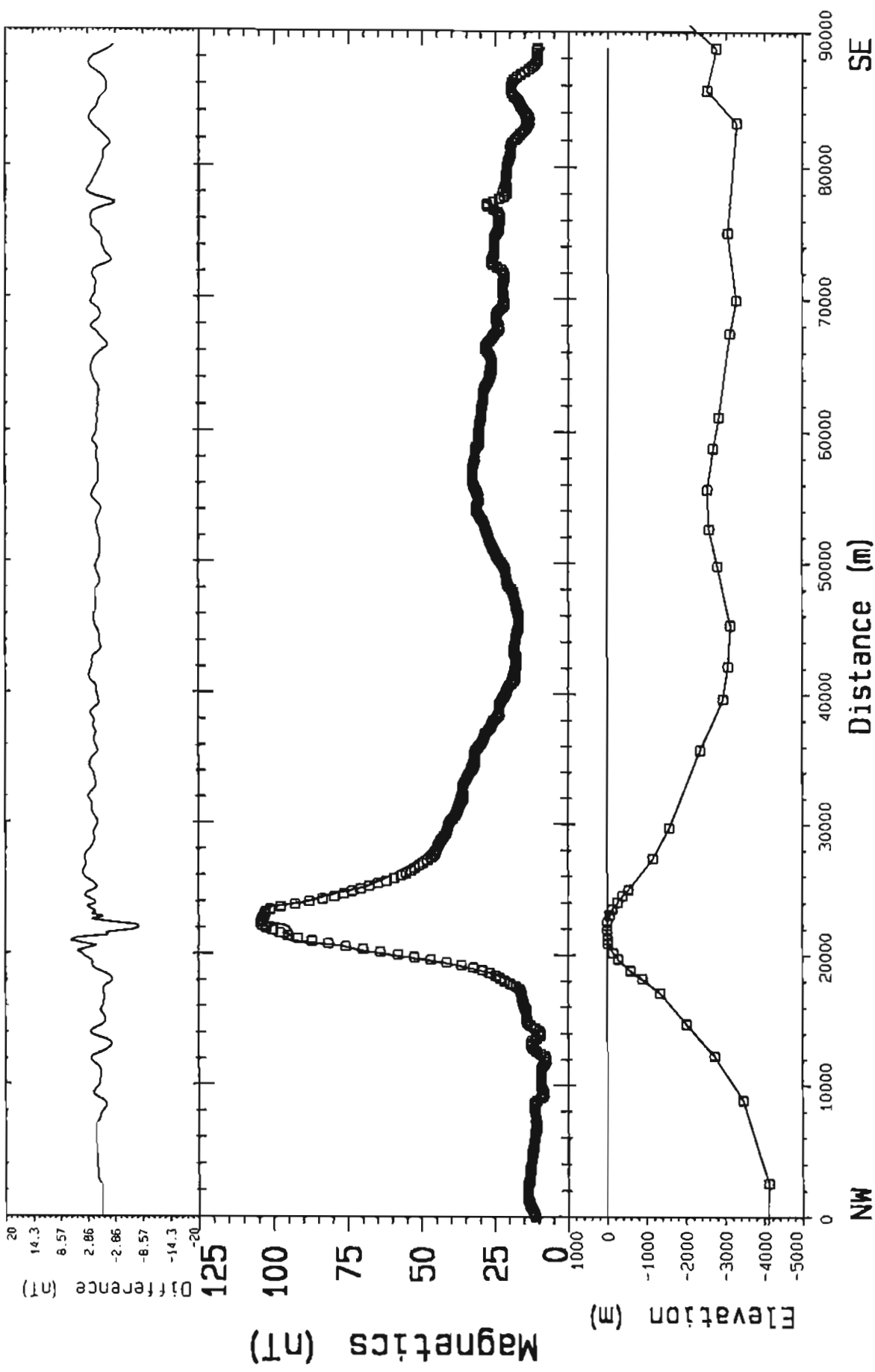


FIGURE 25: 2.5-D modelled magnetic profile 3

Inducing field : 54000. nT	Dept. of Natural Resources	Bedrock magnetization: 0.001
Inc: 72.00 deg Dec: 20.00 deg	SIAL GEOSCIENCES INC.	
Strike Direction : 65.00 de		
Profile Direction : 155.00 de	Data Set: 3	Date: 25 May 98
All Directions are Clockwise from true north		Profile: 3
		Profile Scale: 1:432110 Vert. Exagg. 2.5:1



Distance (m) SE

FIGURE 26: 2.5-D modelled magnetic profile 4

Inducing field : 54000. nT		Bedrock Magnetization: 0.00052	
Inc: 72.00 deg	Dec: 20.00 deg	Dept. of Natural Resources	
Strike Direction : 65.00 de		State of Alaska	
Profile Direction : 155.00 de		Holtina Basin	
All Directions are Clockwise from true north		Data Set: 4	Date: 25 May 98
		Profile: 4	

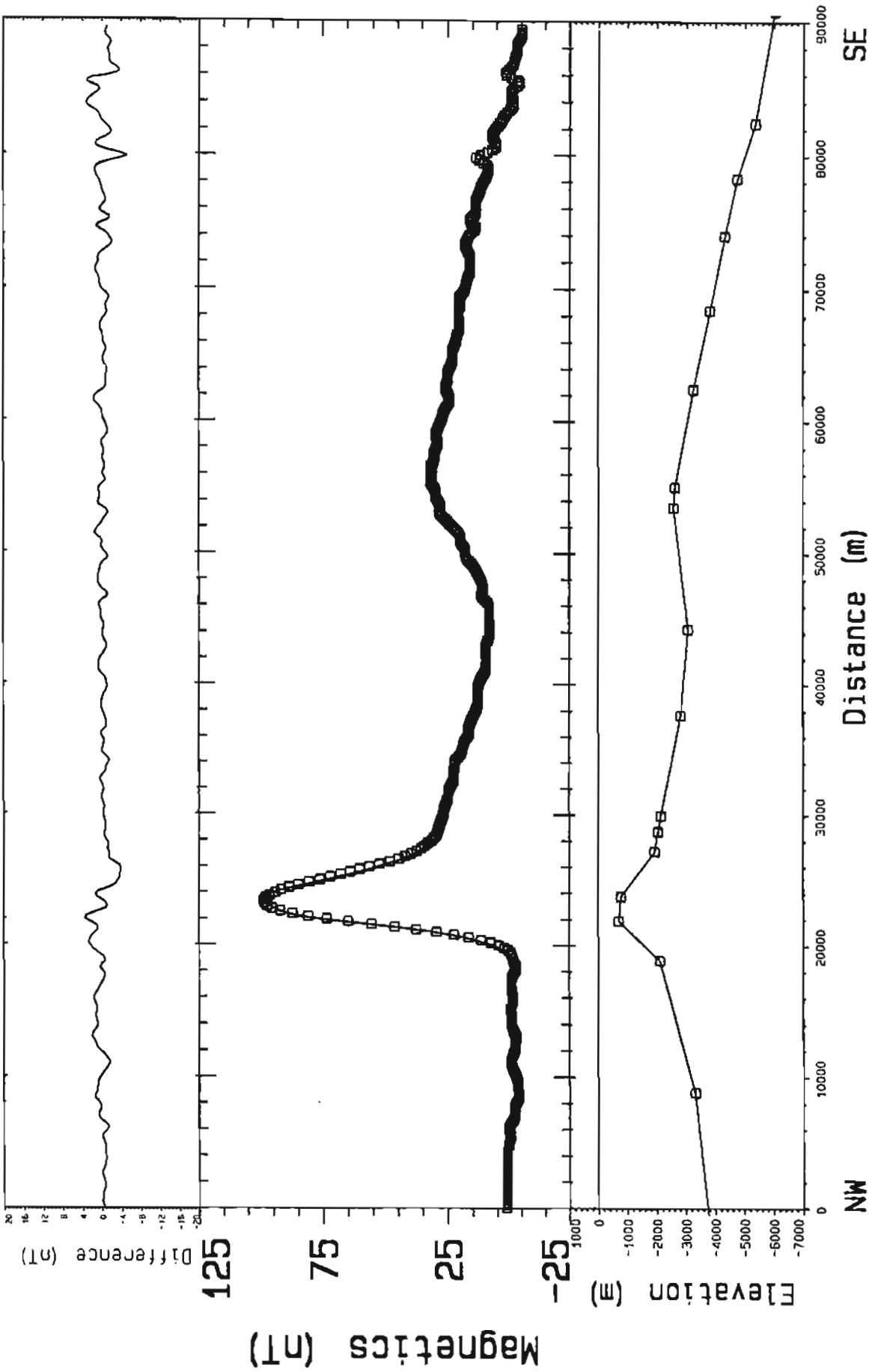


FIGURE 27: 2.5-D modelled magnetic profile 5

Inducing field : 54000. nT		Bedrock Magnetisation: 0.0008	
Inc: 72.00 deg Dec: 20.00 deg		Dept. of Natural Resources	
Strike Direction : 65.00 de		State of Alaska	
Profile Direction : 155.00 de		Holitna Basin	
Data Set: 5	Date: 25 May 98	Profile: 5	
All Directions are Clockwise from true north			
Profile Scale 1 432x10 Vert Exagg 2 20-1			

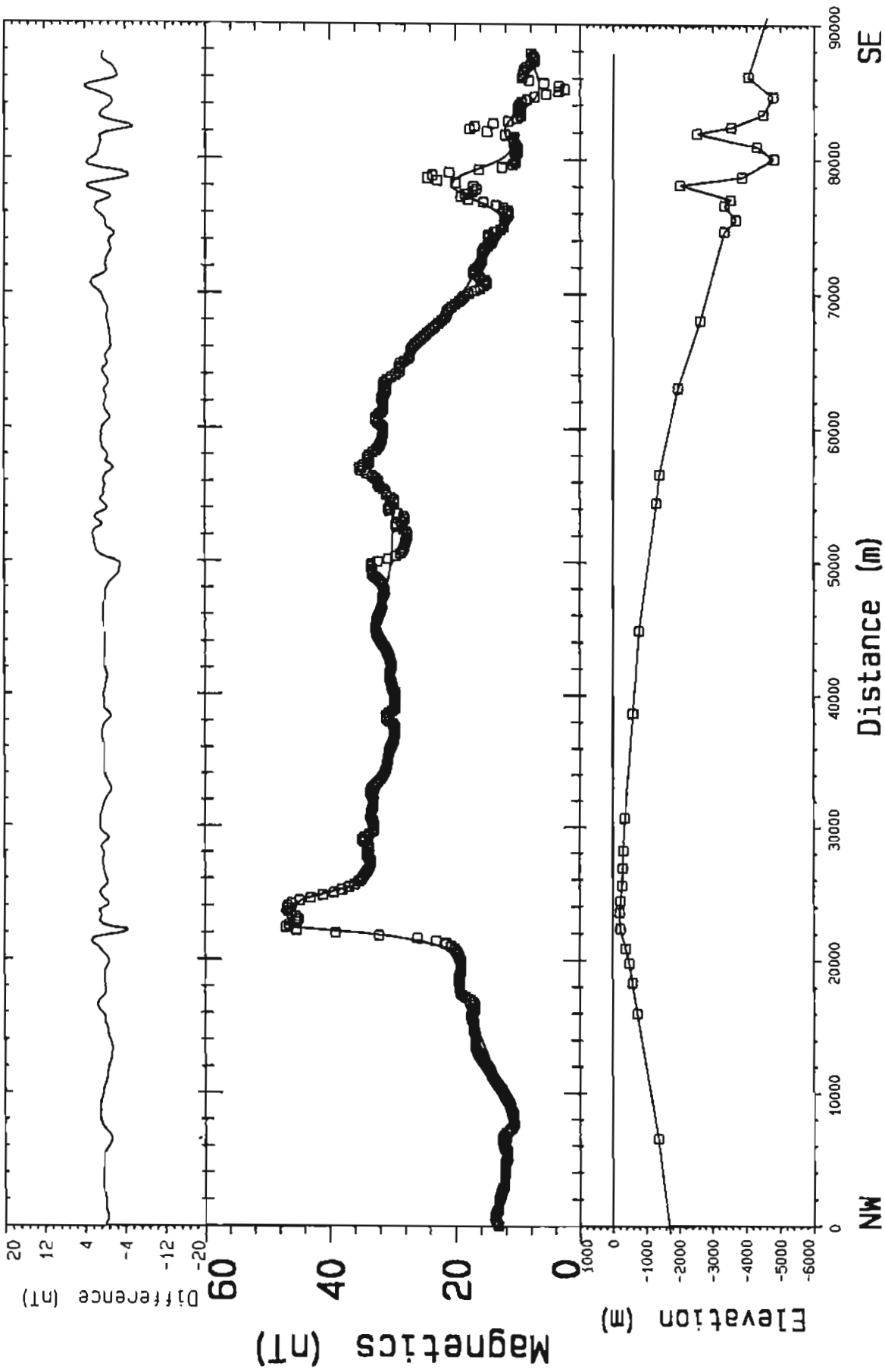


FIGURE 28: 2.5-D modelled magnetic profile 6

Inducing field : 54000. nT	Dept. of Natural Resources		Bedrock Magnetisation: 0.0008
Inc: 72.00 deg Dec: 20.00 deg	SIAL GEOSCIENCES INC.		State of Alaska
Strike Direction : 65.00 de	Date Set: 6	Date: 25 May 98	Holitna Basin
Profile Direction : 155.00 de	Profile: 6		Profile Scale: 1: 62110 Vert. Exagg: 2.5: 1
All Directions are Clockwise from true north			

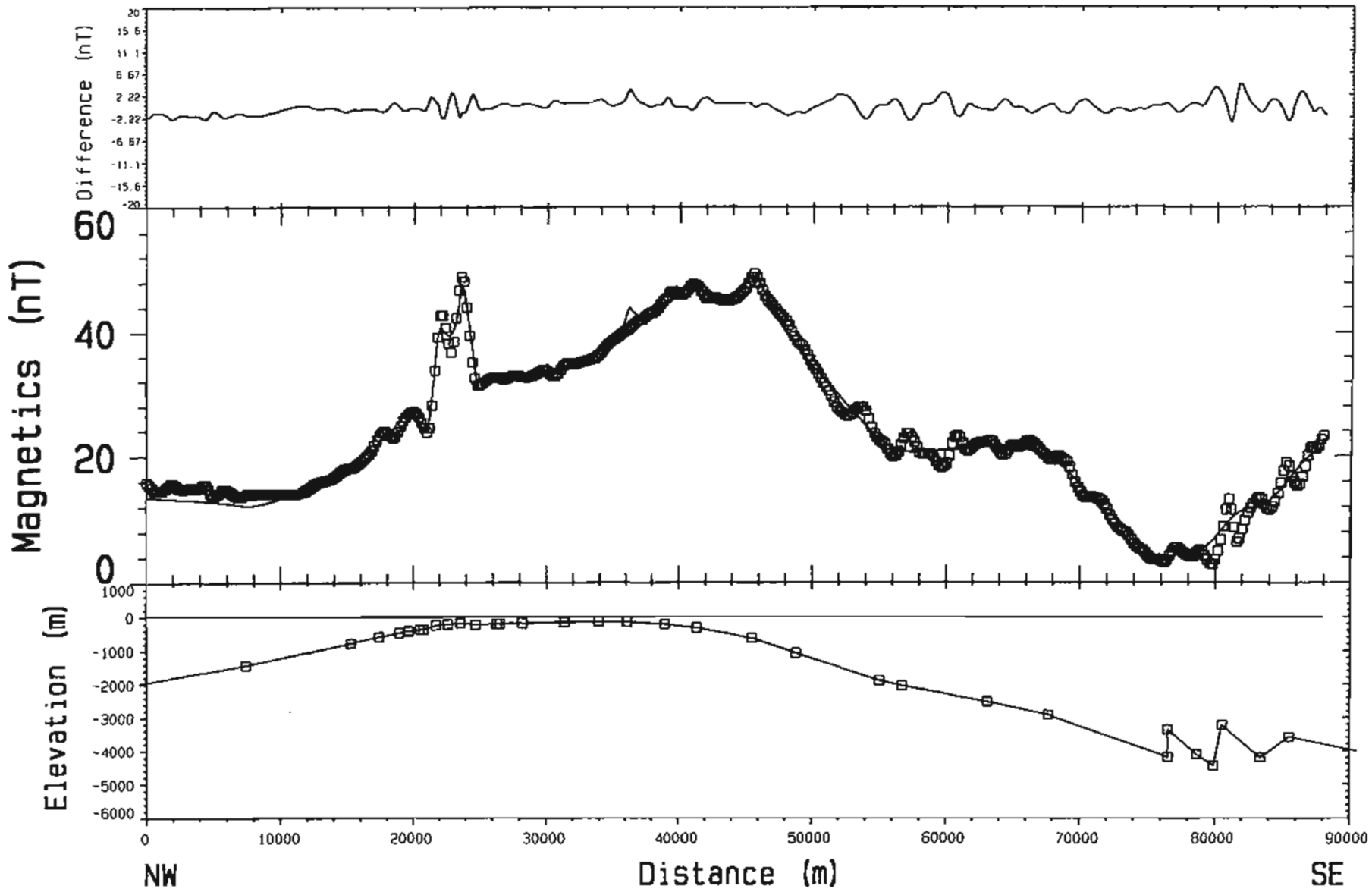


FIGURE 29: 2.5-D modelled magnetic profile 7

Inducing field : 54000. nT	Dept. of Natural Resources	Bedrock Magnetisation: 0.0008
Inc: 72.00 deg Dec: 20.00 deg	SIAL GEOSCIENCES INC.	
Strike Direction : 65.00 de	Data Set: 7	Date: 25 May 98
Profile Direction : 155.00 de	Profile: 7	Profile Scale: 1:432110 Vert. Exagg 2.5:1
All Directions are Clockwise from True North		

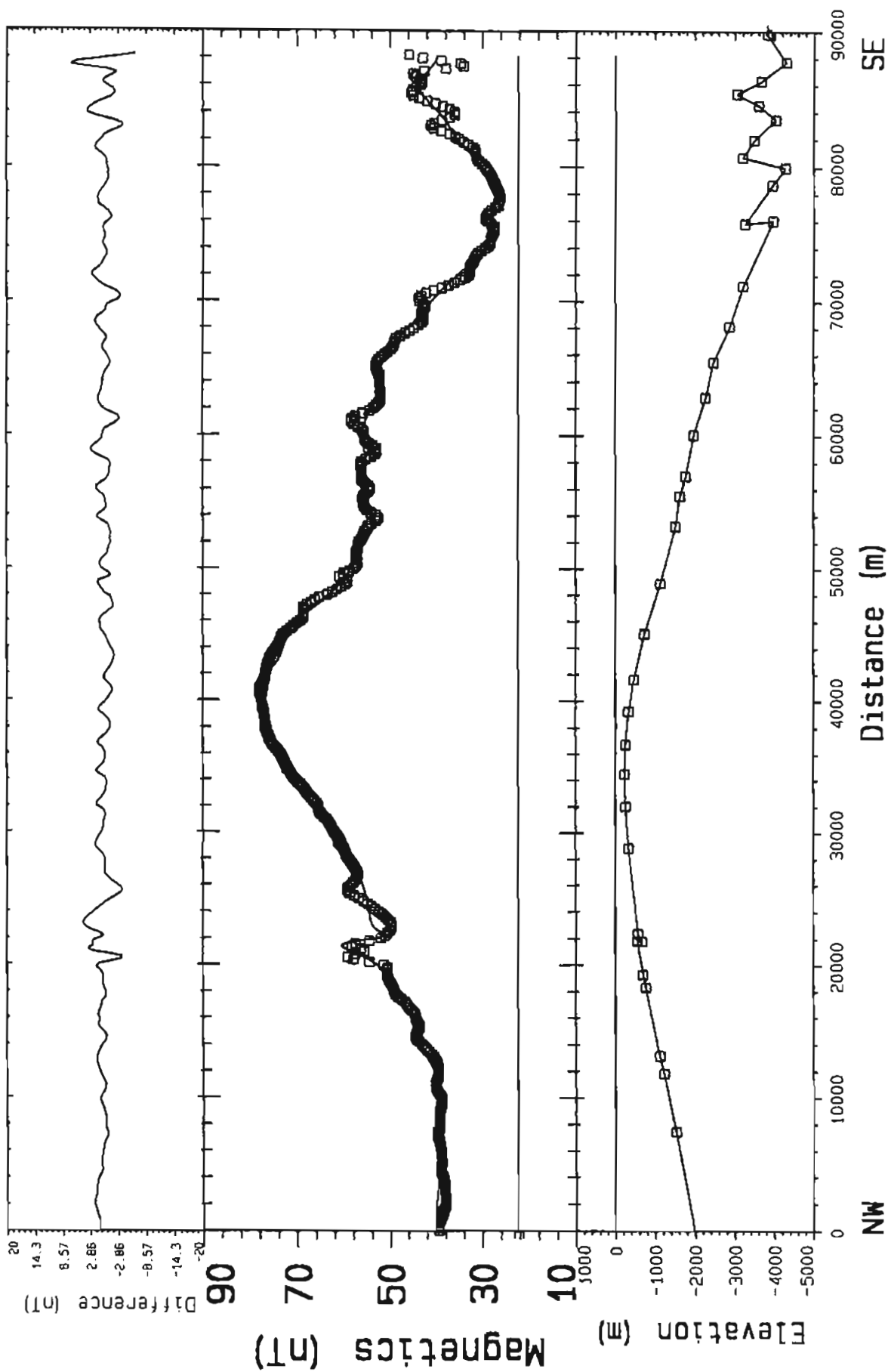


FIGURE 30: 2.5-D modelled magnetic profile 8

Inducing field : 54000. nT		Bedrock Magnetization: 0.001	
Inc: 72.00 deg	Dec: 20.00 deg	Dept. of Natural Resources	
Strike Direction : 65.00 de		SIAL GEOSCIENCES INC.	
Profile Direction : 155.00 de	Date: 25 May 98	Data Set: 8	Profile: 8
All Directions are Clockwise from true north			

State of Alaska  
Holtna Basin

Profile Scale 1:43210 Vert. Engrg 2 93 1

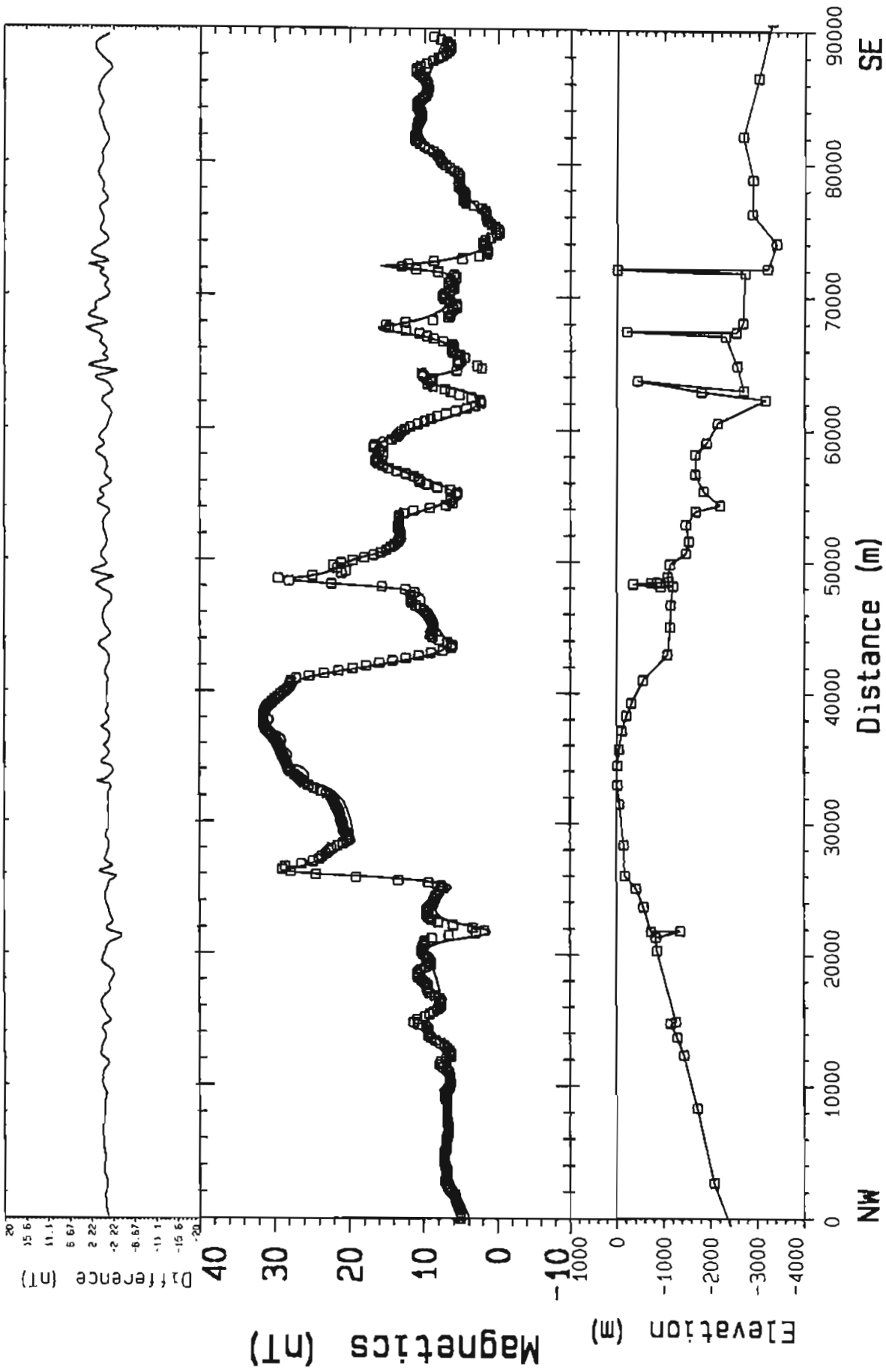


FIGURE 31: 2.5-D modelled magnetic profile 9

Inducing field : 54000 nT		Bedrock Magnetization: 0.0005	
Inc: 72.00 deg	Dec: 20.00 deg	Dept. of Natural Resources	
Strike Direction : 65.00 de		SIAL GEOSCIENCES INC.	
Profile Direction : 135.00 de		Data Set: 9	Date: 25 May 98
All Directions are Clockwise from true north		Profile: 9	
		State of Alaska HOLITNA BASIN	
		Profile Scale: 1:43210 Vert Ekagg 3 51 1	

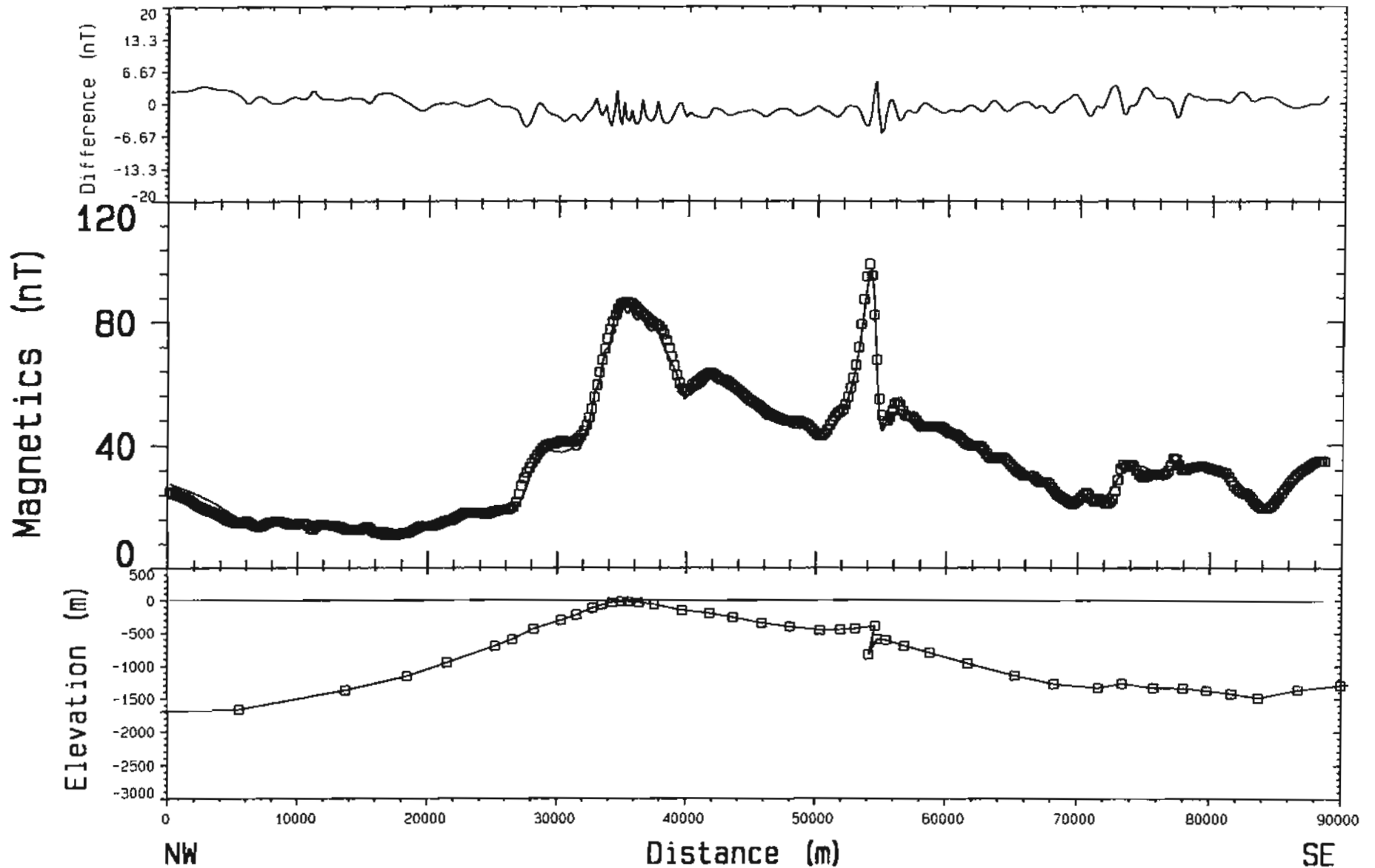


FIGURE 32: 2.5-D modelled magnetic profile 10

Inducing field : 54000. nT	Dept. of Natural Resources		Bedrock Magnetization: 0.0016
inc: 72.00 deg Dec: 20.00 deg	SIAL GEOSCIENCES INC.		State of Alaska Holitna Basin
Strike Direction : 85.00 de	Data Set: 10	Date: 25 May 98	
Profile Direction : 155.00 de		Profile: 10	Profile Scale: 1:43210 Vert. Exagg 5 02 1
All Directions are Clockwise from True north			

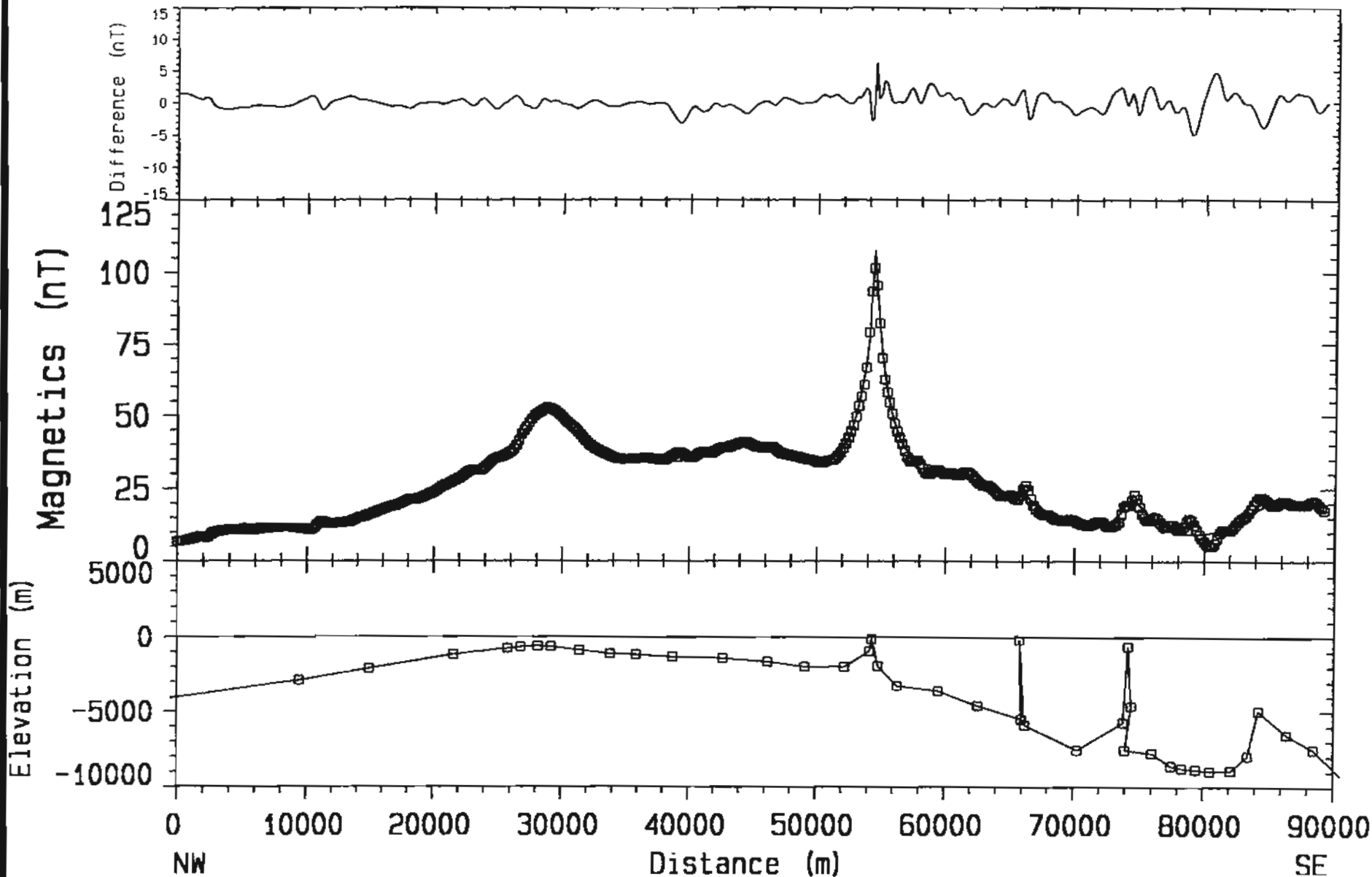


FIGURE 33: 2.5-D modelled magnetic profile 11

Inducing field : 54000. nT	Dept. of Natural Resources	Bedrock Magnetization: 0.0005
Inc: 72.00 deg Dec: 20.00 deg	SIAL GEOSCIENCES INC.	State of Alaska
Strike Direction : 65.00 de	Data Set: 11	Date: 25 May 98
Profile Direction : 155.00 de	Profile: 11	Profile Scale : 432110 Ver. 2 Exagg 1 12 1
All Directions are Clockwise from true north		

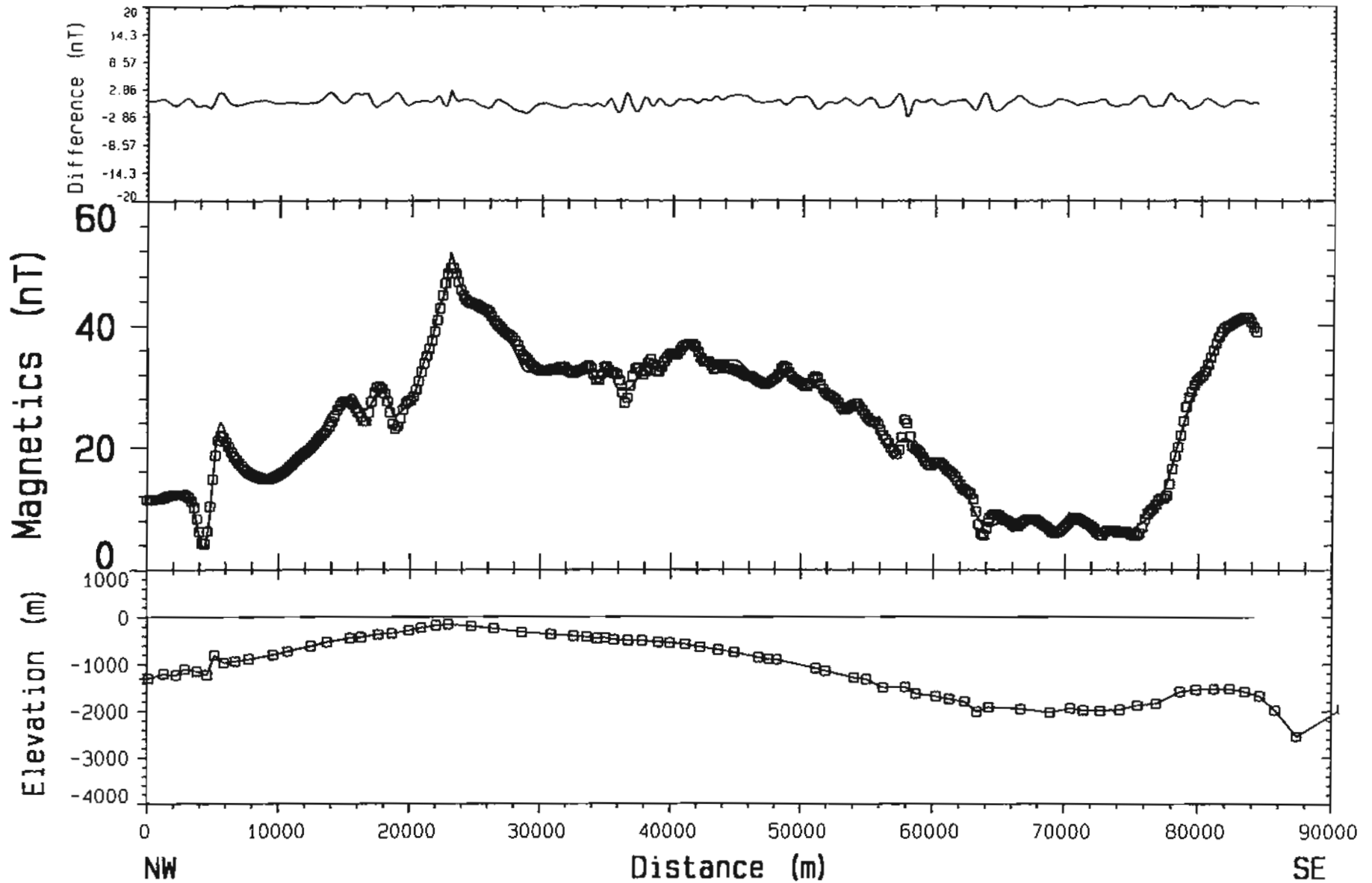


FIGURE 34: 2.5-D modelled magnetic profile 12

Inducing field : 54000. nT	Dept. of Natural Resources	Bedrock Magnetization: 0.001
Inc: 72.00 deg Dec: 20.00 deg	SIAL GEOSCIENCES INC.	
Strike Direction : 65.00 de		
Profile Direction 155.00 de	Data Set: 12	Date: 25 May 98
All Directions are Clockwise from true north		Profile: 12
		State of Alaska Holitna Basin
		Profile Scale: 1:432150 Vert. Exagg 3 5/1

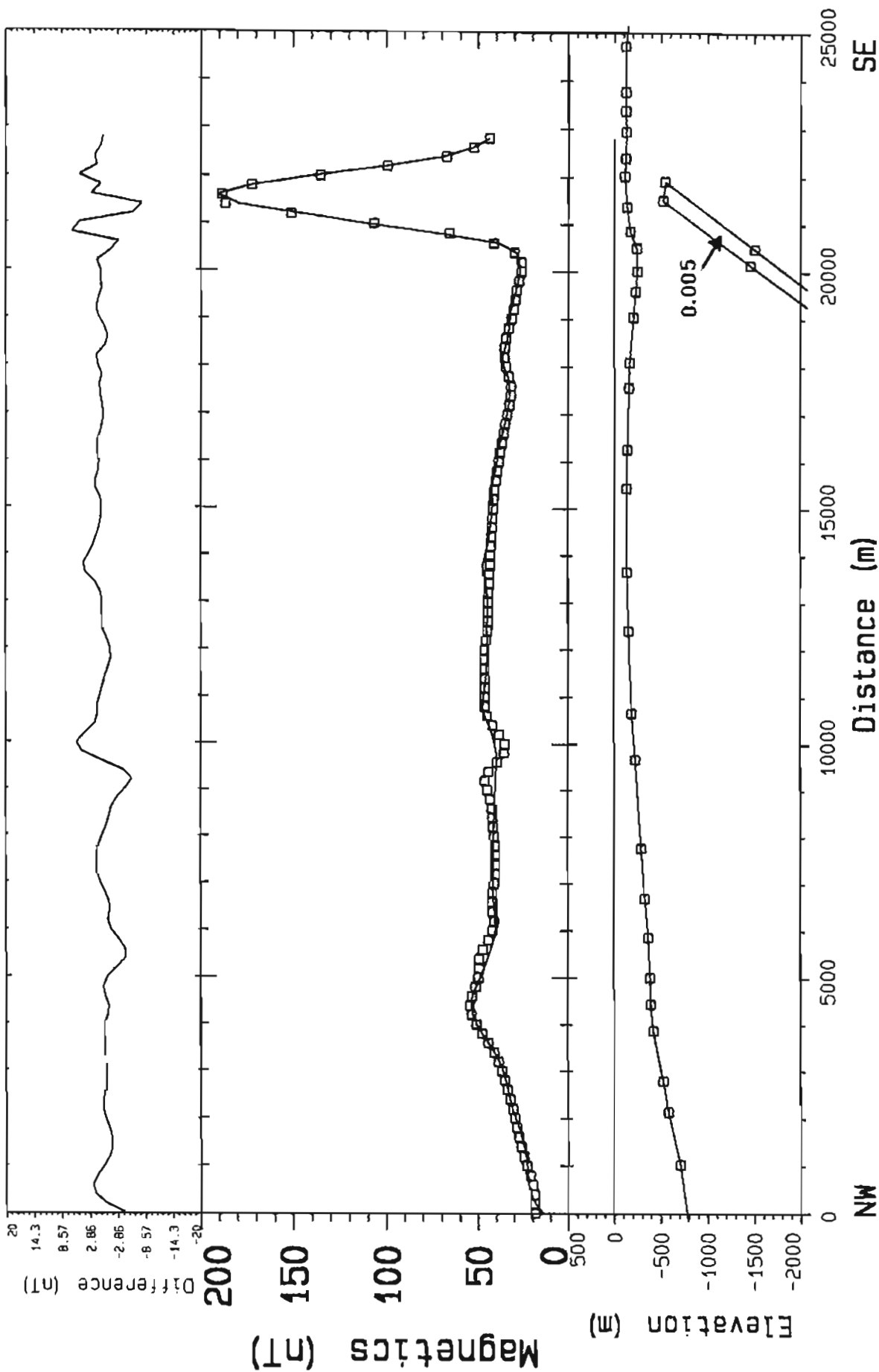


FIGURE 35: 2.5-D modelled magnetic profile 13

Inducing field : 54000. nT		Bedrock Magnetization: 0.001	
Inc: 72.00 deg	Dec: 20.00 deg	Dept. of Natural Resources	
Strike Direction : 65.00 de		State of Alaska	
Profile Direction : 155.00 de		Holitna Basin	
411 Directions are Clockwise from true north		Data Set: 13	Date: 25 May 98
		Profile: 13	
		Profile Scale: 1:120030 Vert. Exagg. 1.95:1	

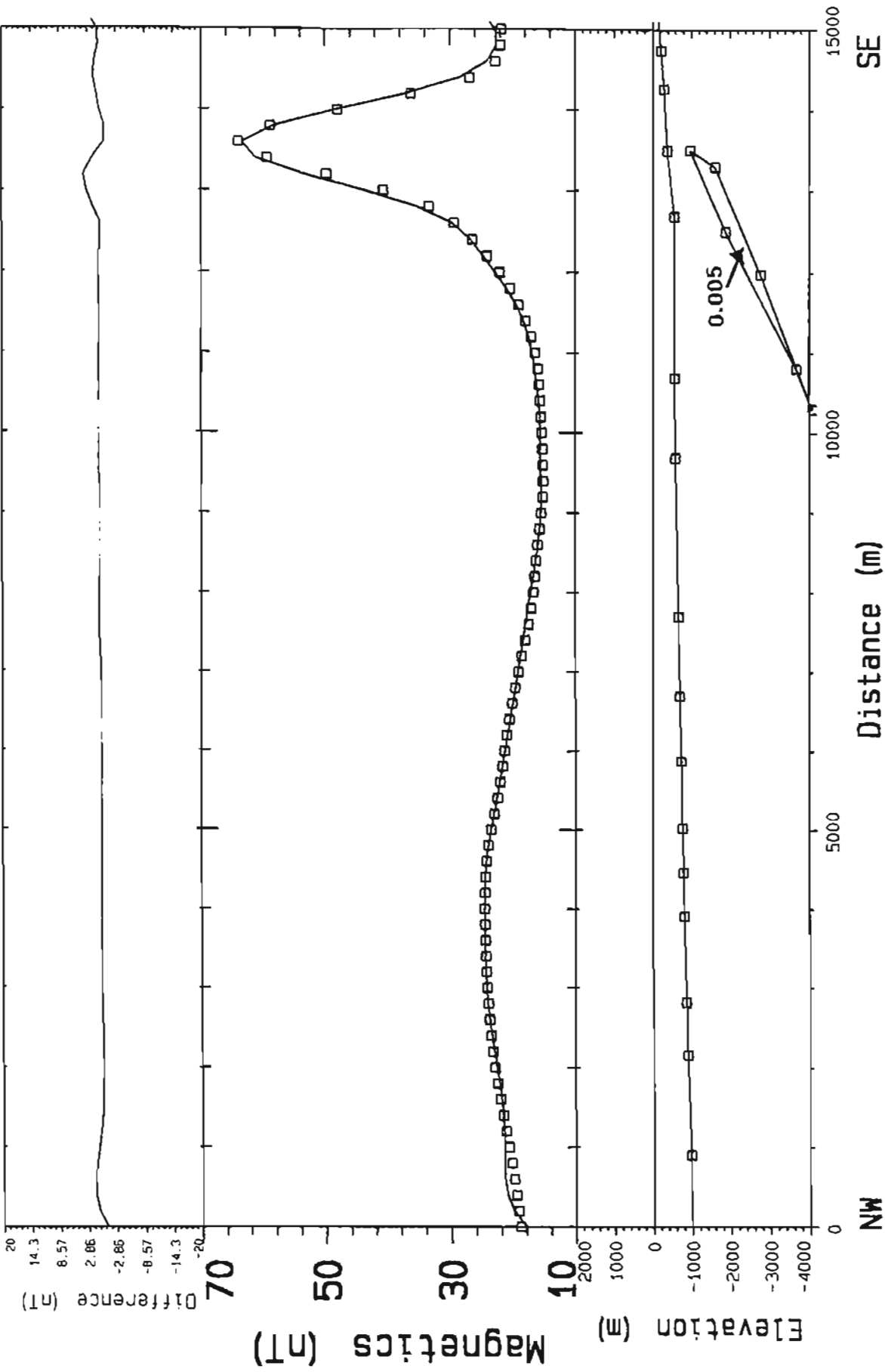


FIGURE 36: 2.5-D modelled magnetic profile 14

Inducing field : 54000. nT	Dept. of Natural Resources	Bedrock Magnetization: 0.001
Inc: 72.00 deg Dec: 20.00 deg	SIAL GEOSCIENCES INC.	State of Alaska
Strike Direction : 65.00 de	Date Set: 14	Holitna Basin
Profile Direction : 155.00 de	Date: 25 May 98	Profile Scale: 1:72018 Vert. Exagg. 0.48:1
All Directions are Clockwise from true north	Profile: 14	

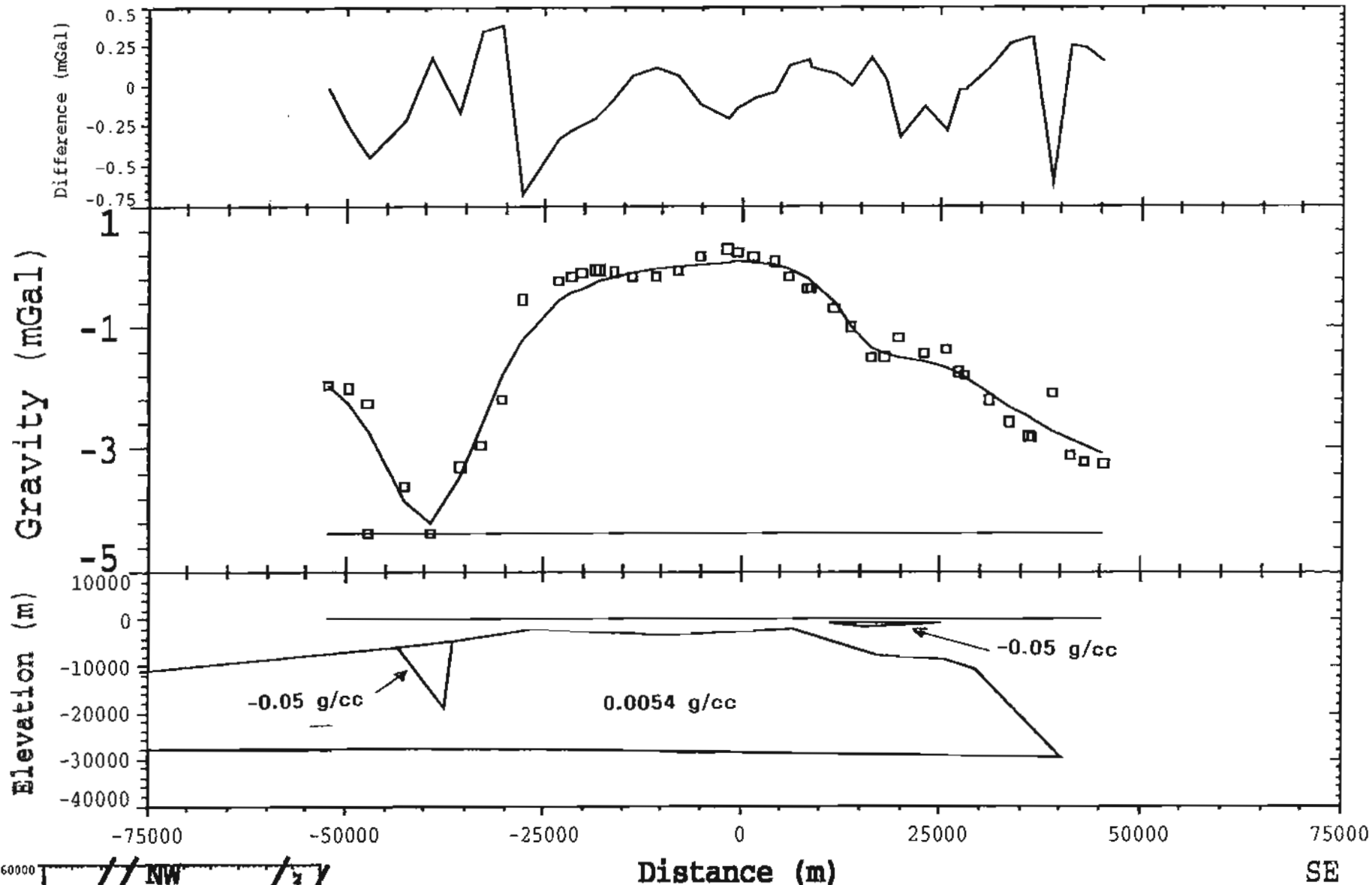
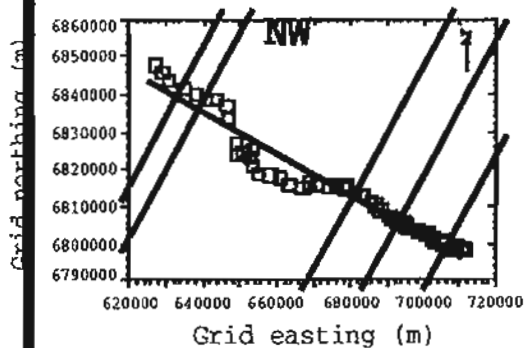


FIGURE 37: 2.5-D modelled gravity profile A-A'



Alaska DNR		Bouguer Gravity	
SIAL GEOSCIENCES INC.		Holitna Basin	
Data Set: g1	Date: Aug 1997	Profile Scale: 1:720183 Vert. Exagg: 0.59:1	
Map Scale: 1:2072106	Profile: A-A'		

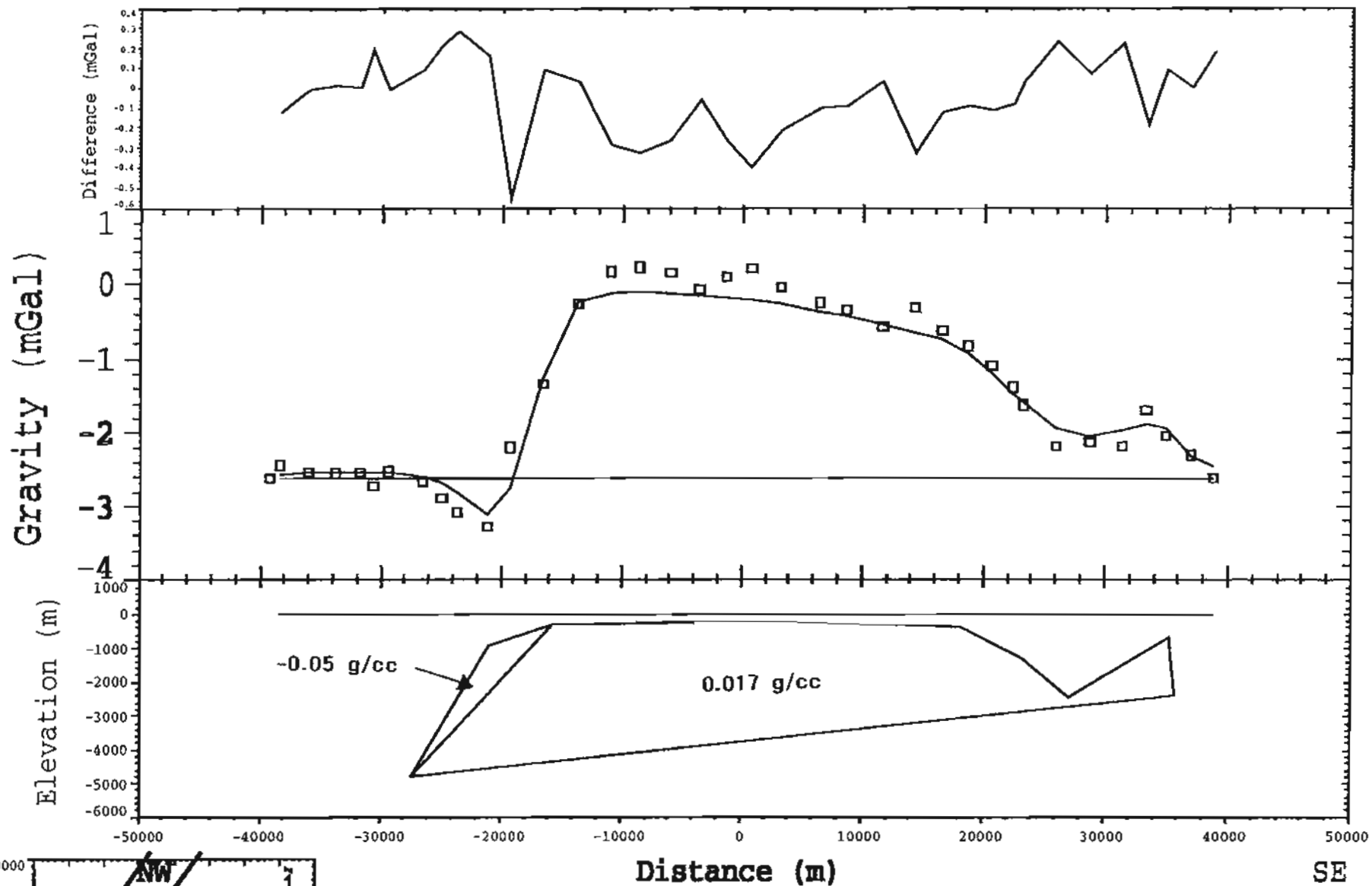


FIGURE 38: 2.5-D modelled gravity profile B-B'

<b>Alaska DNR</b>		<b>Bouger Gravity</b>	
<b>SIAL GEOSCIENCES INC.</b>		<b>Holitna Basin</b>	
<b>Data Set: g3</b>	Date: Aug 1997	Profile Scale: 1:480122 Vert. Exagg: 2.79:1	
Map Scale: 1:1657684	<b>Profile: B-B'</b>		

For all the magnetic profiles, the IGRF was removed prior to modelling, and a constant regional value was selected. It should be noted that the magnetization determined are relative. In addition, since the effect of an infinite slab is zero, the lower surface does not have any effect if it is assumed to be at a constant depth (in this case 30 km).

The variation in gravity values was quite small, ranging from 0 to -4 mgal on profile A-A', and from 0 to -3 mgal on profile B-B'. Note that some of the intermediate values, which lie in scarcely sampled areas, are significantly lower, however more values would have to be collected before reliable interpretation could be carried out over these areas. The present gravity data are mainly along rivers and streams.

Modelling of gravity profiles yielded results compatible with the magnetic modelling.

## 9.6 Euler Deconvolution

The Euler deconvolution method is based on Euler's homogeneous equation (Pilkington and al., 1991), which for data in map form is given by:

$$(1) \quad (x-x_0)\partial T/\partial x + (y-y_0)\partial T/\partial y + (z-z_0)\partial T/\partial z = N (B-T)$$

where:

- $(x_0, y_0, z_0)$  is the position of a magnetic source whose total field effect  $T$ , is detected at  $(x, y, z)$
- $B$  is the regional field
- $N$  is the degree of homogeneity or structural index (Thompson, 1982; Reid et al., 1990) which depends on source type
- $\partial T/\partial x$ ,  $\partial T/\partial y$  and  $\partial T/\partial z$  are two horizontal and the vertical gradients of the magnetic field which are easily calculated using frequency domain processing

If the total field  $T(x,y,z)$  has the general form of:

$$(2) \quad T(x,y,z) = G / r^N$$

where:

- $r = (x^2 + y^2 + z^2)^{1/2}$
- $N = 1, 2, 3, \dots$
- $G$  is not dependant on  $(x, y, z)$

Then  $T$  satisfies Euler's equation.

Many simple magnetic sources types can be described in this way, with the value of the structural index,  $N$ , being indicative of the source geometry. From the equation (2), we see that  $N$  controls the rate of decay of the magnetic field with distance from the source. When  $N$  is large, the field falls off at a greater rate than for small  $N$ . Figure 39 shows how this parameter varies for a number of commonly met geological situations. Although the source geometry controls the value of  $N$ , the direction of the Earth's magnetic field also influences the rate of decay of the field, but we may consider this as a secondary effect.

## Results

Two source geometries were used (Dike and Step model) and the results are presented in figures 40 and 41. On each figure, a scale bar give the color code for the basement depth.

The dike model give a maximum basement depth of 6490 meters and the step model give a maximum basement depth of 5350 meters. Some indeterminate areas are observed on the figures 40 and 41, meaning that no Euler solution has been found at these particular places. Because the dike model is more compatible with the spectral analysis results, this model has been retained for the basement depth contours presented on the interpretation sketch map of figure 42. In order to fill in the indeterminate areas, the evaluated depths have been regridded with a longer radius.

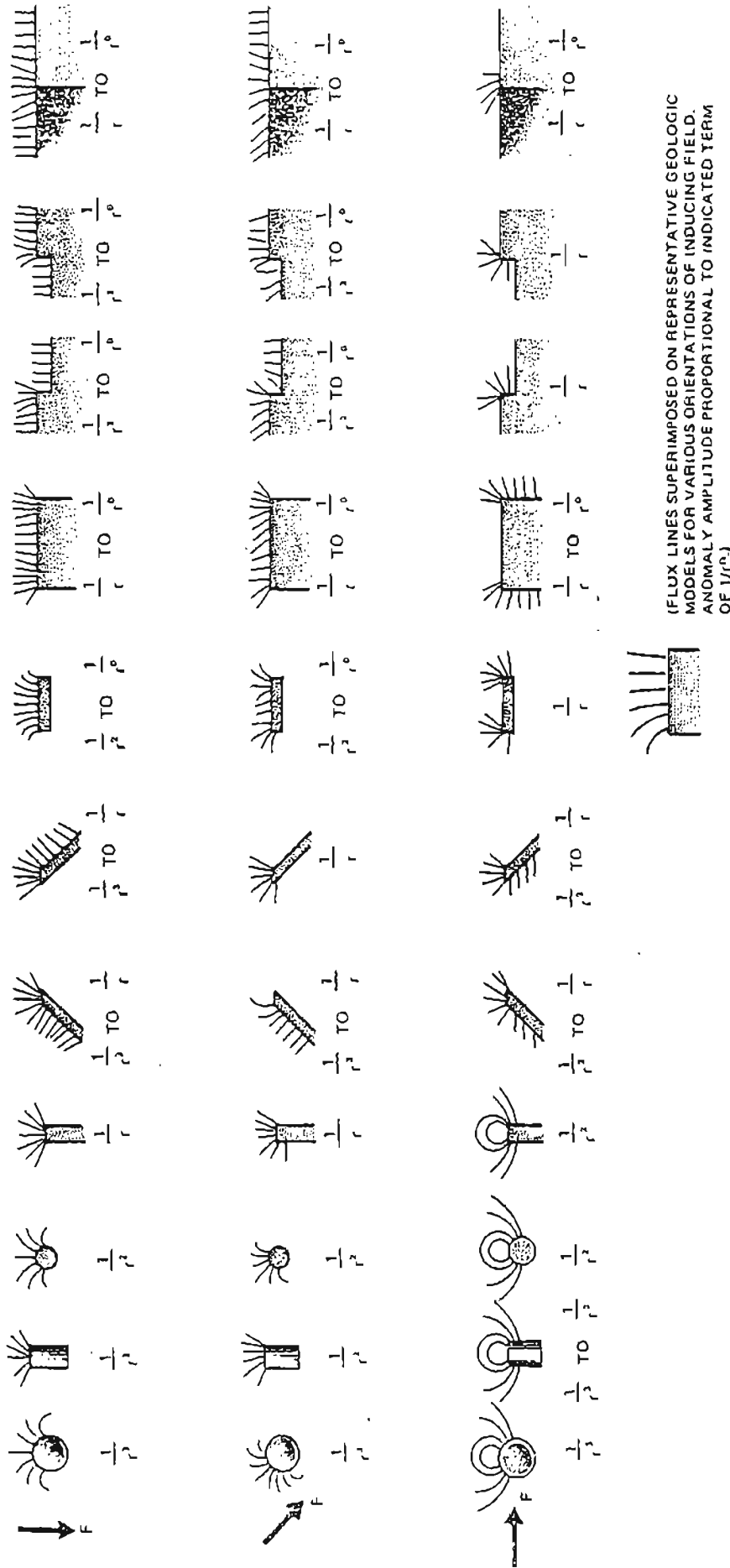
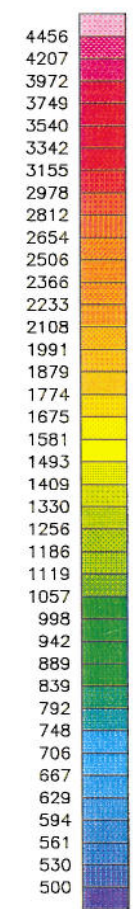
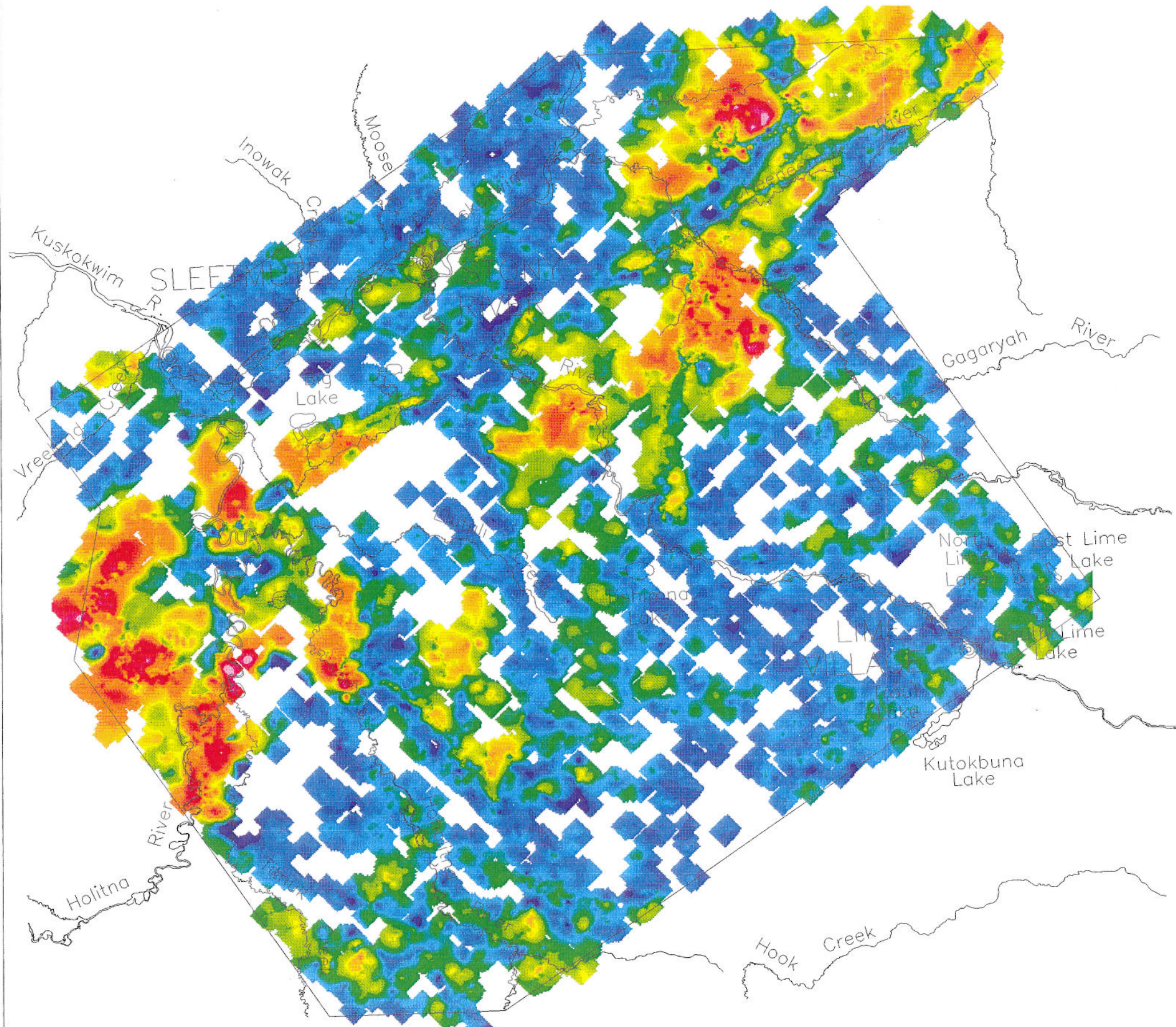


FIGURE 29: Magnetic field (flux lines) and fall-off rates for various geological models (after Breiner, 1973).



BASEMENT DEPTH  
( meters )

Scale 1:500 000

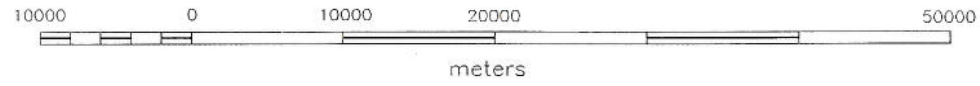
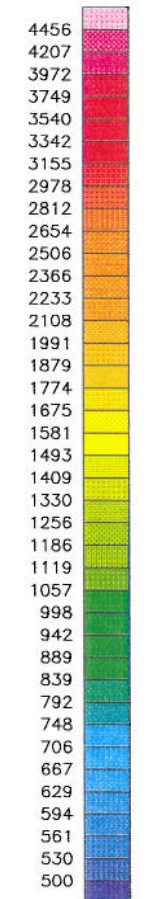
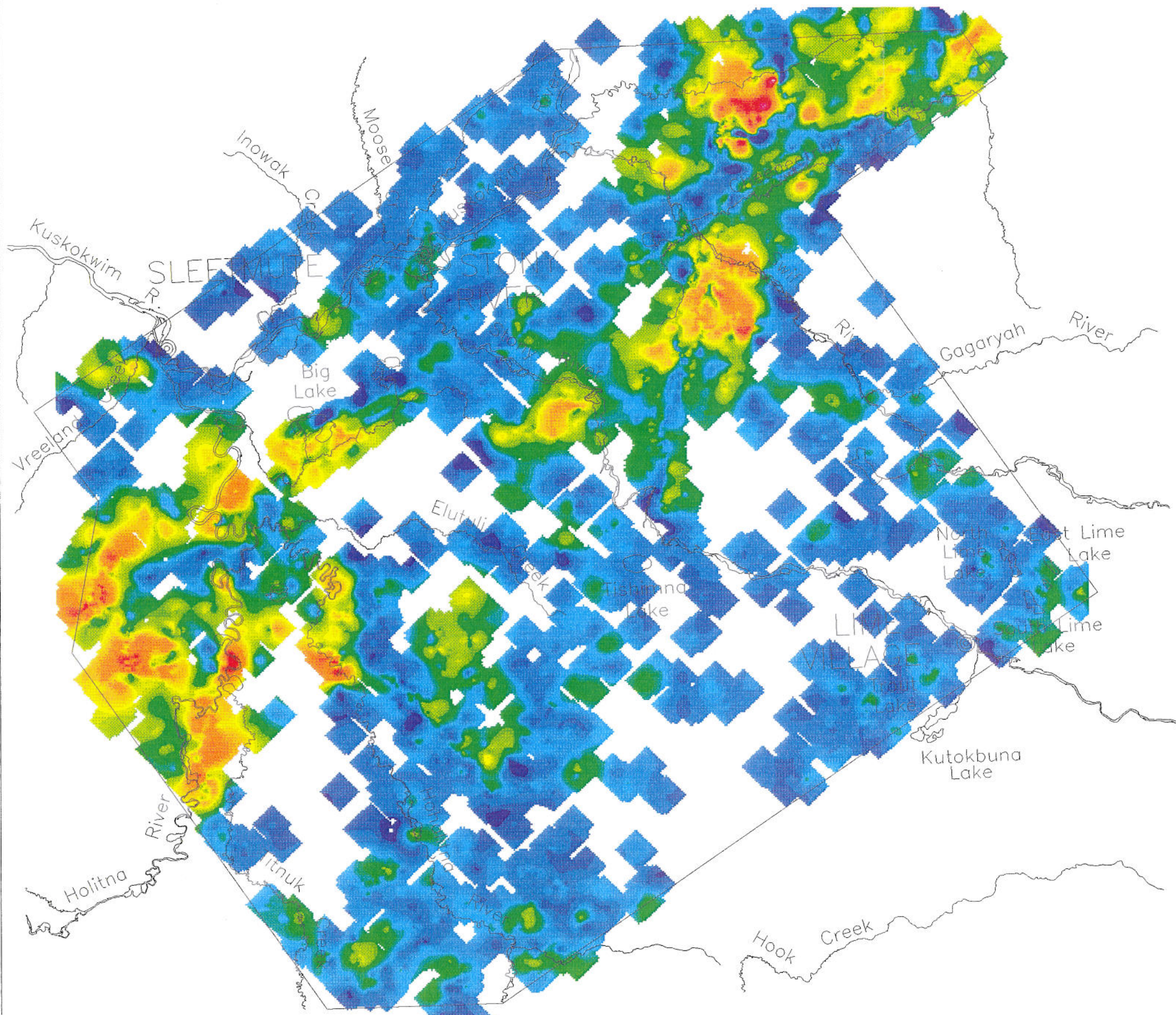


FIGURE 40: Euler depth interpretation (dike model)

<b>STATE OF ALASKA</b>			
HOLITNA BASIN AIRBORNE GEOPHYSICAL SURVEY SOUTHWESTERN ALASKA			
<b>EULER DEPTH INTERPRETATION DIKE MODEL COLOUR MAP</b>			
Map scale :	1: 500 000	Project Ref :	97A03-36 CDIKHOL500
Date Compiled :		Date Flown :	
<b>SIAL</b> Géosciences inc.			



BASEMENT DEPTH  
( meters )

Scale 1:500 000

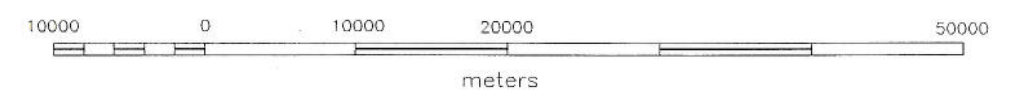
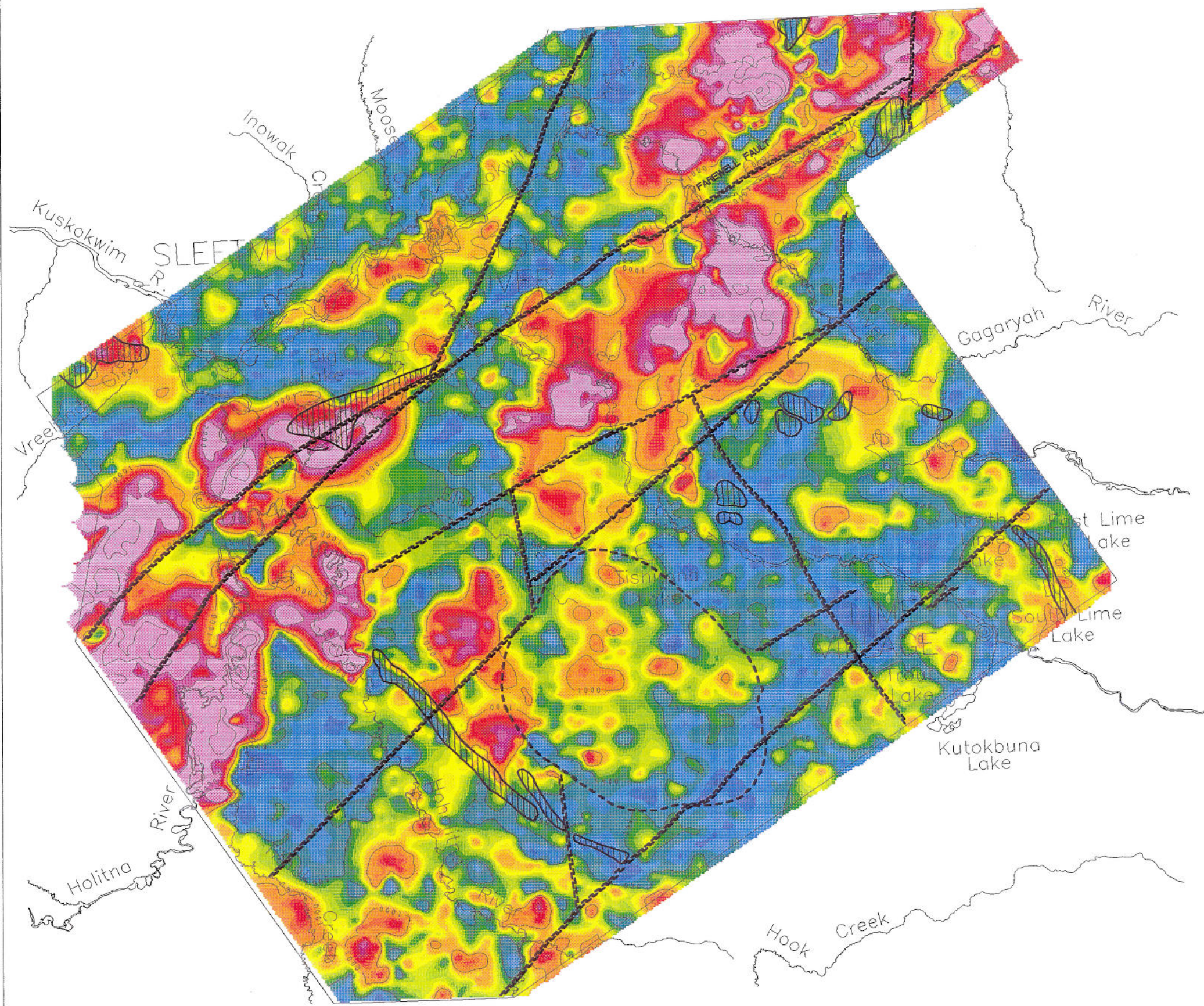


FIGURE 41 : Euler depth interpretation (step model)

<b>STATE OF ALASKA</b>			
HOLITNA BASIN AIRBORNE GEOPHYSICAL SURVEY SOUTHWESTERN ALASKA			
<b>EULER DEPTH INTERPRETATION STEP MODEL COLOUR MAP</b>			
Map scale :	1: 500 000	Project Ref :	97A03-36 CSTPHOL500
Date Compiled :		Date Flown :	
<b>SIAL</b> Géosciences inc.			



**BASEMENT DEPTH**

Map contours are in meters.

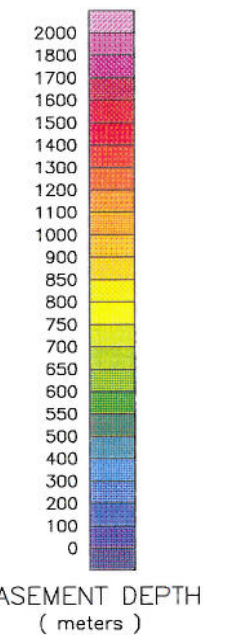
500 m : ——— 500 ———

1000 m : ——— 1000 ———

2000 m : ——— 2000 ———

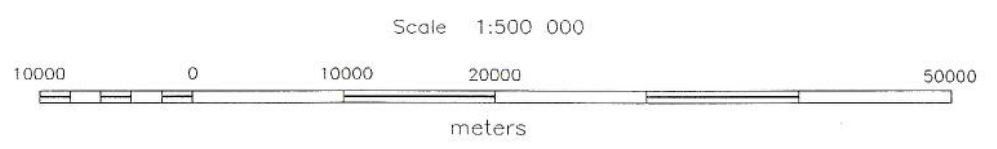
3000 m : ——— 3000 ———

4000 m : ——— 4000 ———



**LEGEND FOR GEOPHYSICAL INTERPRETATION**

- Batholith
- Presumed Fault
- Dike / Intrusif



<b>STATE OF ALASKA</b>			
HOLITNA BASIN AIRBORNE GEOPHYSICAL SURVEY SOUTHWESTERN ALASKA			
<b>INTERPRETATION SKETCH MAP</b>			
FIGURE 42			
Map scale :	1: 500 000	Project Ref :	97A03-36   INTHOL500
Date Compiled :		Date Flown :	
<b>SIAL Géosciences inc.</b>			

## 10.0 CONCLUSIONS

All airborne and ground-based records were of excellent quality. Radar altitude tolerance was well respected with very few exceptions in very rugged terrain (Lime Hills mountains).

Data acquisition was generally done in easy diurnal conditions. There was a generally good correlation between the diurnal records of the two base stations and the diurnal correction, although beneficial, was not by itself effective enough to produce acceptable final maps. The remaining diurnal levelling error, that does not affect map and calculated gradient quality, is however estimated to be in the 2-5 nT range.

GPS results proved to be of high quality and very few intersection displacements were required. Most re-flights were caused by diurnal and bad GPS. The main causes of down-time were the weather, diurnal activity and aircraft maintenance.

The data were interpreted through a qualitative review of the color and shadow maps of the total field magnetic and the aeromagnetic structural interpretation and basement depth are presented at figure 42 at a scale of 1:500,000.

It is hoped that the information presented in this report and on the accompanying interpretation map will be useful both in planning subsequent exploration efforts and in the interpretation of related exploration data.

Respectfully Submitted,



Camille St-Hilaire, M.Sc.A.  
Senior Geophysicist



Josée Potvin, P.Eng.  
Senior Geophysicist

**SELECTED REFERENCES**

- Barnes, D.F., 1977. Bouguer gravity map of Alaska: U.S. Geological Survey Geophysical Investigations Map GP-913, 1 sheet, scale 1:250,000.
- Bhattacharya, B.K., 1966. Continuous Spectrum of Total Magnetic Field due to a Rectangular Body. *Geophysics*, v.31, p.97-121.
- Breiner, S., 1973. Applications manual for portable magnetometers: Geometrics, Sunnyvale, California.
- Bundtzen, T.K., Laird, G.M., Blodgett, R.B., Clautice, K.H., and Harris, E.E., 1994. Geology of the Gagaryah River Area Lime Hills, C-5 and C-6 Quadrangles, Southwest Alaska: Department of Natural Resources, Division of Geological & Geophysical Surveys, State of Alaska.
- Cady, W.M., Wallace, R.E., Hoare, J.M., and Webber, E.J., 1955. The Central Kuskokwim Region Alaska: U.S. Geological Survey Professional Paper 268, 132 p.
- Decker, J., Bergman, S.C., Blodgett, R.B., Box, S.E., Bundtzen, T.K., Clough, J.G., Coonrad, L.W., Gilbert, W.G., Miller, L.M., Murphy, J.M., Robinson, M.S., and Wallace, W.K., 1994. Geology of Southwestern Alaska: The Geology of North America, Vol. G-1, Geology of Alaska. The Geological Society of America, pp. 285-310.
- Decker, J., Reifenstuhl, R.R., Robinson, M.S., Waythomas, C.F., and Clough, J.G., 1995. Geologic of the Sleetmute A-5, A-6, B-5 and B-6 Quadrangles, Southwestern Alaska: Department of Natural Resources, Division of Geological & Geophysical Surveys, State of Alaska. Professional Report 99.
- Grant, F.S. and west, G.F., 1965. Interpretation Theory in Applied Geophysics: MacGraw-Hill Inc., New York.
- Hall, E.L., 1979. Computer Image Processing and Recognition: Academic press, Toronto.
- Kirschner, C.E., 1994. Interior basins of Alaska: The Geology of North America, Vol. G-1, Geology of Alaska. The Geological Society of America, pp. 469-493.
- Nettleton, L.L., 1976. Gravity and Magnetics in Oil Prospecting: MacGraw-Hill Inc., New York.

**SELECTED REFERENCES (Cont'd)**

- Nokleberg, W.J., Plafker, G., and Wilson, F.H., 1994. Geology of South-Central Alaska: The Geology of North America, Vol. G-1, Geology of Alaska. The Geological Society of America, pp. 311-366.
- Pilkington, M., Keating, P., 1991. Recent advances in interpretation techniques for magnetic and gravity anomalies. In Interpretation of Gravity and Magnetic Anomalies for Non-Specialists. Note for Canadian Geophysical Union Short Course, January 23 and 24, 1991. Geological Survey of Canada.
- Powell, M.J.D., 1965. A method for minimizing a sum of squares of nonlinear functions without calculating derivatives. Computer Journal, vol. 7. p. 303-307.
- Rasmussen, R. and Pederson, L.B., 1979. End corrections in potential field modelling. Geophysical Prospecting, vol. 27, no. 4, p. 749-760.
- Reid, A.B., Allsop, J.M., Granser, H., Millet, A.J. and Somerton, I.W., 1990. Magnetic interpretation in three dimensions using Euler deconvolution. Geophysics, v.55, p. 88-91.
- Reifenstuhel, R.R., Robinson, M.S., Smith, T.E., Albanese, M.S., and Allegro, G.A., 1984. Geologic Map of the Sleetmute B-6 Quadrangle, Alaska: Department of Natural Resources, Division of Geological & Geophysical Surveys, State of Alaska. Report of Investigations 84-12.
- Robinson, M.S., Decker, J., Reifenstuhel, R.R., Murphy, J.M., and Box, S.E., 1984. Geologic Map of the Sleetmute B-5 Quadrangle, Alaska: Department of Natural Resources, Division of Geological & Geophysical Surveys, State of Alaska. Report of Investigations 84-10.
- Schaff, R.G., 1983. Oil and Gas Basins Map of Alaska: Department of Natural Resources, Division of Geological & Geophysical Surveys, State of Alaska. Special report 32
- Shuey, R.T. and Pasquale, A.S., 1973. End correction in magnetic profile interpretation. Geophysics, vol. 38, no. 3, p. 507-512.
- Spector, A., 1968. Spectral Analysis of Aeromagnetic Data, Ph.D. Thesis. University of Toronto, Toronto, Ontario, Canada.

**SELECTED REFERENCES (Cont'd)**

- Spector, A. and Grant, F.S., 1970. Statistical Models for Interpretating Aeromagnetic Data, *Geophysics*, v.35, 293-302.
- Talwani, M. and Heirtzler, J.R., 1964. Computation of magnetic anomalies caused by two dimensional structures of arbitrary shape. In "Computers in the Mineral Industries, part 1", Stanford University Publications Geological Sciences, vol. 9, p. 464-480.
- Telford, W.M., Geldart, L.P., Sheriff, R.E., and Keys, D.A., 1976. Applied Geophysics: Cambridge University Press, Cambridge.
- Thompson, D.T., 1982. A new technique for making computer assisted depth estimates from magnetic data. *Geophysics*, v.47, p. 31-37.
- Zonge Engineering and Research Organization and Geonex Aero Service, 1995. High Resolution Aeromagnetic Survey Southeastern Bethel Basin, Alaska, Data Acquisition, data processing, and interpretation report: Department of Natural Resources, Division of Geological & Geophysical Surveys, State of Alaska.